

# DOCTORAL PROGRAMME

## **Information Management**

# GLOBAL AND LOCAL PROCESSES INFLUENCING ALTIMETRIC ERROR PATTERNS IN DIGITAL ELEVATION MODELS (DEM)

An approach on vertical accuracy assessment and spatial aspects of DEM error

Zuleide Alves Ferreira

A thesis submitted in partial fulfillment of the requirements for the degree of Doctor in Information Management

NOVA Information Management School
Instituto Superior de Estatística e Gestão de Informação

Universidade Nova de Lisboa

## **NOVA Information Management School** Instituto Superior de Estatística e Gestão de Informação

Universidade Nova de Lisboa

## GLOBAL AND LOCAL PROCESSES INFLUENCING ALTIMETRIC ERROR PATTERNS IN

ι	DIGITAL ELEVATION MODELS (DEM)	
	by	
	Zuleide Alves Ferreira	
Doctoral Thesis presented as r	partial requirement for obtaining the PhD in Information Manageme	ant
Doctoral mesis presented as p	varital requirement for obtaining the FID in information Manageme	:110
Supervisors:	Pedro da Costa Brito Cabral, PhD	
	Ana Cristina Marinho da Costa, PhD	

November 2023

## **STATEMENT OF INTEGRITY**

I hereby declare having conducted this academic work with integrity. I confirm that I have not used plagiarism or any form of undue use of information or falsification of results along the process leading to its elaboration. I further declare that I have fully acknowledged the Rules of Conduct and Code of Honor from the NOVA Information Management School.

Zuleide Alves Ferreira

Lisbon, 23 November 2023

## **DEDICATION**

To my dear parents, Antônio and Nilda, for unconditional support throughout my life.

To my dear husband, Rodrigo Alexandre, for his dedication and companionship.

To my beloved brothers, Paulo Ricardo (*in memoriam*) and Arthur Santhiago (*in memoriam*), who will forever be alive in my heart.

#### **ACKNOWLEDGEMENTS**

Firstly, I thank God for the gift of life and the opportunity for intellectual and spiritual evolution.

I am deeply grateful to my supervisors, Pedro Cabral and Ana Cristina Costa, whose guidance, expertise, and unwavering commitment played a pivotal role in shaping the direction of my research and the overall quality of this thesis.

I extend my appreciation to my fellow researchers and colleagues for their intellectual support, collaborative spirit, and the stimulating academic environment they provided. The exchange of ideas and discussions greatly enriched my research experience.

I want to thank Bruna Almeida and Leonardo Barbosa for their valuable contributions to specific aspects of this research. Their expertise enhanced the depth and scope of my work.

Heartfelt thanks to my family for their unwavering support and encouragement, especially to my parents, Antônio and Nilda, for all their love, dedication, and trust at all stages of my life.

I want to express my deep gratitude to my husband, Rodrigo Alexandre and my godson, Paulo Júnior, who faced this extraordinary experience living in a foreign country with me. Gratitude for their companionship, affection, and patience in all the challenging moments we lived on this journey.

My sincere thanks to my friends, Renata Cristina and Krammoer Paz, whose support was fundamental the whole time we lived in Portugal.

I am very grateful to my colleagues from the IFTO Geomatics Department, Eduardo, Érika, Heloísa, Itamara, Jonathas, Lidiane and Luiz Antônio, for the encouragement, and understanding during the challenging phases of this journey.

I acknowledge the financial support provided by the *Instituto Federal de Educação, Ciência e Tecnologia do Tocantins – Campus Palmas"*, *Fundação para a Ciência e a Tecnologia (FCT)* and *Centro de Investigação em Gestão de Informação (MagIC)* for providing the necessary resources for the successful completion of this research.

Finally, I would like to express my gratitude to anyone else who played a role in this academic journey, whether through discussions, assistance, or moral support. This thesis would not have been possible without the collective contributions of these individuals and institutions. Thank you all for your support and encouragement.

#### **ABSTRACT**

The field of geospatial data quality assessment is critical for ensuring the reliability and utility of Digital Elevation Models (DEM). DEM provide detailed elevation information, impacting various Earth sciences applications, including hydrology, geomorphology, environmental monitoring, land-use planning, and disaster management. However, uncertainties in DEM can propagate to derived products, which may lead to inaccurate predictions and decisions. This research addresses a significant knowledge gap in the field, particularly in understanding how terrain characteristics influence DEM vertical accuracy and how this impact varies across different spatial scales. The main objectives of this research are to investigate the vertical uncertainty of four open-source DEM, classify them according to cartographic standards, explore the correlation between DEM vertical error and terrain characteristics, provide a better understanding of error factors, identify local factors affecting DEM vertical accuracy, and investigate how terrain characteristics relate to altimetric error at different spatial scales. To achieve these objectives, we employed advanced geospatial techniques, including Geographically Weighted Regression (GWR) and Multiscale Geographically Weighted Regression (MGWR) to analyse local relationships and spatial variability in DEM altimetric errors. Our research reveals that elevation and slope impact DEM vertical accuracy, with higher altitudes and steeper terrains corresponding to increased altimetric errors. Furthermore, Land Use and Land Cover (LULC) also influence altimetric errors, particularly in areas with artificial structures and forest vegetation. The major contributions of this work include a nuanced understanding of DEM vertical accuracy and the role of terrain characteristics, emphasizing the importance of addressing spatial non-stationarity in DEM vertical accuracy assessments. Our research highlights the significance of terrain characteristics on DEM vertical error at different spatial scales and offers valuable guidance for researchers and practitioners working with these data. By enhancing the understanding of these influences, this research advances the field of geospatial data quality assessment, leading to better-informed decisions in several applications relying on these products.

## **KEYWORDS**

Local Spatial Regression; Spatial Error Analysis; Geographically Weighted Regression; Moran; Voronoi; Vertical Accuracy

## **Sustainable Development Goals (SGD):**





#### **RESUMO**

O campo da avaliação da qualidade dos dados geoespaciais é fundamental para garantir a confiabilidade e a utilidade dos Modelos Digitais de Elevação (MDE). O MDE fornece informações detalhadas de elevação, impactando diversas aplicações de ciências da Terra, incluindo hidrologia, geomorfologia, monitoramento ambiental, planejamento do uso da terra e gestão de desastres. No entanto, as incertezas nos MDE podem propagar-se em seus produtos derivados, o que pode levar a previsões e decisões imprecisas. Esta pesquisa aborda uma lacuna significativa de conhecimento na área, particularmente na compreensão de como as características do terreno influenciam a acurácia vertical do MDE e como esse impacto varia em diferentes escalas espaciais. Os principais objetivos desta pesquisa são investigar a incerteza vertical de quatro MDE de código aberto, classificá-los de acordo com padrões cartográficos, explorar a correlação entre o erro vertical do MDE e as características do terreno, fornecer uma melhor compreensão dos fatores de erro, identificar fatores locais que afetam a acurácia vertical do MDE e investigar como as características do terreno se relacionam com o erro altimétrico em diferentes escalas espaciais. Para atingir esses objetivos, empregamos técnicas geoespaciais avançadas, incluindo Regressão Geograficamente Ponderada (GWR) e Regressão Geograficamente Ponderada Multiescala (MGWR) para analisar as relações locais e a variabilidade espacial em erros altimétricos nos MDE. Nossa pesquisa revela que a elevação e a inclinação impactam a acurácia vertical do MDE, com altitudes mais altas e terrenos mais íngremes correspondendo a maiores erros altimétricos. Além disso, o uso e cobertura da terra (LULC) também influencia os erros altimétricos, particularmente em áreas com estruturas artificiais e vegetação florestal. As principais contribuições deste trabalho incluem uma compreensão diferenciada da acurácia vertical do MDE e do papel das características do terreno, enfatizando a importância de abordar a não-estacionariedade espacial nas avaliações de acurácia vertical do MDE. Nossa pesquisa destaca a importância das características do terreno no erro vertical em MDE em diferentes escalas espaciais e oferece orientação valiosa para pesquisadores e profissionais que trabalham com esses dados. Ao melhorar a compreensão destas influências, esta pesquisa avança no campo da avaliação da qualidade de dados geoespaciais, permitindo decisões mais bem informadas em diversas aplicações que dependem destes produtos.

## **PALAVRAS-CHAVE**

Regressão Espacial Local; Análise de Erros Espaciais; Regressão Geograficamente Ponderada; Moran; Voronoi; Acurácia Vertical

## Objetivos de Desenvolvimento Sustentável (ODS):





## **PUBLICATIONS AND AWARDS**

## **Journal articles**

Ferreira, Z., & Cabral, P. (2022). A comparative study about vertical accuracy of four freely available Digital Elevation Models: A case study in the Balsas River Watershed, Brazil. *ISPRS International Journal of Geo-Information*, 11(2), 106. https://doi.org/10.3390/ijgi11020106.

Ferreira, Z., Costa, A. C., & Cabral, P. (2023). Analysing the spatial context of the altimetric error pattern of a digital elevation model using multiscale geographically weighted regression. *European Journal of Remote Sensing*, 56(1), 2260092. https://doi.org/10.1080/22797254.2023.2260092.

Ferreira, Z., Almeida B., Costa, A. C., Fernandes, M. C. & Cabral, P. (2024). Insights into landslide susceptibility: A comparative evaluation of multi-criteria analysis and machine learning techniques. *Manuscript submitted for publication in a Scopus first-quartile journal*.

## **Conference paper**

Ferreira, Z., & Cabral, P. (2021). Vertical accuracy assessment of ALOS PALSAR, GMTED2010, SRTM and Topodata Digital Elevation Models. *Proceedings of the 7th International Conference on Geographical Information Systems Theory, Applications and Management (GISTAM 2021)*, 116-124. https://doi.org/10.5220/0010404001160124.

## **Award**

Best Student Paper Award Certificate for the paper entitled: Vertical accuracy assessment of ALOS PALSAR, GMTED2010, SRTM and Topodata Digital Elevation Models. *Proceedings of the 7th International Conference on Geographical Information Systems Theory, Applications and Management (GISTAM 2021).* 

## **INDEX**

1	Introduction	1
	1.1 Research questions	4
	1.2 Research objectives	4
	1.3 Research Methodology	4
	1.4 Dissertation structure	6
2	A comparative study about vertical accuracy of four freely available digital	elevation
m	odels: a case study in the Balsas River watershed, Brazil	7
	2.1 Introduction	7
	2.2 Materials and Methods	9
	2.2.1 Study area	9
	2.2.2 Data	.10
	2.2.3 Methods	.13
	2.3 Results	.15
	2.4 Discussion	.25
	2.5 Conclusions	.26
3	Analysing the spatial context of the altimetric error pattern of a digital elevation	on model
us	sing multiscale geographically weighted regression	.28
	3.1 Introduction	.29
	3.2 Materials	.31
	3.2.1 Study area	.31
	3.2.2 Data and preprocessing	.32
	3.2.3 Methods	.39
	3.3 Results	.43
	3.3.1 Statistical analysis	.43
	3.3.2 Models' performance and diagnostics	.47
	3.4 Discussion	.52
	3.5 Conclusion	54

4	Final Considerations	.55
5	Limitations and recommendations for future works	.58
Re	eferences	.59
Αŗ	opendices	.80
	Appendix A1/A2 – Correlation between the elevation of the reference points (BGN	) and the
el	evation	.80
	Appendix A3 – Histogram of the altimetric error	.81
	Appendix A4 – Boxplots of the elevation differences	.82
	Appendix B – Statistical analysis of the altimetric error	.83
	Appendix C – Correlation matrix of the candidate explanatory variables	.84
	Appendix D – Statistics of significant coefficient estimates (MGWR)	.85

## **LIST OF FIGURES**

Figure 1.1 – Research methodology5
Figure 2.1 – Study area9
Figure 2.2 – Hypsometric maps of Balsas River watershed derived from: (a) ALOS PALSAR, (b)
GMTED2010, (c) SRTM and (d) Topodata10
Figure 2.3 – Flowchart of methodology14
Figure 2.4 – Histogram of the altimetric error for ALOS PALSAR (a), GMTED2010 (b), SRTM (c)
and Topodata (d)16
Figure 2.5 – Linear correlation between the reference points altitudes of the Brazilian geodetic
network and altitudes extracted from each DEM: ALOS PALSAR (a), GMTED2010 (b),
SRTM (c) and Topodata (d)17
Figure 2.6 – Slope map for ALOS PALSAR (a), GMTED2010 (b), SRTM (c) and Topodata (d) 18
Figure 2.7 – Spatial distribution of the altimetric error for ALOS PALSAR (a), GMTED2010 (b),
SRTM (c) and Topodata (d) elaborated through the Inverse Distance Weighting (IDW)
method23
Figure 3.1 – Study area and reference points in the hydrographic region of Uruguay (Brazil)32
Figure 3.2 – LULC in the hydrographic region of Uruguay
Figure 3.3 – Voronoi map of the altimetric error45
Figure 3.4 – Local Moran's I statistic (a) and Hot Spot Analysis (b) of the altimetric error 46
Figure 3.5 – Voronoi map of the Local $R^2$ (a) and Local Condition Number (b) of the MGWR
model48
Figure 3.6 – Voronoi map of the spatial distribution of MGWR local coefficients: (a) aspect, (b)
curvature, (c) elevation, (d) LULC (class 1 – Artificial area)49

## **LIST OF TABLES**

Table 1.1 – Dissertation structure 6
Table 2.1 – GMTED2010 – Input source data characteristics adapted from Danielson & Gesch
(2011)
Table 2.2 – Original characteristics of the four assessed DEM
Table $2.3$ – Statistical metrics of the altitude difference between control points and DEM $15$
Table 2.4 – Spatial distribution of each slope class of the Balsas River watershed
Table 2.5 – Statistical analysis of altimetric error regarding slope classes
Table 2.6 – Statistical analysis of altimetric error as regarding altitude21
Table 2.7 – Altimetric Cartographic Accuracy Standard of the Elevation Points and the Digital
Terrain Model, Digital Elevation Model and Digital Surface Model for Digital Cartographic
Products production (Brazil, 2016)24
Table 2.8 – Extracted points from the DEM which had altimetric errors less than 15 and 25
meters24
Table 2.9 – DEM classification according to Altimetric Cartographic Accuracy Standard for
Digital Cartographic Products
Table 3.1 – Main characteristics of BGN (IBGE, 2019), SRTM (NASA, 2013) and Topodata DEM
(Garofalo & Liesenberg, 2015; Miceli et al., 2011; Valeriano, 2008)34
Table 3.3 – Spatial distribution of LULC classes in the hydrographic region of Uruguay 39
Table 3.4 – Statistical accuracy indicators of the Topodata DEM43
Table 3.5 – Parameter estimates for the OLS model
Table 3.6 – Metrics of OLS, GWR and MGWR models
Table 3.7 – Frequency distribution of Local R2 values of the MGWR model 50
Table 3.8 – Summary of local regression results

## **LIST OF ABBREVIATIONS AND ACRONYMS**

AIC Akaike's Information Criterion

**ALOS** Advanced Land Observing Satellite

**ALS** Airborne Laser Scanning

ANA Agência Nacional de Águas e Saneamento Básico

ASTER Advanced Spaceborne Thermal Emission and Reflection Radiometer

**AVNIR-2** Advanced Visible and Near Infrared Radiometer type 2

**BGN** Brazilian Geodetic Network

**BGS** Brazilian Geodetic System

**CDED** Canadian Digital Elevation Data

**DEM** Digital Elevation Model (s)

**DTED** Digital Terrain Elevation Data

**EGM96** Earth Gravitational Model 1996

**ESDA** Exploratory Spatial Data Analysis

**GDA 94** Geocentric Datum of Australia 1994

**GMTED2010** Global Multi-resolution Terrain Elevation Data 2010

**GTOPO30** Global 30-Arc-Second Elevation Dataset

**GWR** Geographically Weighted Regression

IBGE Instituto Brasileiro de Geografia e Estatística

INPE Instituto Nacional de Pesquisas Espaciais

**InSAR** Interferometric Synthetic Aperture Radar

**LiDAR** Light Detection and Ranging

MGWR Multiscale Geographically Weighted Regression

MODIS Moderate-Resolution Imaging Spectroradiometer

NAD 83 North American Datum of 1983

NASA National Aeronautics and Space Administration

**NED** National Elevation Dataset

NGA National Geospatial-Intelligence Agency

**OLS** Ordinary Least Squares

PALSAR Phased Array type L-band Synthetic Aperture Radar

PEC Padrão de Exatidão Cartográfica

**PRISM** Panchromatic Remote-sensing Instrument for Stereo Mapping

**SIRGAS2000** Sistema de Referência Geocêntrico para as Américas

**SPOT** Satellite Pour l'Observation de la Terre

**SRTM** Shuttle Radar Topography Mission

**TPI** Topographic Position Index

TRI Terrain Ruggedness Index

**USGS** United States Geological Survey

**VRM** Vector Ruggedness Measure

WGS 84 World Geodetic System 1984

"Education does not transform the world. Education changes people. People transform the world." (Paulo Freire)

"If I have seen further, it is by standing on the shoulders of giants." (Isaac Newton)

## 1 INTRODUCTION

A Digital Elevation Model (DEM) is a raster representation of the Earth's surface topography where each cell (pixel) contains information about the elevation (height) of the terrain (Abrams et al., 2020; Chaplot et al., 2006; Chen & Yue, 2010; Guth, 2006; Hirt et al., 2010; Smith et al., 2022). Generating a DEM involves collecting tree-dimensional data from the ground surface using miscellaneous technologies, namely, photogrammetry, Interferometric Synthetic Aperture Radar (InSAR), Light Detection and Ranging (LiDAR), Airborne Laser Scanning (ALS) and field surveying (Chang et al., 2004; Hodgson et al., 2003; Miller et al., 2022; Mondal et al., 2017).

Considering that DEM provide detailed three-dimensional information about the terrestrial surface (Guth et al., 2021), they have become valuable tools for Earth sciences applications concerning hydrology (Roostaee & Deng, 2020; Tran et al., 2023; Wechsler, 2007; Zhang & Montgomery, 1994), geomorphology (Dhont & Chorowicz, 2006; Hancock et al., 2006; S. Li et al., 2020; Walker & Willgoose, 1999; Xiong et al., 2021), environmental monitoring (Ahmad, 2018; Carrol & Morse, 1996; Florinsky, 1998; Mansour et al., 2020), land-use planning (Hammer et al., 1995; Munoth & Goyal, 2020; Tan et al., 2020; Tang et al., 2020), and disaster management (Demirkesen, 2012; Griffin et al., 2015; Manfreda & Samela, 2019; Naderpour et al., 2019; Saleem et al., 2019). However, it is improbable that DEM provide a perfect representation of the Earth's surface owing to various sources of uncertainty related to sampling, topographic complexity, geodetic control, survey point accuracy, processing techniques, interpolation, and resolution (Williams, 2012).

A DEM is an approximation representing an actual terrain surface and, inherently, includes a level of uncertainty that can affect DEM derivatives (i.e., slope, aspect, curvature, etc.), which may lead to an imprecise representation of terrain features (Aerts et al., 2003; Darnell et al., 2008; Zhou & Liu, 2002). Since some products derived from DEM, such as slope and aspect, are key parameters influencing landscape natural processes, DEM accuracy may affect predictions involving natural hazards, land-use potential, and environmental planning (Gonga-Saholiariliva et al., 2011). Hence, a better understanding of these models' errors is crucial to reduce the potential error propagation, given that the greater the vertical error of a DEM, the greater the error in their derived products (Oksanen, 2006). Nonetheless, developing a

comprehensive error model for DEM uncertainty has proven to be challenging due to the complexity of the rigorous analysis of error propagation (Oksanen & Sarjakoski, 2006).

The essential role of DEM in supporting decision-making processes justifies the critical importance of assessing the uncertainties of these products (Altunel, 2019; Oksanen, 2006; Soliman & Han, 2019; Wechsler, 2003) because the outcomes from DEM applications are directly influenced by their quality, which is affected mainly by their vertical accuracy and spatial resolution (Soliman & Han, 2019). Thereupon, quantifying a DEM accuracy can be challenging due to the absence of an absolute "true" reference, leading to uncertainty and subjectivity when evaluating the correctness and quality of these models (Zhou & Liu, 2002), not to mention that the primary indicator of DEM quality should not only rely on the absolute accuracy of elevation values within a sample (Reuter et al., 2009).

DEM vertical accuracy is typically assessed using metrics that do not incorporate spatial dimensions, such as the mean error (ME), mean absolute error (MAE), and root mean square error (RMSE) (Chaplot et al., 2006; Erdoğan, 2010; J. Li et al., 2020; Thomas et al., 2014). RMSE is the parameter most used to assess DEM accuracy (Mesa-Mingorance & Ariza-López, 2020; Nadi et al., 2020), but it offers a generalized overview of the error, lacking the capability to differentiate areas with varying levels of uncertainty (Aerts et al., 2003). These metrics are typically obtained by comparing the elevations extracted from the assessed DEM and a reference dataset acquired from a more accurate data source (Mesa-Mingorance & Ariza-López, 2020; Polidori & El Hage, 2020; Temme et al., 2009).

DEM error metrics (i.e., ME, MAE and RMSE) provide an overall assessment of their accuracy (Erdoğan, 2010). However, spatial aspects of DEM error are constantly overlooked (Oksanen & Sarjakoski, 2006), and thus, users have to consider the assumption that error rates remain homogeneous everywhere in the DEM (Erdoğan, 2010). Therefore, modelling the DEM error magnitude is fundamental in overall surface characteristics production (Ehlschlaeger, 2002), as it can offer assessments of the potential impacts of data quality, allowing users to make informed judgments about the appropriateness of spatial data for particular tasks (Fisher, 1998). In this way, extensive research in uncertainty analysis has yielded a wide array of methods for exploring DEM errors and their propagation (Darnell et al., 2008) once a more

comprehensive explanation of the errors facilitates a deeper understanding of DEM quality and its level of uncertainty when applied to analytical scenarios (Erdoğan, 2010).

DEM errors, arising from sampling, measurement, and interpolation processes, are often considered to have no spatial distribution and to be statistically stationary over a region, but both are unrealistic assumptions (Fisher, 1998). Hence, deep investigation is needed to identify the optimal statistical representation for errors in specific applications, as different applications require tailored statistical combinations (Ehlschlaeger, 2002).

Regression modelling may be a good approach as it has the potential to generate error surfaces considering spatial non-stationarity, spatial correlation, and heteroscedasticity (Carlisle, 2005). Generally, DEM error varies spatially across an area (spatial variability) besides being sometimes related to errors from neighbouring cells (spatial autocorrelation) (Carlisle, 2005; Darnell et al., 2008; Williams, 2012). Accordingly, a global model, such as Ordinary Least Squares (OLS), may not accurately represent spatial non-stationarity relationships and can be highly misleading locally (Erdoğan, 2010; Fotheringham et al., 2002) because even when the global average DEM error is small, local error values can exhibit significant magnitudes as well as present spatial correlations among them (Holmes et al., 2000).

Despite being a linear regression model, the OLS technique considers the investigated processes to be constant across space, which is often an invalid assumption (Erdoğan, 2010). Thus, to overcome this issue, Geographically Weighted Regression (GWR) was developed as an alternative approach for analysing local relationships within multivariate datasets (Fotheringham et al., 2002).

GWR investigates the potential spatial variability in relationships and offers insight into the spatial scale at which processes operate by identifying an optimal bandwidth, presuming that all variables operate at the same spatial scale (Fotheringham et al., 2017). On the other hand, Multiscale Geographically Weighted Regression (MGWR) explores spatial heterogeneity by identifying the spatial scale at which different processes operate (Fotheringham et al., 2017). In other words, it allows us to identify if the relationships between dependent and independent variables occur at local, regional, or global scales. Given these considerations and the factors above-mentioned, there is a compelling opportunity to investigate the global and

local processes influencing the quality of DEM to ensure the reliability and utility of these products.

## 1.1 RESEARCH QUESTIONS

The hypotheses under the research are the following:

- Can the terrain characteristics explain the altimetric error in a DEM?
- What are the spatial variations in the magnitude of the relationship between altimetric error and terrain characteristics?
- What are the spatial scales over which terrain characteristics affect local variations in DEM vertical errors?

## 1.2 RESEARCH OBJECTIVES

The main goal of our study is to provide a better understanding of the global and local processes influencing the quality of DEM products. To accomplish the overall goal, we had to divide our research into some specific objectives, as follows:

- To investigate the vertical uncertainty of four open-source DEM.
- To classify four open-source DEM according to the Brazilian Cartographic Accuracy Standard.
- To investigate the correlation between DEM vertical error and terrain characteristics.
- To provide a better comprehension of DEM vertical error influencing factors.
- To identify the local factors that may explain the vertical error of an open-source DEM.
- To investigate if the relationship between terrain characteristics and altimetric error operates at different spatial scales.

#### 1.3 RESEARCH METHODOLOGY

The research methodology for the DEM vertical accuracy analysis carried out in this dissertation is summarized in Figure 1.1.

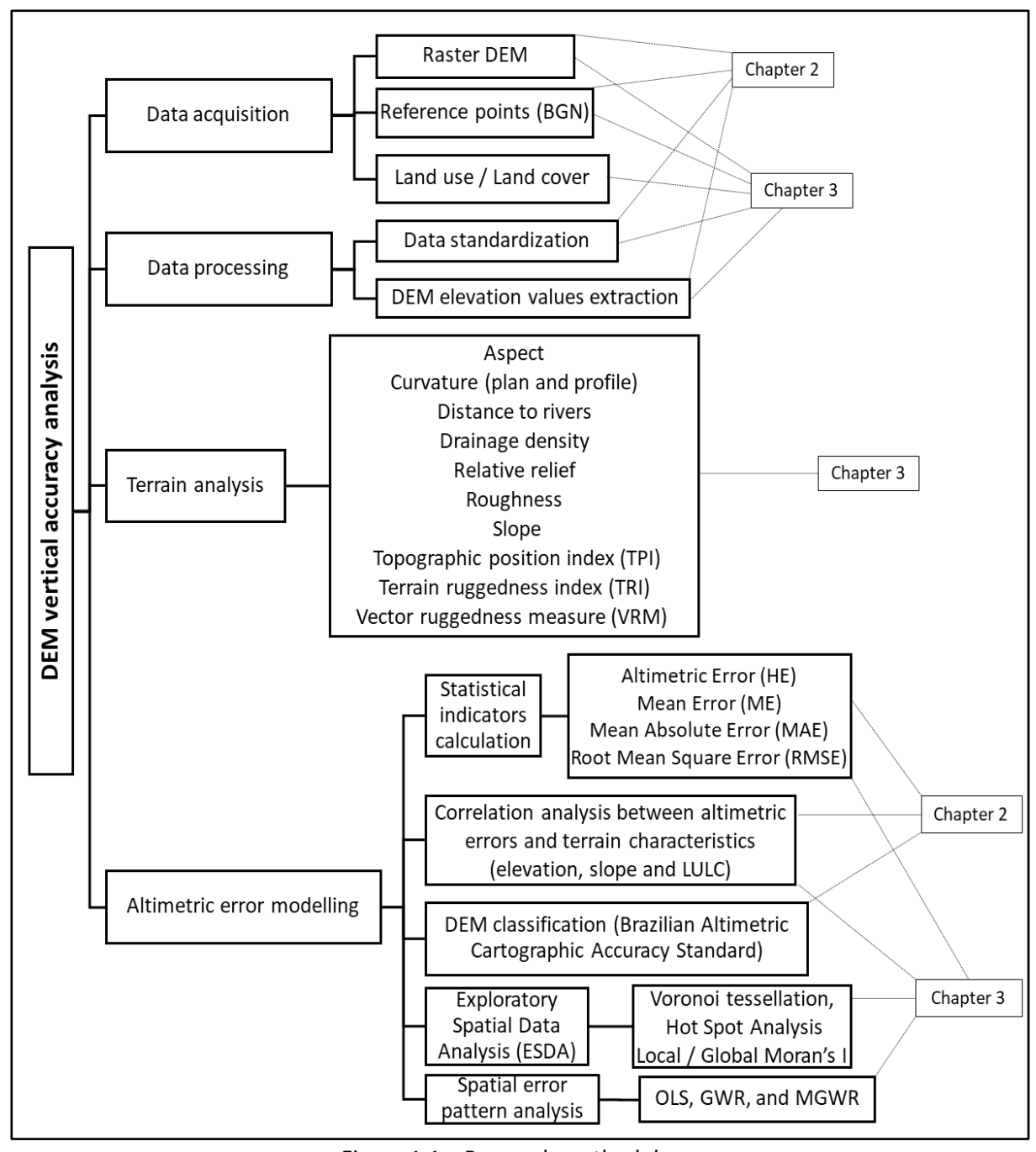


Figure 1.1 – Research methodology

## 1.4 DISSERTATION STRUCTURE

This dissertation is organized into five chapters, which include three research articles. The first chapter is an introduction section that addresses the background contextualization, research questions, objectives and the research path performed.

Regarding the research path, the first paper (Ferreira & Cabral, 2021) was published in the 7<sup>th</sup> International Conference on Geographical Information Systems Theory, Applications and Management (GISTAM 2021). Since this study won the GISTAM 2021 Best Student Paper Award, it was invited for a conference post-publication. Therefore, the second chapter of this dissertation refers to the second paper (full version) published in the International Journal of Geo-Information (Ferreira & Cabral, 2022), which incorporated the first article. The third chapter refers to the article published in the European Journal of Remote Sensing (Ferreira et al., 2023). The fourth chapter summarizes the main findings of our study, whereas the fifth chapter brings some limitations of this research and recommendations for future works. Table 1.1 shows how this dissertation is organized.

Table 1.1 – Dissertation structure

Chapter	Title	Status	Journal Ranking <sup>1</sup>
1	Introduction	N/A	N/A
2	Vertical accuracy assessment of ALOS PALSAR, GMTED2010, SRTM and Topodata Digital Elevation Models <sup>2</sup>	Published in the 7 <sup>th</sup> International Conference on Geographical Information Systems Theory, Applications and Management (GISTAM 2021)	N/A
	A comparative study about vertical accuracy of four freely available Digital Elevation Models: A case study in the Balsas River Watershed, Brazil <sup>3</sup>	Published in the International Journal of Geo-Information (ISPRS)	Scopus – Q1
3	Analysing the spatial context of the altimetric error pattern of a digital elevation model using multiscale geographically weighted regression	Published in the European Journal of Remote Sensing	Scopus – Q1
4	Final Considerations	N/A	N/A
5	Limitations and recommendations for future works	N/A	N/A

<sup>&</sup>lt;sup>1</sup> Journal ranking at the submission date.

<sup>&</sup>lt;sup>2</sup>This paper won the GISTAM 2021 Best Student Paper Award and it was invited for a conference post-publication.

<sup>&</sup>lt;sup>3</sup> This paper is the full version of the special issue of the conference post-publication.

# 2 A COMPARATIVE STUDY ABOUT VERTICAL ACCURACY OF FOUR FREELY AVAILABLE DIGITAL ELEVATION MODELS: A CASE STUDY IN THE BALSAS RIVER WATERSHED, BRAZIL<sup>1</sup>

Abstract: Digital Elevation Models (DEM) provide important support to research since these data are freely available for almost all areas of the terrestrial surface. Thus, it is important to assess their accuracy for correct applicability regarding the correct use scale. This paper aims to assess the vertical accuracy of ALOS PALSAR, GMTED2010, SRTM and Topodata DEM according to the Brazilian Cartographic Accuracy Standard through the official high accuracy network data of the Brazilian Geodetic System. This study also seeks to investigate whether the altimetric error is correlated with altitude and slope in the study area. Our results showed that the four assessed DEM in this study demonstrated satisfactory accuracy to provide mappings in scales up to 1: 100,000 because more than 90% of the extracted points presented altimetric errors of less than 25 meters when compared to the reference points from the high accuracy network of the Brazilian Geodetic System. Regarding the altimetric error, we could not find a significant correlation coefficient with altitude or slope in the study area. In this sense, future DEM assessments should be based on the investigation of other factors that may influence altimetric error.

## 2.1 Introduction

Digital Elevation Models (DEM) provide an important topographic product that is fundamental for many scientific and commercial applications (Rizzoli et al., 2017; Uysal et al., 2015). However, traditional methods to acquire information for DEM generation are often expensive and time-consuming due to land surveying necessity (Uysal et al., 2015). On the other hand, several DEM products from many sources have been made freely available to geoinformation users in the last decade, so it is important to investigate their possible applications by assessing their accuracy (Moura et al., 2014).

<sup>1</sup> The text from this chapter has been published in the International Journal of Geo-Information (ISPRS). https://doi.org/10.3390/ijgi11020106. DEM products accuracy has been regularly investigated to evaluate their applicative potentialities thus improving the mapping methods (Polidori et al., 2014). Most of these experiments are performed by comparing the extracted data from DEM to a set of reference data, i.e., control points, through accuracy statistical indicators, such as mean difference, standard deviation or root mean square error (Polidori et al., 2014).

DEM accuracy assessment requires further attention considering that, despite technological advances in the creation and availability of these products, there are still no specific standardized guidelines regarding this assessment process (Mesa-Mingorance & Ariza-López, 2020). Nonetheless, in Brazil, there is a decree that regulates the quality of cartographic products by establishing instructions for the technical standards of national cartography. The Decree n° 89,817/1984 determines criteria for cartographic products classification regarding their accuracy and the distribution of errors using a statistical indicator of positional quality named Cartographic Accuracy Standard (*Padrão de Exatidão Cartográfica - PEC*). Therefore, 90% of the extracted points from the cartographic product must not present errors higher than those predicted in the PEC when their coordinates are compared with those from surveyed points in the field through a high accuracy method (Brazil, 1984, 2016).

There are a lot of studies on DEM accuracy assessment (Hu et al., 2017; Jain et al., 2018; Mouratidis & Ampatzidis, 2019; Varga & Bašić, 2015; Wessel et al., 2018), but none assessed the vertical accuracy of the ALOS PALSAR, GMTED2010, SRTM and Topodata DEM according to the Brazilian Cartographic Accuracy Standard (PEC). Thus, the purpose of this study is to assess the vertical accuracy of the above-mentioned DEM by using the official high accuracy network data of the Brazilian Geodetic System. This study also seeks to investigate whether the altimetric error is correlated with altitude and slope in the study area. We expect that results contribute to the correct applicability of the analysed DEM according to an appropriate use scale in Brazil and other places dealing with the same problem context.

## 2.2 MATERIALS AND METHODS

## 2.2.1 Study area

The Balsas River watershed covers thirteen municipalities and its area is 12,352.50 km², corresponding to nearly 4.5% of the State of Tocantins (Figure 2.1) (Brazil, 2012). Its altitudes are approximately between 200 and 800 meters considering the sea level and inside this area, we can find 105 stations of the official Brazilian geodetic network situated along the main highways of the region (Figure 2.2). It is worth noting the absence of high accuracy three-dimensional data available for free to the community in various regions of the planet. In this sense, the Balsas River watershed was selected due to the lack of accurate three-dimensional data available for this area.

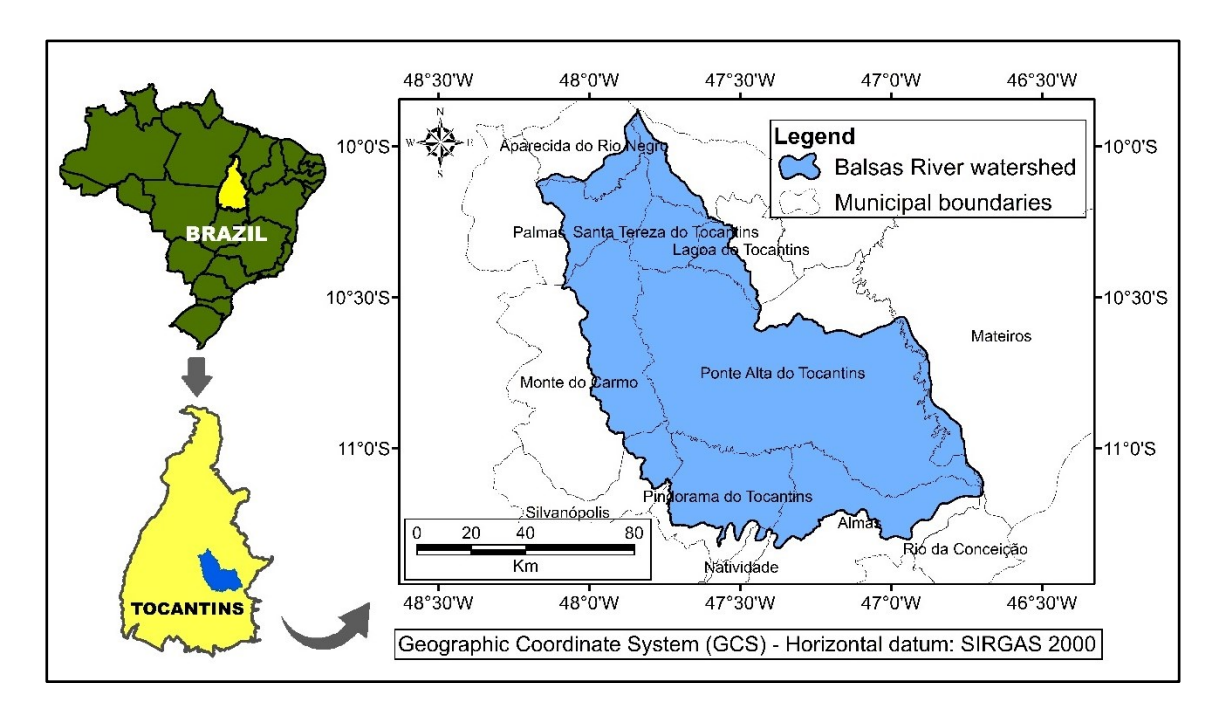


Figure 2.1 – Study area

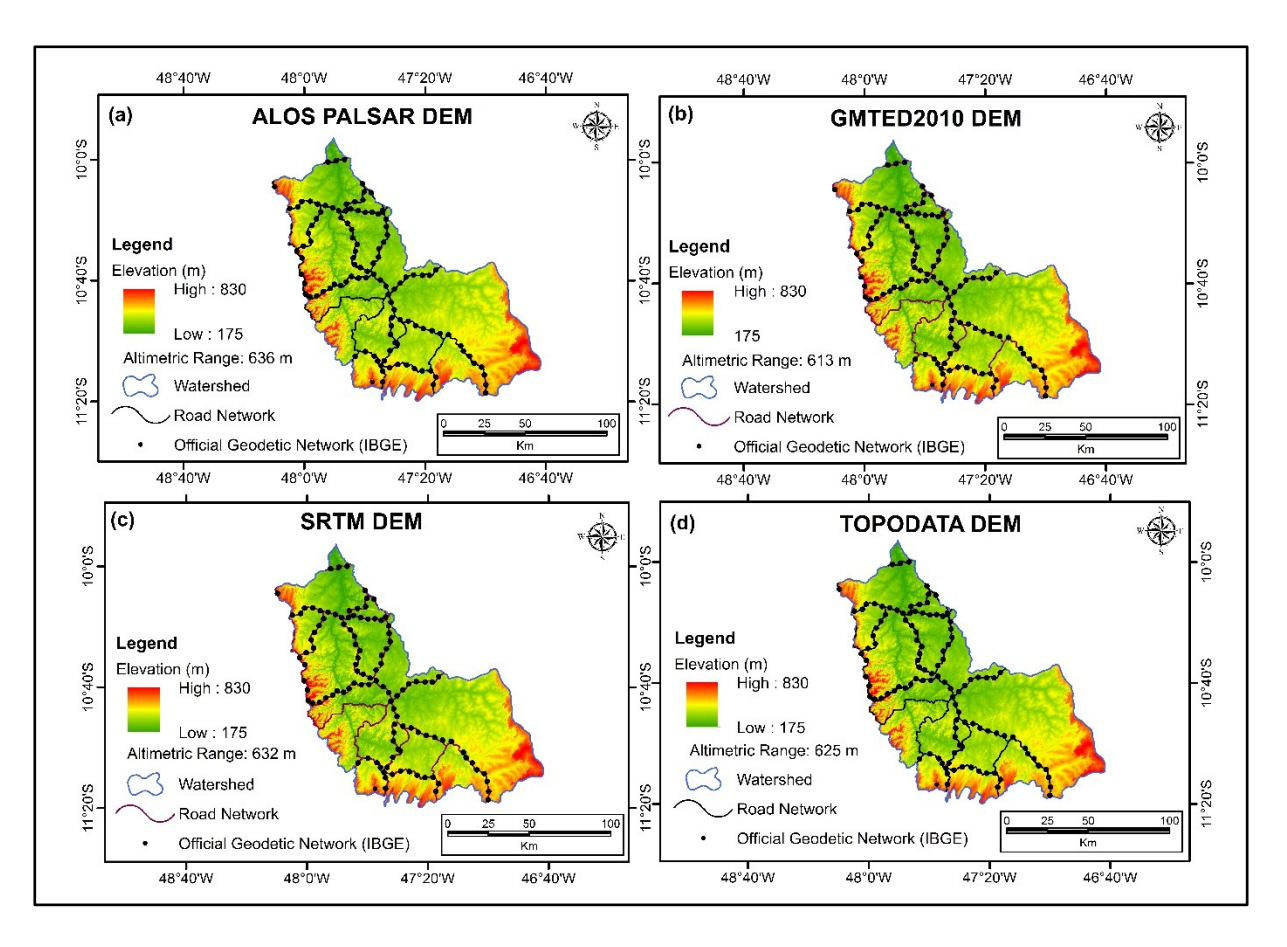


Figure 2.2 – Hypsometric maps of Balsas River watershed derived from: (a) ALOS PALSAR, (b) GMTED2010, (c) SRTM and (d) Topodata

## 2.2.2 Data

In this accuracy assessment, we compared the extracted points from the four DEM with the official network data of the Brazilian Geodetic System. This network is composed of geodesic stations located along the main highways throughout the Brazilian territory which was implemented in 1945 through the high accuracy geometric levelling method (IBGE, 2019). Since then, these altitudes are regularly recalculated owing to the addition of new geometric levelling lines, development of new data measurement and processing techniques, where new observations of geometric levelling and gravimetry are added aiming to ensure the integrity, consistency, and reliability of the information from the Geodetic Database. According to the quality assessment of these altimetric data performed in 2018, 87.5% of the adjusted geopotential values presented standard deviations between 6 and 10 centimetres in absolute terms (IBGE, 2019).

The Advanced Land Observing Satellite "DAICHI" (ALOS) was designed to supply land coverage mapping, resource surveying and disaster monitoring (JAXA, 2020b). It was launched on January 24, 2006, from the Tanegashima Space Center with three sensors onboard namely Panchromatic Remote-sensing Instrument for Stereo Mapping (PRISM), Advanced Visible and Near Infrared Radiometer type 2 (AVNIR-2), and Phased Array type L-band Synthetic Aperture Radar (PALSAR). ALOS mission was completed on May 12, 2011, but during its 5-years operation, it shot 6.5 million scenes around the Earth, which have been used in many fields, such as agriculture, natural environment maintenance, forest monitoring and disaster mitigation (JAXA, 2020b). The PRISM sensor is a panchromatic radiometer and has three sets of optical systems with 2.5 meters spatial resolution at nadir, the AVNIR-2 sensor is a visible and near-infrared radiometer that provides 10 meters spatial resolution images and PALSAR is an active microwave sensor that uses L-band frequency to obtain cloud-free and day-and-night land observation (JAXA, 2020a, 2020b).

The acquired data during the ALOS mission were geometrically and radiometrically corrected. Firstly, the geometric distortions were corrected using some DEM, then the radiometry correction was executed by adjusting the brightness of the individual SAR image pixels in the affected foreshortening and layover regions (Gens, 2015; Laurencelle et al., 2015). Succeeding the radiometric terrain correction, these products were distributed at two resolutions, 12.5 and 30 meters pixel size generated from high-resolution (NED13) and mid - resolution DEM (SRTM30, NED1 and NED2), respectively (Gens, 2015).

The Shuttle Radar Topography Mission (SRTM) is an international project developed by the National Aeronautics and Space Administration (NASA) and the National Geospatial-Intelligence Agency (NGA). This mission started on February 11, 2000, and during 10 days, SRTM acquired data over approximately 80 percent of Earth's land surface through two radar antennas to create the first near-global data set of land elevations (NASA, 2020). Initially, SRTM data were made publicly available at 3 arc-seconds resolution, or 90 meters of pixel size, for regions outside the United States. However, in 2014, the topographic data were released globally with the full resolution originally measured, that is 1 arc-second (30 meters) (NASA, 2020).

The Topodata project is a topographic database generated from the refinement of SRTM data. Due to the general lack of topographic data at adequate scales in some Brazilian regions, this project was released in 2008 aiming to refine SRTM data from the 3 arc-seconds to 1 arc-second resolution through kriging techniques as well as to provide the derivation of geomorphometric data for the whole Brazilian territory (Valeriano, 2008; Valeriano & Rossetti, 2012). The Topodata project resulted in an extensive structured database freely available for the scientific community which offers several products such as slope, slopes orientation, horizontal curvature, vertical curvature, inputs for the drainage structure design among others (Valeriano, 2008).

The Global Multi-resolution Terrain Elevation Data 2010 (GMTED2010) was developed by the United States Geological Survey (USGS) in partnership with the National Geospatial-Intelligence Agency (NGA) to replace the Global 30 Arc-Second Elevation (GTOPO30) as the elevation dataset for global and continental scale applications (Danielson & Gesch, 2011). GMTED2010 was elaborated using derived data from 11 raster-based elevation sources (Table 2.1), which provides global coverage from latitude 84°N to 56°S for most products at three different resolutions 7.5, 15 and 30 arc-seconds, that corresponds to nearly 250, 500 and 1,000 meters of pixel size, respectively (Danielson & Gesch, 2011). In this study, we selected the GMTED2010 product available in 7.5 arc-seconds resolution, which is widely used in several scientific studies (Amatulli et al., 2018; Athmania, 2014; Janiec, 2020; Pakoksung, 2021; Tan et al., 2015; Thomas et al., 2014; Thomas et al., 2015; Varga & Bašić, 2015) despite its bigger pixel size when compared with SRTM, for instance. Table 2.2 presents the original main characteristics of the four DEM assessed in this study.

Table 2.1 – GMTED2010 – Input source data characteristics adapted from Danielson & Gesch (2011)

Dataset	Resolution	Horizontal unit	Horizontal datum
SRTM DTED® 2	1	Arc-second	WGS 84
DTED® 1	3	Arc-second	WGS 84
CDED1	0.75	Arc-second	NAD 83
CDED3	3	Arc-second	NAD 83
15-arc-second SPOT 5 Reference3D	0.00416666	Decimal degree	WGS 84
NED	0.00027777	Decimal degree	NAD 83
NED – Alaska	0.00055555	Decimal degree	NAD 83
GEODATA 9 second DEM version 2	0.0025	Decimal degree	GDA 94
Greenland satellite radar altimeter DEM	1,000	Meter	WGS 84
Antarctica satellite radar and laser altimeter DEM	1,000	Meter	WGS 84
GTOPO30	0.00833333	Decimal degree	WGS 84

(DTED®, Digital Terrain Elevation Data; WGS 84, World Geodetic System 1984; CDED, Canadian Digital Elevation Data; NAD 83, North American Datum of 1983; SPOT, Satellite Pour l'Observation de la Terre; NED, National Elevation Dataset; DEM, digital elevation model; GDA 94, Geocentric Datum of Australia 1994; GTOPO30, Global 30-Arc-Second Elevation Dataset).

Table 2.2 – Original characteristics of the four assessed DEM

DEM	Coordinate System	Horizontal Datum	Vertical Reference	Pixel Size	Radiometric Resolution
ALOS PALSAR	UTM	WGS 84	Ellipsoid*	12.5 meters	16 bits (signed integer)
CNATED 2010	Geographic	WGS 84	Geoid	231 meters	16 bits
GMTED2010		WG3 64	(EGM96)	(7.5 arc-seconds)	(signed integer)
SRTM	Geographic	WGS 84	Geoid	30 meters	16 bits
SKTIVI		WG3 84	(EGM96)	(1 arc-second)	(signed integer)
Tonodata		MCC 94	Geoid	30 meters	32 bits
Topodata	Geographic	WGS 84	(EGM96)	(1 arc-second)	(floating point)

<sup>\*</sup>The orthometric heights with EGM96 vertical datum were converted to ellipsoid heights using the ASF MapReady tool named "geoid\_adjust" (Laurencelle et al., 2015).

## 2.2.3 Methods

Figure 2.3 summarizes the methodology used in this study. Firstly, we downloaded the data from the study area, such as raster DEM and Brazilian official geodetic network points. Then, we proceeded with the radiometric resolution conversion of the Topodata DEM from 32 bits (floating point) to 16 bits (signed integer) to standardize the data. The following step was to extract the altitudes of the ALOS PALSAR, GMTED2010, SRTM and Topodata DEM at the same coordinates of the reference points from the official geodetic network. However, we needed

to convert the ellipsoidal altitudes of the ALOS PALSAR DEM to orthometric altitudes (geoid) since the GMTED2010, SRTM and Topodata DEM were available with altitudes referenced to the geoid (EGM96). For this conversion process, we used the MAPGEO2015 software (IBGE, 2015) developed by the *Instituto Brasileiro de Geografia e Estatística* (IBGE) in collaboration with the *Escola Politécnica da Universidade de São Paulo*.

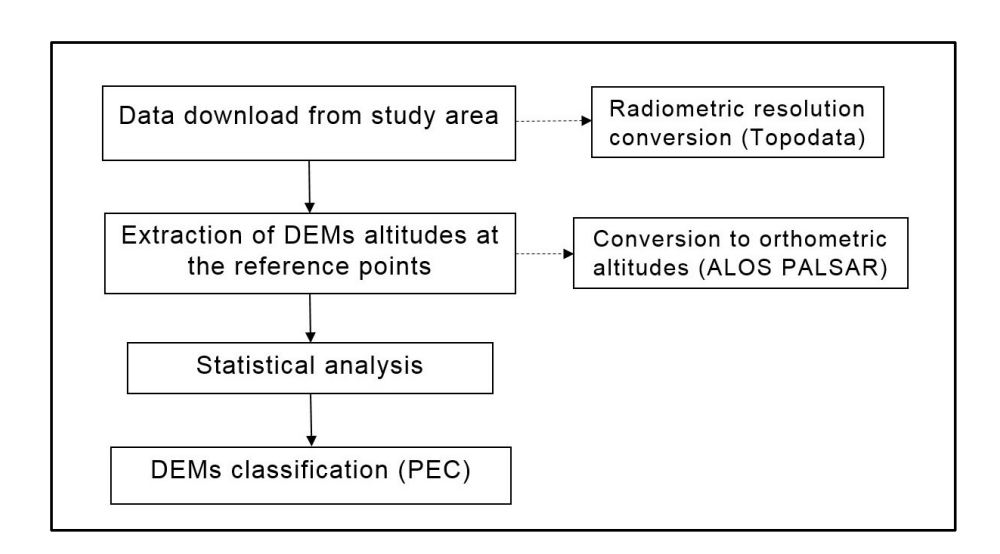


Figure 2.3 – Flowchart of methodology

Afterwards, accuracy statistical indicators were calculated such as Altimetric Error (HE) (1), Mean Error (ME) (2), Mean Absolute Error (MAE) (3) and Root Mean Square Error (RMSE) (4), as performed in some previous studies (Jain et al., 2018; Varga & Bašić, 2015; Wessel et al., 2018). We also analysed the correlation between the altimetric error and altitude/slope in the study area through the coefficient of determination ( $R^2$ ) (5). Finally, we could classify the four DEM according to the Brazilian Cartographic Accuracy Standard (PEC) (Iorio et al., 2012; Moura et al., 2014).

$$H_E = H_{REF} - H_{DEM} \tag{1}$$

$$ME = \frac{1}{n} \sum_{i=1}^{n} (HREF - HDEM)$$
 (2)

$$MAE = \frac{1}{n} \sum_{i=1}^{n} |HREF - HDEM|$$
 (3)

$$RMSE = \sqrt{\frac{1}{n} \sum_{i=1}^{n} (HE - ME)^2}$$
 (4)

$$R^2 = 1 - \frac{\text{RSS}}{\text{TSS}} \tag{5}$$

where  $H_E$  = altimetric error;  $H_{REF}$  = reference point altitude from Brazilian geodetic system official altimetric network;  $H_{DEM}$  = altitude extracted from DEM at reference point coordinates; ME = Mean Error; MAE = Mean Absolute Error; RMSE = Root Mean Square Error; n = number of reference points;  $R^2$  = coefficient of determination; RSS = sum of squares of residuals; and TSS = total sum of squares.

## 2.3 RESULTS

Results show that regarding the mean error and mean absolute error, the values of the statistical analysis are similar for the four DEM (Table 2.3). Actually, we observe that ALOS PALSAR, SRTM and Topodata DEM present similarity in all statistical indicators, as well as it is possible to notice that GMTED2010 shows the worst performance mainly when we consider the RMSE (7.48 m) and the error range (54.00 m), i.e., the difference between the minimum and maximum altimetric errors.

Table 2.3 – Statistical metrics of the altitude difference between control points and DEM

	ALOS PALSAR	GMTED2010	SRTM	Topodata
ME (m)	12.70	13.31	12.82	12.87
MAE (m)	12.88	13.86	12.96	13.22
RMSE (m)	4.95	7.48	4.76	5.38
H <sub>E</sub> min (m)	-3.58	-14.22	-3.21	-6.17
H <sub>E</sub> max (m)	22.04	39.78	20.93	23.60
Error Range (m)	25.62	54.00	24.14	29.77

Figure 2.4 presents the histogram of the altimetric error of each DEM where we can see a positive distortion in all four DEM and higher variability of the errors in the GMTED2010 product. Nevertheless, we can also notice a very strong correlation between the altitudes of the reference points from the Brazilian official network and the altitudes extracted from the assessed DEM, where it is possible to verify a determination coefficient (R<sup>2</sup>) of approximately 0.99 in all of them (Figure 2.5).

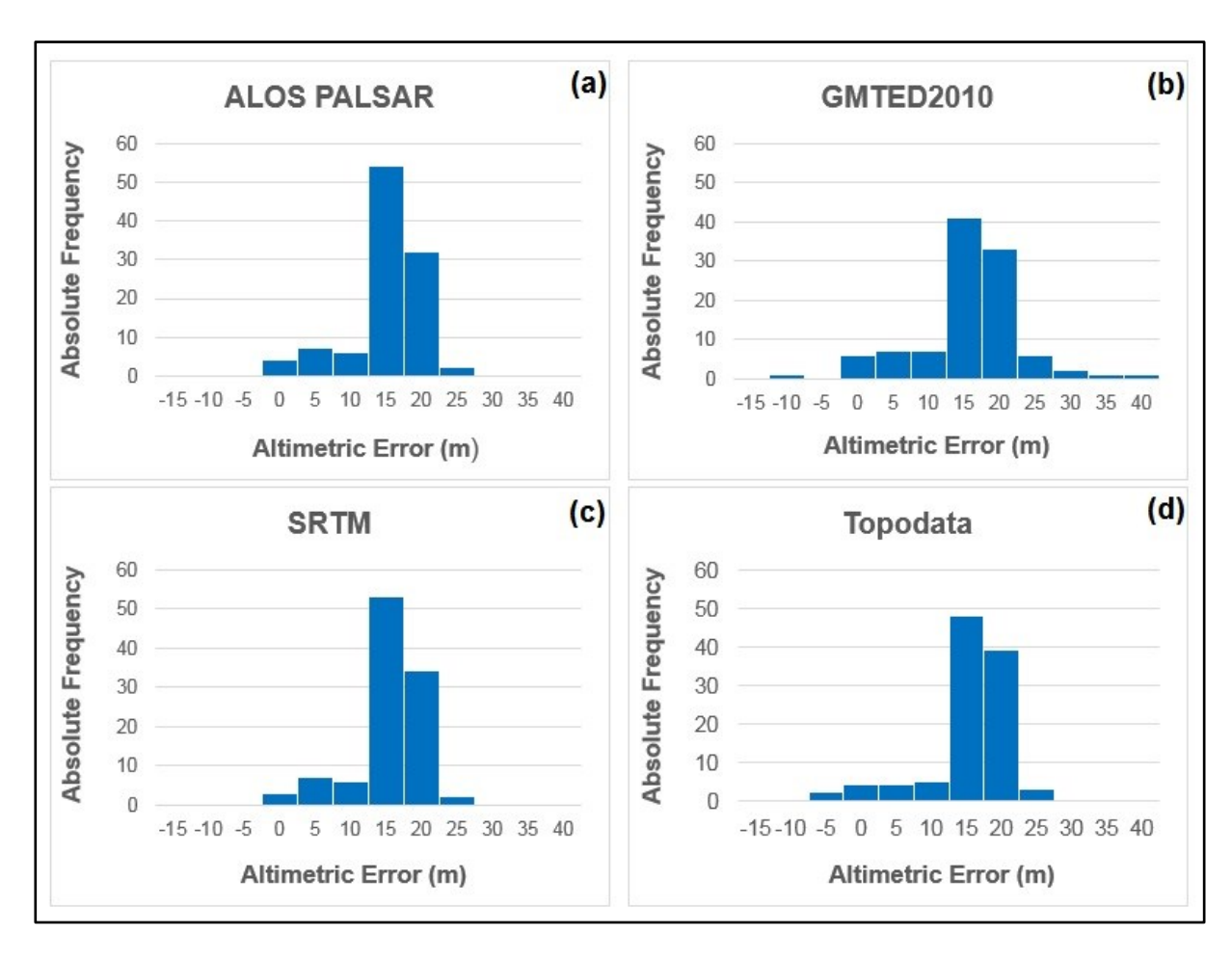


Figure 2.4 – Histogram of the altimetric error for ALOS PALSAR (a), GMTED2010 (b), SRTM (c) and Topodata (d)

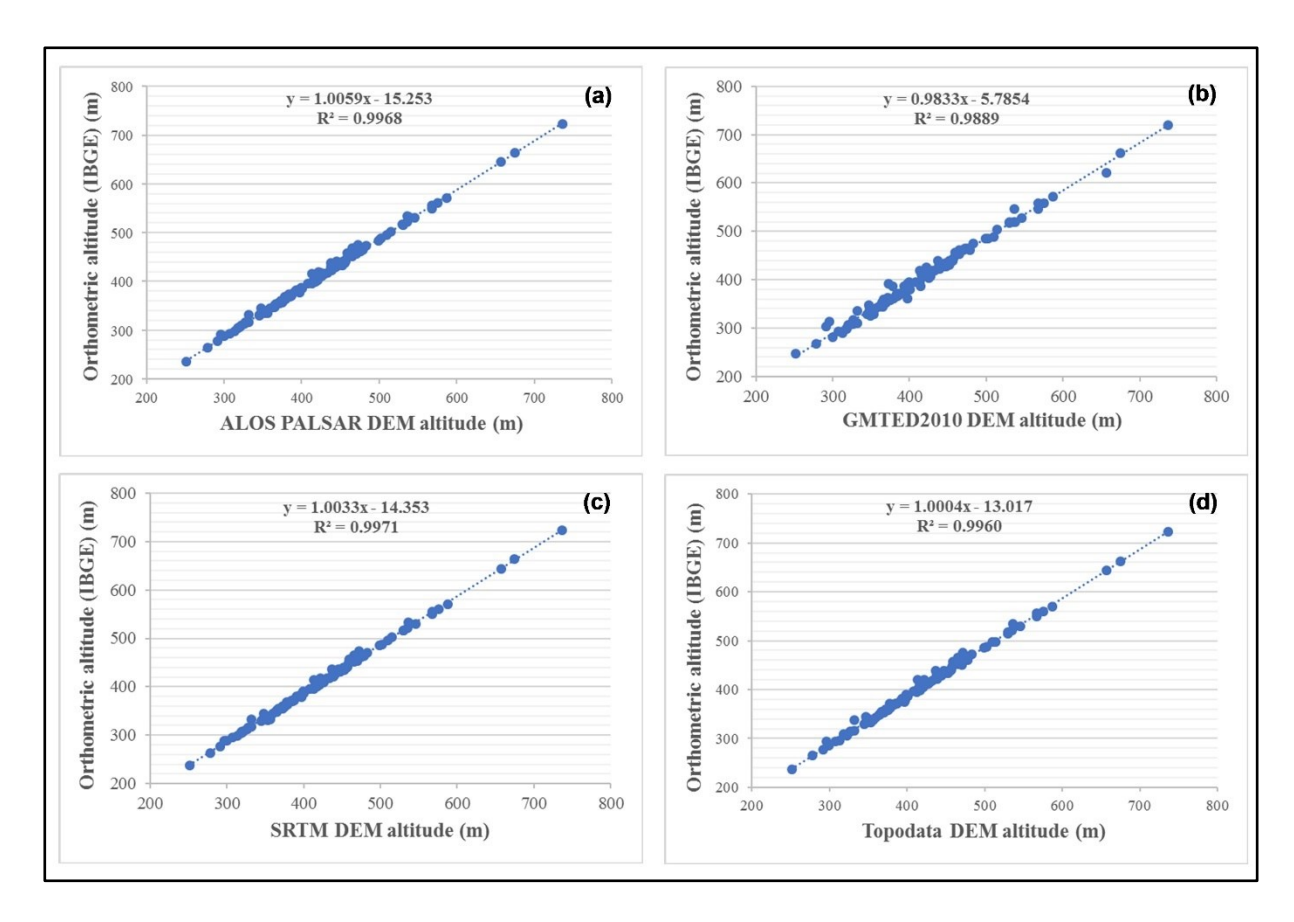


Figure 2.5 – Linear correlation between the reference points altitudes of the Brazilian geodetic network and altitudes extracted from each DEM: ALOS PALSAR (a), GMTED2010 (b), SRTM (c) and Topodata (d)

Aiming to investigate whether there is a correlation between slope and altimetric error, slope maps of the Balsas River watershed were generated from each DEM, where six slope classes were established according to IBGE (IBGE, 2007) (Figure 2.6).

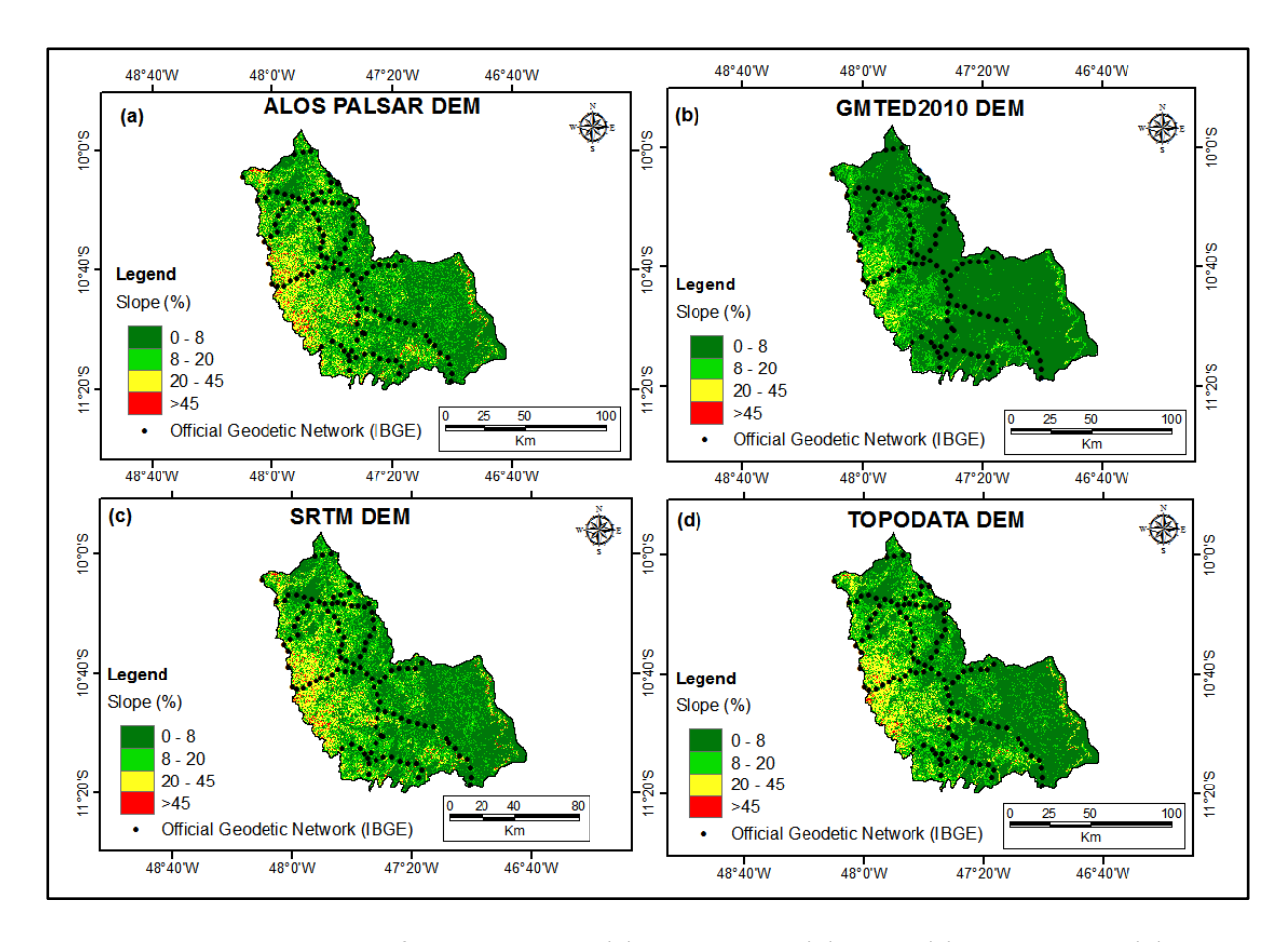


Figure 2.6 – Slope map for ALOS PALSAR (a), GMTED2010 (b), SRTM (c) and Topodata (d)

The spatial distribution of each slope class in the Balsas River watershed can be seen in Table 2.4, where we observe that the four DEM presented approximated values regarding the second slope class (3 to 8%). However, the first class (0 to 3%) shows that the values differ importantly and that SRTM and Topodata presented more similar values in this slope class than the other DEM. Concerning the other slope classes, ALOS PALSAR, SRTM and Topodata presented similar results but the GMTED2010 showed very different results, what was expected, due to its pixel size.

Table 2.4 – Spatial distribution of each slope class of the Balsas River watershed

	ALOS PA	LSAR	GMTED	GMTED2010 SRTM		Topodata		
Slope	Area (Km²)	%	Area (Km²)	%	Area (Km²)	%	Area (Km²)	%
0 to 3%	992.55	8.04	4,103.36	33.22	1,776.15	14.38	2,297.57	18.60
3 to 8%	5,459.72	44.20	5,881.54	47.61	5,155.10	41.73	5,295.32	42.87
8 to 20%	3,879.34	31.41	2,075.17	16.80	3,579.51	28.98	3,222.54	26.09
20 to 45%	1,813.29	14.68	292.36	2.37	1,696.15	13.73	1,454.33	11.77
45 to 75%	200.78	1.63	0.07	0.00	142.65	1.15	82.15	0.67
>75%	6.83	0.06	0.00	0.00	2.94	0.02	0.59	0.00
Total	12,352.50	100.00	12,352.50	100.00	12,352.50	100.00	12,352.50	100.00

In this analysis, no significant correlation coefficient was observed between slope and altimetric error (Table 2.5). Nonetheless, it is possible to notice that the RMSE increases as the slope increases in all DEM except in the ALOS PALSAR DEM.

 ${\sf Table~2.5-Statistical~analysis~of~altimetric~error~regarding~slope~classes}$ 

		•		Ü			
ALOS DEM							
Slope	lope ME (m) MAE (m) RMSE (m) R <sup>2</sup>				Points		
0 to 3%	13.89	13.89	3.81	0.0004	17		
3 to 8%	12.94	13.21	5.03	0.0005	62		
>8%	11.61	11.64	4.71	0.0088	26		
					Σ = 105		
		GMTED2	010 DEM				
Slope	ME (m)	MAE (m)	RMSE (m)	R²	Points		
0 to 3%	12.42	13.24	6.45	0.0000	54		
3 to 8%	13.19	14.59	9.10	0.0014	43		
>8%	13.45	20.96	17.57	0.0278	8		
					Σ = 105		
		SRTIV	I DEM				
Slope	ME (m)	MAE (m)	RMSE (m)	R²	Points		
0 to 3%	14.44	14.44	2.86	0.0005	28		
3 to 8%	12.43	12.52	4.86	0.0175	52		
>8%	12.46	12.61	5.13	0.0206	25		
					Σ = 105		
		Topoda	ita DEM				
Slope	ME (m)	MAE (m)	RMSE (m)	R²	Points		
0 to 3%	14.71	14.71	2.75	0.0250	38		
3 to 8%	13.01	13.29	5.13	0.0003	47		
>8%	8.88	10.01	7.06	0.0024	20		
					Σ = 105		

We also did not find a significant correlation coefficient between altimetric error and altitude, although we have noticed a higher value in R<sup>2</sup> for all assessed DEM considering the altitudes above 550 meters, except for GMTED2010, as can be seen in Table 2.6. Regarding ME and MAE, we observe that all DEM also present the highest values in this same altitude class.

Table 2.6 – Statistical analysis of altimetric error as regarding altitude

Гable 2.6 – Sta	tisticai ana	alysis of altir	netric error a	s regardin	ig altitude		
ALOS PALSAR DEM							
Altitude (m)	ME (m)	MAE (m)	RMSE (m)	R²	Points		
250-350	12.10	12.10	4.21	0.0395	20		
350-450	13.51	13.62	4.56	0.1384	53		
450-550	11.52	11.99	5.92	0.0040	25		
>550	13.48	13.48	2.37	0.2223	7		
					Σ = 105		
		GMTED20	LO DEM				
Altitude (m)	ME (m)	MAE (m)	RMSE (m)	R²	Points		
250-350	11.00	14.34	11.10	0.1037	20		
350-450	12.92	14.40	8.79	0.0002	53		
450-550	12.58	13.36	6.52	0.0092	25		
>550	18.01	18.01	7.73	0.0615	7		
					Σ = 105		
		SRTM [	DEM				
Altitude (m)	ME (m)	MAE (m)	RMSE (m)	R²	Points		
250-350	12.00	12.00	4.00	0.0411	20		
350-450	13.72	13.78	4.45	0.0971	53		
450-550	11.94	12.14	5.36	0.0002	25		
>550	13.86	13.86	1.91	0.3375	7		

					Σ = 105			
Topodata DEM								
Altitude (m)	ME (m)	MAE (m)	RMSE (m)	R²	Points			
250-350	11.45	12.03	5.46	0.0345	20			
350-450	13.47	13.79	5.00	0.0870	53			
450-550	12.18	12.46	6.06	0.0034	25			
>550	14.44	14.44	2.50	0.2060	7			
					Σ = 105			

The interpolated surface of the altimetric error (Figure 2.7) does not show correlation between altimetric error and slope or altitude when we compare it with Figures 2.2 and 2.6. In fact, Figure 2.7 shows very similar surfaces for the SRTM and Topodata DEM and allows us to verify that the highest altimetric errors coincide with the coordinates of the samples from the Brazilian official network in the central area and that negative errors are concentrated in the southwest region of the watershed.

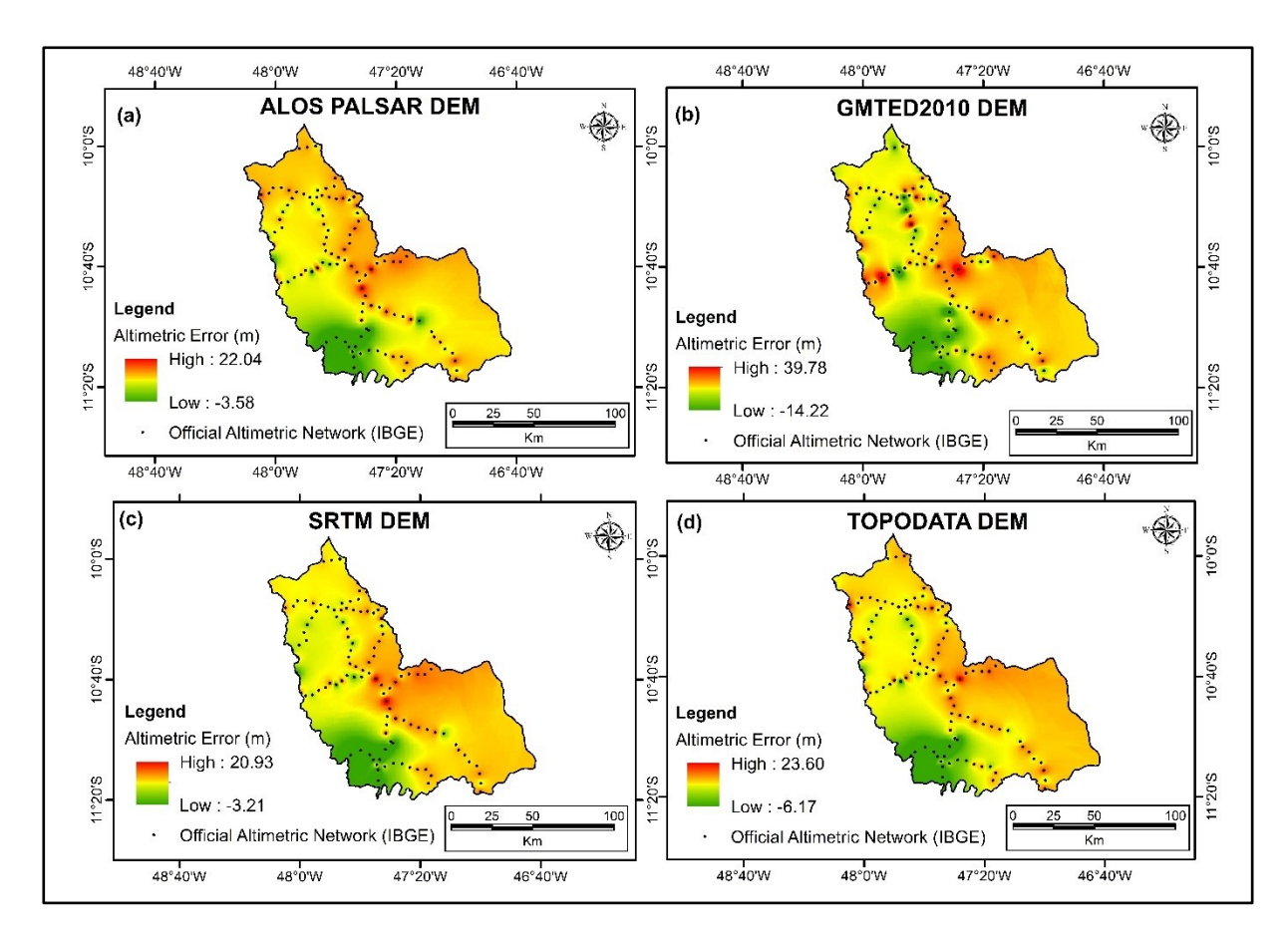


Figure 2.7 – Spatial distribution of the altimetric error for ALOS PALSAR (a), GMTED2010 (b), SRTM (c) and Topodata (d) elaborated through the Inverse Distance Weighting (IDW) method

To classify each DEM product according to the appropriate application scale, we used the altimetric cartographic accuracy standard for digital cartographic product development (Table 2.7), which determines that 90% of point errors collected in the cartographic product must present the same values or less than those predicted in each class.

Table 2.7 – Altimetric Cartographic Accuracy Standard of the Elevation Points and the Digital Terrain Model, Digital Elevation Model and Digital Surface Model for Digital Cartographic Products production (Brazil, 2016)

SCALE	1:25,000		1:50	1:50,000		1:100,000		1:250,000	
PEC	PEC*	RMSE	PEC*	RMSE	PEC*	RMSE	PEC*	RMSE	
Class	(m)	(m)	(m)	(m)	(m)	(m)	(m)	(m)	
Α	2.70	1.67	5.50	3.33	13.70	8.33	27.00	16.67	
В	5.00	3.33	10.00	6.66	25.00	16.66	50.00	33.33	
С	6.00	4.00	12.00	8.00	30.00	20.00	60.00	40.00	
D	7.50	5.00	15.00	10.00	37.50	25.00	75.00	50.00	

<sup>\*90%</sup> of point errors collected in the cartographic product must have the same values or less than the predicted when compared with the ones surveyed in the field by a high-precision method.

Analysing Table 2.8, we can verify that the four assessed DEM can be included in Class B for the 1:100,000 scale and in Class A for the 1:250,000 scale (Table 2.9) because more than 90% of the extracted points from them had altimetric errors of less than 25 meters when compared to the reference points from the Brazilian geodetic network. In addition, the four DEM also presented the RMSE less than 16.66 meters as predicted in Table 2.7.

Table 2.8 – Extracted points from the DEM which had altimetric errors less than 15 and 25 meters

DEM	H <sub>E</sub> < <b>15m</b>		H <sub>E</sub> < <b>25m</b>		
DEIVI	Points	%	Points	%	RMSE (m)
ALOS PALSAR	71	67.6	105	100	4.95
SRTM	69	65.7	105	100	4.76
Topodata	63	60.0	105	100	5.38
GMTED2010	62	59.0	101	96.2	6.54

Table 2.9 – DEM classification according to Altimetric Cartographic Accuracy Standard for Digital Cartographic Products

Scale	ALOS PALSAR	GMTED2010	SRTM	Topodata
1:100,000	В	В	В	В
1:250,000	Α	Α	Α	Α

#### 2.4 DISCUSSION

We assessed the vertical accuracy of the ALOS PALSAR, GMTED2010, SRTM and Topodata DEM and could classify them according to the Brazilian cartographic accuracy standard. Our results showed that more than 90% of the extracted points from the four DEM presented altimetric errors less than 25 meters when compared to the reference points from the Brazilian geodetic network. Indeed, ALOS PALSAR, SRTM and Topodata DEM presented 100% of altimetric errors less than 25 meters and only GMTED2010 DEM presented 3.8% of altimetric errors higher than 25 meters. Therefore, the four analysed DEM demonstrated satisfactory accuracy in providing mappings in scales up to 1:100,000.

Regarding the statistical indicators, we can see that ALOS PALSAR and SRTM demonstrated the best performance since ALOS PALSAR had the lowest ME and MAE, while the SRTM showed the lowest RMSE and the smallest error range. The Topodata product presented slightly larger errors when compared to these two DEM, which can be interpreted as a satisfactory performance since this is a refinement of the SRTM data at 3 arc-seconds (90 meters). On the other hand, the GMTED2010 demonstrated the worst accuracy, probably due to its pixel size (231 meters), even though, it also could be classified in the same accuracy category according to the Brazilian PEC.

According to some studies (Arabameri et al., 2019; Rabby et al., 2020), ALOS PALSAR demonstrated a better performance when compared to SRTM and the Advanced Spaceborne Thermal Emission and Reflection Radiometer (ASTER), but in others, when some specific parameters were compared, the SRTM performance was better than ALOS PALSAR (Andrades Filho & Rossetti, 2012), ASTER and GMTED2010 (Thomas et al., 2014; Thomas et al., 2015). Nonetheless, the Topodata product demonstrated better accuracy in the characterization of

drainage networks and watershed vectors when compared with SRTM and ASTER (Mantelli et al., 2011).

Although our results have indicated compatibility of the four assessed DEM with a scale of 1: 100,000 regarding the Brazilian cartographic accuracy standard, Moura et al. (2014) stated that Topodata, SRTM and ASTER are compatible with the scale of 1:50,000 in watersheds with little rugged relief. But, in watersheds with higher slopes and higher drainage density, their results also showed compatibility with scales up to 1:100,000 (Moura et al., 2014).

The above-mentioned findings may indicate that some terrain physical characteristics might influence the results of the DEM accuracy assessment. Although some studies have found a strong correlation between slope and altimetric error (Gorokhovich & Voustianiouk, 2006; Satgé et al., 2015; Varga & Bašić, 2015), no significant correlation coefficient was observed between these variables in this analysis.

#### 2.5 CONCLUSIONS

The acquisition of three-dimensional data from the Earth's surface in the field is a process that requires appropriate equipment and qualified professionals. Furthermore, this process can be expensive and time-consuming depending on the type of methodology used. In this sense, using DEM is an attractive alternative for many researchers, consequently, it is very important to assess their accuracy to ensure their correct applicability concerning the appropriate use scale. Nevertheless, a limitation for assessing the accuracy of DEM is the absence of accurate data freely available, making fieldwork essential, which makes the assessment process difficult and expensive.

Even though some authors have stated the absence of specific standardized guidelines for DEM accuracy assessment, in Brazil, the Cartographic Accuracy Standard regulates the quality of cartographic products and according to this regulation the four assessed DEM in this study can supply mappings in scales up to 1: 100,000. Regarding the altimetric error, we could not find a significant correlation coefficient with altitude or slope though some authors have found such a correlation in other studies.

A limitation found in this study is that there were few control points from the Brazilian geodetic network inside the Balsas River watershed, and they were badly distributed in the study area because they were located on the banks of the highways. However, the availability of these free data makes possible DEM accuracy assessment through an accurate data analysis without the need for fieldwork. We suggest that future similar studies be based on the accuracy of a specific application as well in the investigation about other factors that may influence altimetric error, such as watershed roughness, vegetal coverage and/or land use.

# 3 ANALYSING THE SPATIAL CONTEXT OF THE ALTIMETRIC ERROR PATTERN OF A DIGITAL ELEVATION MODEL USING MULTISCALE GEOGRAPHICALLY WEIGHTED REGRESSION<sup>2</sup>

Abstract: Many freely available Digital Elevation Models (DEM) have increasingly been used worldwide due to the difficulty in acquiring accurate elevation data in some regions, emphasizing the need to investigate their accuracy and the factors that may influence their uncertainties. We performed an accuracy analysis of the Topodata DEM in the hydrographic region of Uruguay (Brazil) assuming that its vertical accuracy may be related to terrain characteristics. Multiscale Geographically Weighted Regression (MGWR) was applied to investigate the spatial scales over which terrain characteristics affect local variations in altimetric errors. MGWR outperformed Ordinary Least Squares (OLS) and Geographically Weighted Regression (GWR). MGWR results also showed that aspect, curvature, and artificial areas operate at much smaller scales than elevation and have a higher influence in areas with high positive altimetric errors. The model explains about 41% of the total variation of the altimetric error of the Topodata DEM in the study area. Our findings enrich the understanding of the global and local processes affecting the accuracy of the Topodata DEM and shed light on the importance of local terrain characteristics in effective DEM product development.

# **Key policy highlights**

- DEM products provide fundamental information for several research areas.
- OLS, GWR and MGWR were applied to identify the factors explaining the altimetric error of a DEM.
- MGWR investigated the spatial scales over which terrain characteristics affect local variations in altimetric errors.
- MGWR outperformed OLS and GWR proving that terrain characteristics operate at different scales.

<sup>&</sup>lt;sup>2</sup> The text from this chapter has been published in the European Journal of Remote Sensing. https://doi.org/10.1080/22797254.2023.2260092.

#### 3.1 Introduction

Products extracted from Digital Elevation Models (DEM) are an important data source on the physical characteristics of the terrestrial surface since these data are the primary means of visualizing terrain texture and relief classification that should be observed in essential research topics (Xu et al., 2021). DEM products provide fundamental information for several approaches, such as precipitation estimation (Chen et al., 2021; Taheri et al., 2020; Xu et al., 2015), landslide susceptibility (Bui et al., 2020; Bui et al., 2016; Chen & Chen, 2021; Merghadi et al., 2020; Saleem et al., 2019), flood prediction (Sarma et al., 2020; Suliman et al., 2021; Vignesh et al., 2021), and geomorphometric analysis (Abdelkarim et al., 2020; Gorini & Mota, 2016; Lindsay, 2016; Pipaud et al., 2015; Sánchez-Guillamón et al., 2018). Furthermore, they are extremely important in risk assessment of natural disasters (Saleem et al., 2019).

Although traditional methods to generate DEM are expensive and time-consuming (Uysal et al., 2015), Earth's surface analysis is becoming increasingly viable due to the rising availability of DEM products at different spatial resolutions (Drăguţ & Eisank, 2011). Moreover, due to the lack of more accurate three-dimensional data for geographic studies at a regional scale, freely available DEM are frequently used in several scientific applications which evidences the need to investigate the accuracy of DEM products (Liu et al., 2020). Approaches regarding the assessment of DEM quality are usually based on altimetric discrepancies between the DEM and the reference data, which must present reasonable density and be well-distributed in the study area (Polidori & El Hage, 2020). In addition, it is essential that these reference data have greater accuracy than the evaluated DEM to ensure a relevant statistical analysis as well as a spatial error analysis (Polidori & El Hage, 2020).

In recent decades, many technological advances in the creation and in the process of making available DEM products have been made, despite there are not enough specific guidelines yet regarding the assessment of the accuracy nor a perspective of suitability for the use of these products (Mesa-Mingorance & Ariza-López, 2020). In this sense, scale effects modelling has been considered an important research topic since there are not many studies dealing with the potential influence that such effects may have on some factors' modelling related to hydrology, soil science and geomorphology (Chang et al., 2019; Drăguţ & Eisank, 2011). Moreover, mathematical modelling of the predicted DEM error as a function of the landscape characteristics is also a promising research path (Polidori & El Hage, 2020).

Many studies have addressed the vertical accuracy of DEM (Hawker et al., 2019; Hirano et al., 2003; Hladik & Alber, 2012; Wessel et al., 2018; Weydahl et al., 2007) through external and internal quality assessment, i.e., with or without reference data, respectively (Polidori & El Hage, 2020). The vertical accuracy is often assessed through the comparison of the elevation of the DEM product with a reference elevation collected from a greater accuracy source where parameters such as mean, standard deviation and root mean square error (RMSE) are obtained to analyse the elevation discrepancies (Mesa-Mingorance & Ariza-López, 2020; Wise, 2000).

The most common parameter to assess the vertical accuracy of a DEM is the RMSE (Mesa-Mingorance & Ariza-López, 2020) but, it is also possible to use information entropy (Wise, 2012) as well as geomorphometric analyses to measure the quality of a DEM (Pipaud et al., 2015; Szypuła, 2019; Temme et al., 2009). Furthermore, some studies have addressed spatial statistics techniques such as Ordinary Least Squares (OLS) and Geographically Weighted Regression (GWR) to model errors in DEM (Carlisle, 2005; DeWitt et al., 2015; Erdoğan, 2010; Gallay et al., 2010).

OLS is a technique used to estimate the parameters of multiple linear regression models, which is based on the principle of minimizing the sum of squared differences between the observed dependent variable values and the predicted values (Brunsdon et al., 1996; Hutcheson, 2011). OLS assumes that the relationship between variables is constant across the entire study area, disregarding any spatial variations. On the other hand, GWR (Brunsdon et al., 1996; Fotheringham et al., 2002) and MGWR - Multiscale Geographically Weighted Regression (Fotheringham et al., 2017) are both spatial regression techniques that explicitly account for spatial heterogeneity by estimating relationships locally, allowing for spatially varying coefficients. GWR operates at a local scale, where the relationships between variables are estimated for each individual location within the study area, while MGWR simultaneously estimates the relationships at different scales. This allows MGWR to capture variations in relationships at local, regional, and global scales. Thereby, MGWR can model the relationship between the dependent and the independent variables considering the geographic scale at which processes occur, allowing it to differentiate spatial homogeneous and heterogeneous relationships that may influence the dependent variable at different locations (Fotheringham et al., 2017). Hence, it is possible to identify if an explanatory factor of the altimetric error operates locally, regionally, or globally in the study area. However, there is still no evidence of studies that have modelled the pattern of the altimetric error through MGWR.

Our study performs a vertical accuracy analysis using MGWR, aiming to identify the local factors that may explain the altimetric error of the Topodata DEM in the hydrographic region of Uruguay (Brazil), accounting for possible different spatial scales in the relationship between such local factors and the altimetric error. Accordingly, this research study aims to investigate not only if the vertical accuracy of DEM products is related to local terrain characteristics but also if there are spatial variations in the magnitude of those relationships. Additionally, this study aims to determine if the relationships between the terrain characteristics and the altimetric error operate at different spatial scales. Besides MGWR, two additional models were used for comparison purposes, namely OLS and GWR.

Our findings are expected to provide a better understanding of the global and local processes influencing the quality of Topodata products and highlight the importance of terrain characteristics in effective DEM product development, besides shedding light on some limitations of regression modelling applications. Providing a further understanding of the features influencing DEM vertical accuracy may also contribute to improving the applications that rely on the altimetric data extracted from DEM.

### 3.2 MATERIALS

# 3.2.1 Study area

The Uruguay River watershed is approximately 385,000 km<sup>2</sup> with 174,412 km<sup>2</sup> of this area placed in the southern part of Brazil, covering 2% of the national territory, which is named in the hydrographic region of Uruguay (Brazil, 2006). The study area's altimetry ranges from 32 to 1822 meters above sea level (Figure 3.1).

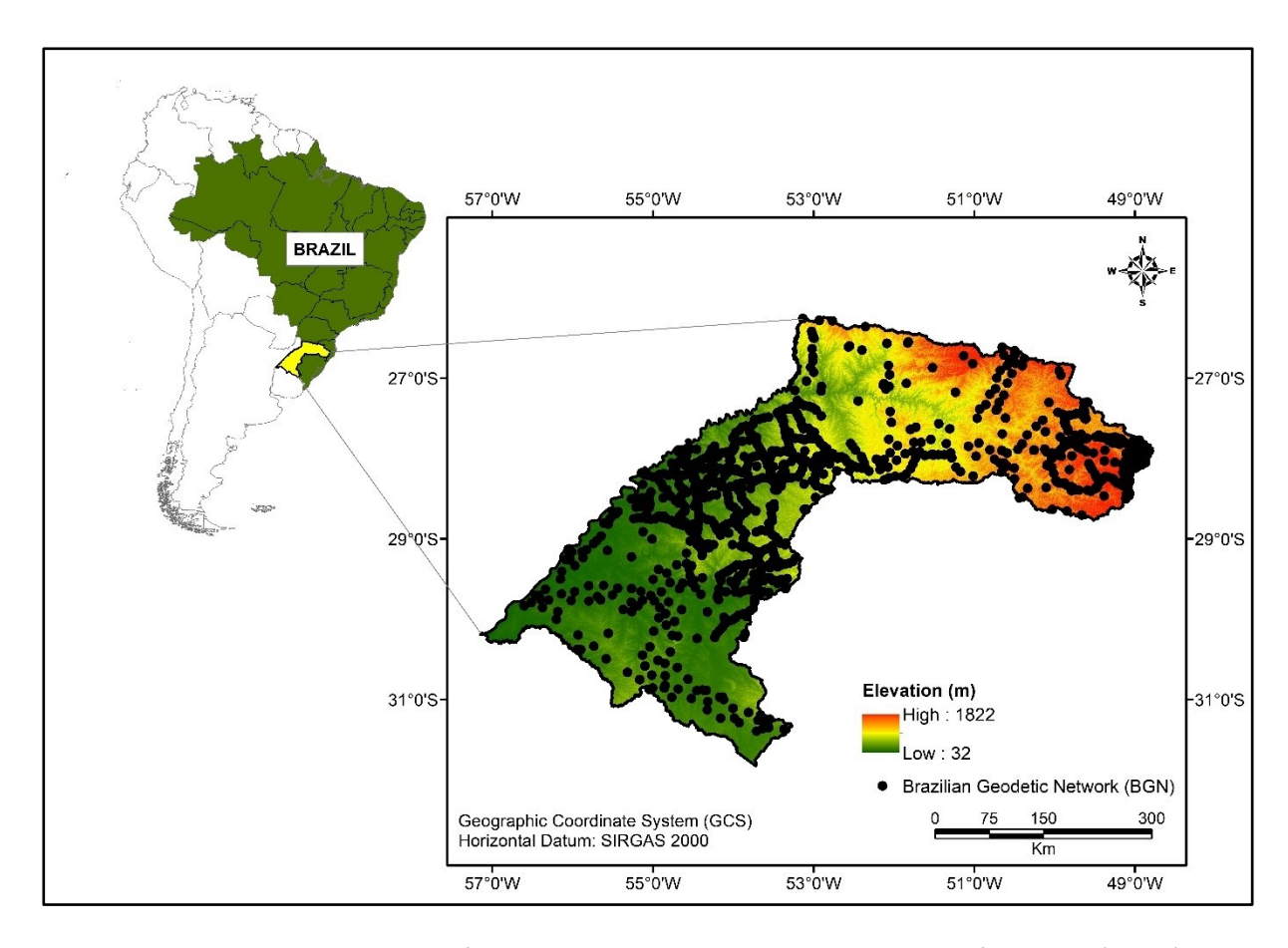


Figure 3.1 – Study area and reference points in the hydrographic region of Uruguay (Brazil)

# 3.2.2 Data and preprocessing

# 3.2.2.1 SRTMGL1v003 DEM and Topodata DEM

Shuttle Radar Topography Mission (SRTM) was released in 2000 onboard the Space Shuttle Endeavour aiming to generate a near-global DEM of the Earth through radar interferometry (NASA, 2013). Initially, SRTM data was made available with a resolution of 1 arc-second for the United States territory and with 3 arc-seconds for other regions of the world. In 2015, the data with full resolution (1 arc-second) was released globally (NASA, 2022). In this context, the Topodata project was developed by the Brazilian National Institute for Space Research (Instituto Nacional de Pesquisas Espaciais - INPE) to refine, through kriging techniques, SRTM data from the resolution of 3 arc-seconds (≈ 90 meters) into 1 arc-second (≈ 30 meters) over the Brazilian territory (Valeriano & Rossetti, 2012). This project also derived geomorphometric data from SRTM products providing information, such as slope, aspect, and curvatures, ready for use by the scientific community (Valeriano, 2008; Valeriano & Rossetti, 2008). Despite there being other DEM with better resolution, SRTM-90 (90-meter pixel) and Topodata are

highly applied in research over the Brazilian territory (Silva et al., 2022). Moreover, Topodata DEM is still widely used due to the unavailability of cartographic products in suitable scales for some Brazilian regions (Ferreira & Cabral, 2022).

Topodata DEM was released in 2008 and had been revised regularly by INPE (INPE, 2008). SRTM datasets most recent version (SRTMGL1v003) eliminated voids that were present in previous versions of SRTM products by using data from ASTER Global Digital Elevation Model (GDEM) Version 2.0, the Global Multi-resolution Terrain Elevation Data 2010 (GMTED2010), and the National Elevation Dataset (NED) (NASA, 2013).

#### 3.2.2.2 Brazilian Geodetic Network

The accuracy analysis in this study is based on official data from the Brazilian Geodetic System (IBGE, 2022a). The Brazilian Geodetic Network (BGN) contains geodesic stations implemented throughout the national territory with essential planimetric, altimetric and gravimetric information used as a reference in positioning activities as well as for correction and verification of Brazilian territory images (IBGE, 2019, 2022a). Most stations are materialized through concrete landmarks with a metal plate on the top, identifying their coordinates, altitudes and gravity obtained by using high-precision geodetic procedures and models (IBGE, 2022a). A total of 1,068 reference points from the BGN are present in the hydrographic region of Uruguay (Figure 3.1) georeferenced to the Geocentric Reference System for the Americas (SIRGAS2000 - horizontal datum) and Imbituba (vertical datum). It is important to mention that the Imbituba datum is defined by the calculated middle level of the sea with data from a tide gauge station and then propagating it throughout the Brazilian territory by high-precision geometric levelling (IBGE, 2019). The main characteristics of BGN, SRTM and Topodata DEM are shown in Table 3.1.

Table 3.1 – Main characteristics of BGN (IBGE, 2019), SRTM (NASA, 2013) and Topodata DEM (Garofalo & Liesenberg, 2015; Miceli et al., 2011; Valeriano, 2008)

DEM	Coordinate System	Horizontal Datum	Vertical Datum	Pixel Size	Radiometric Resolution	Extension
BGN	Geographic	SIRGAS2000*	Imbituba***	-	-	SHP
SRTMGL1 v003	Geographic	WGS 84**	EGM-96****	30 meters (1 arc-second)	16 bits (signed integer)	HGT
Topodata	Geographic	WGS 84**	EGM-96****	30 m (1 arc-second)	32 bits (floating point)	TIF

<sup>\*</sup>Sistema de Referência Geocêntrico para as Américas (Geocentric Reference System for the Americas); \*\*World Geodetic System 1984; \*\*\* Brazilian official vertical datum; \*\*\*\* Earth Gravitational Model 1996.

# 3.2.2.3 Independent variables

Aiming to investigate the factors that may explain the altimetric error of Topodata DEM in the hydrographic region of Uruguay, the following candidate explanatory variables were chosen according to previous studies: altitude/elevation (Das et al., 2016; González-Moradas & Viveen, 2020; Szypuła, 2019), aspect (Dong & Shortridge, 2019; Gorokhovich & Voustianiouk, 2006; Leon et al., 2014; Sharma et al., 2021; Szypuła, 2019), curvature (plan/profile) (Leon et al., 2014; Sharma et al., 2021; Szypuła, 2019), distance to rivers (Mahalingam & Olsen, 2016; Yap et al., 2019), drainage density (Das et al., 2016; Shaikh et al., 2021), land use/land cover (LULC) (Dong & Shortridge, 2019; Leon et al., 2014; Satgé et al., 2015; Yap et al., 2019), relative relief (Das et al., 2016; Ganie et al., 2023), roughness (Habib, 2021; L. Li et al., 2020; Schwendel & Milan, 2020), slope (Das et al., 2016; Dong & Shortridge, 2019; González-Moradas & Viveen, 2020; Gorokhovich & Voustianiouk, 2006; Habib, 2021; Leon et al., 2014; L. Li et al., 2020; Satgé et al., 2015; Sharma et al., 2021; Szypuła, 2019; Yap et al., 2019), terrain ruggedness index (TRI) (Dong & Shortridge, 2019; Leon et al., 2014), topographic position index (TPI) (Dong & Shortridge, 2019; Leon et al., 2014) and vector ruggedness measure (VRM) (Leon et al., 2014; Pipaud et al., 2015).

The variables aspect, curvature (plan/profile), elevation, relative relief, roughness, slope, TPI, TRI and VRM were derived from the SRTM DEM (NASA, 2013) to ensure that their values are independent of the altimetric error derived from the Topodata DEM. If we used the same DEM to derive the explanatory variables, then their values would be a function of the values of the dependent variable. Hence, the regression model would not be correctly specified (i.e., it would be an inappropriate model). On the other hand, distance to rivers and drainage density were derived from the drainage data of the National Water and Sanitation Agency (*Agência Nacional de Águas e Saneamento Básico - ANA*) (ANA, 2022).

Aspect measures the orientation of the slope for each location on which the compass direction ranges from 0° to 360° clockwise, where 0°, 90°, 180° and 270° correspond to north, east, south, and west, respectively (Kaliraj et al., 2015; Lei et al., 2022).

Curvature is one of the most relevant parameters to be considered when analysing the land surface topography (Krebs et al., 2015). Curvature refers to a morphological measure of the terrain topography, where positive values mean that the surface is upwardly convex, negative values reveal an upwardly concave whereas zero values indicate that the surface is flat (Lee & Sambath, 2006). Through different methodologies, it is possible to compute the curvature in the horizontal plane (plan curvature) or in the vertical plane (profile curvature) for every single cell of a digital elevation model (DEM) (Krebs et al., 2015; Ohlmacher, 2007).

It is crucial to consider functional distances based on hydrology in environmental analysis since the physical attributes of the stream network offer valuable insights into environmental conditions, especially at unobserved locations (Peterson et al., 2007). In this sense, distance to rivers was also included in this analysis.

Drainage density is a key characteristic of natural landscapes and serves as a fundamental indicator that reflects local climate, topography, geological composition, and other pertinent variables (Tucker et al., 2001). It is defined by the length of rivers per unit of area (Horton, 1932).

Relative relief is a metric used for analysing the morphological features of the terrain, given by the difference value between the highest and lowest altitude in a region (Das et al., 2016; Mustak et al., 2012; Smith, 1935).

Roughness denotes the slope variability of terrain and reveals the undulating nature of its relief (Samadrita Mukherjee et al., 2013). Higher roughness values are typical of hilly or rocky areas, meaning that these places have increased surface runoff, reduced water percolation, and groundwater recharge (Mukherjee & Singh, 2020).

The slope is useful in characterizing and delimiting geomorphological units and regions since it represents the variation in terrain gradients, where lower values indicate flatter terrain and higher values indicate steeper terrain (IBGE, 2009).

The Terrain Ruggedness Index (TRI) computes the sum variation in elevation between a cell and its neighbouring cells within a DEM, providing a quantitative magnitude estimative of the topographic heterogeneity of an area (Riley et al., 1999).

The Topographic Position Index (TPI) evaluates the elevation of each cell in a DEM relative to the average elevation of a given neighbourhood, with positive values indicating elevations higher than the surrounding average (ridges), negative values indicating lower elevations (valleys), and values close to zero signifying either flat areas or regions with a consistent slope (Weiss, 2001).

The Vector Ruggedness Measure (VRM) gauges the ruggedness of the terrain by assessing the variability in the three-dimensional orientations of grid cells within a given neighbourhood (Arosio et al., 2023). VRM offers a more direct measurement of terrain heterogeneity less dependent on slope than TRI, allowing the treatment of terrain components as distinct variables during the landscape analysis (Sappington et al., 2007).

The LULC mapping was performed by the Brazilian Institute of Geography and Statistics (Instituto Brasileiro de Geografia e Estatística - IBGE) based on images from the Moderate-Resolution Imaging Spectroradiometer (MODIS) sensor and from LANDSAT-5 and LANDSAT-7 satellites, with a spatial resolution of 250m, 30m and 30m, respectively. In addition, the technical review process also involved the incorporation of polygons from the vegetation maps and auxiliary information from the Continuous Cartographic Base of Brazil at a scale of 1:250,000 (IBGE, 2017, 2022b). Since SRTM data were collected in the year 2000, we use the LULC data from the same year trying to be as faithful as possible to the reality of the terrestrial

surface at the mission's time. The following LULC classes are found in the hydrographic region of Uruguay (IBGE, 2017):

- **1. Artificial area** characterized by urban use, structured by buildings and road systems, where non-agricultural artificial surfaces predominate.
- **2. Agricultural area** characterized by temporary and permanent crops, irrigated or not, with the land used for food production, fibre, and agribusiness commodities. It includes all cultivated land, which may be planted or fallow, and cultivated wetlands. It can be represented by heterogeneous agricultural zones or extensive areas of plantations.
- **3. Pasture** area intended for the grazing of cattle and other animals, with cultivated herbaceous vegetation or natural grassland vegetation, both presenting high-intensity anthropic interference.
- **4. Mosaic of agriculture and forest remnants** area characterized by the mixed occupation of agriculture, pasture and forestry associated with forest remnants. Other plant formations (herbaceous and shrubby) may occur to a lesser extent.
- **5. Forestry** area characterized by forest plantations of exotic and/or native species as monocultures.
- **6. Forest vegetation** area occupied by forests. Trees taller than 5 meters are considered forest formations, including areas of dense forest, open forest, and seasonal forest, in addition to the mixed ombrophiles forest.
- **7. Grassland** area characterized by natural grassland vegetation subject to grazing and other low-intensity anthropic interference.
- **8. Mosaic of anthropic areas and grassland** area characterized by the mixed occupation of agriculture, pasture and/or forestry with remnants of grassland vegetation. Arboreal plant formations may occur to a lesser extent proportion.
- **9. Water body** It includes all inland waters such as rivers, streams, canals, and other linear bodies of water. It also encompasses naturally closed bodies of water (natural lakes) and artificial reservoirs (artificial water dams built for irrigation, flood control, water supply and

electricity generation). Figure 3.2 and Table 3.2 show the spatial distribution of each LULC class.

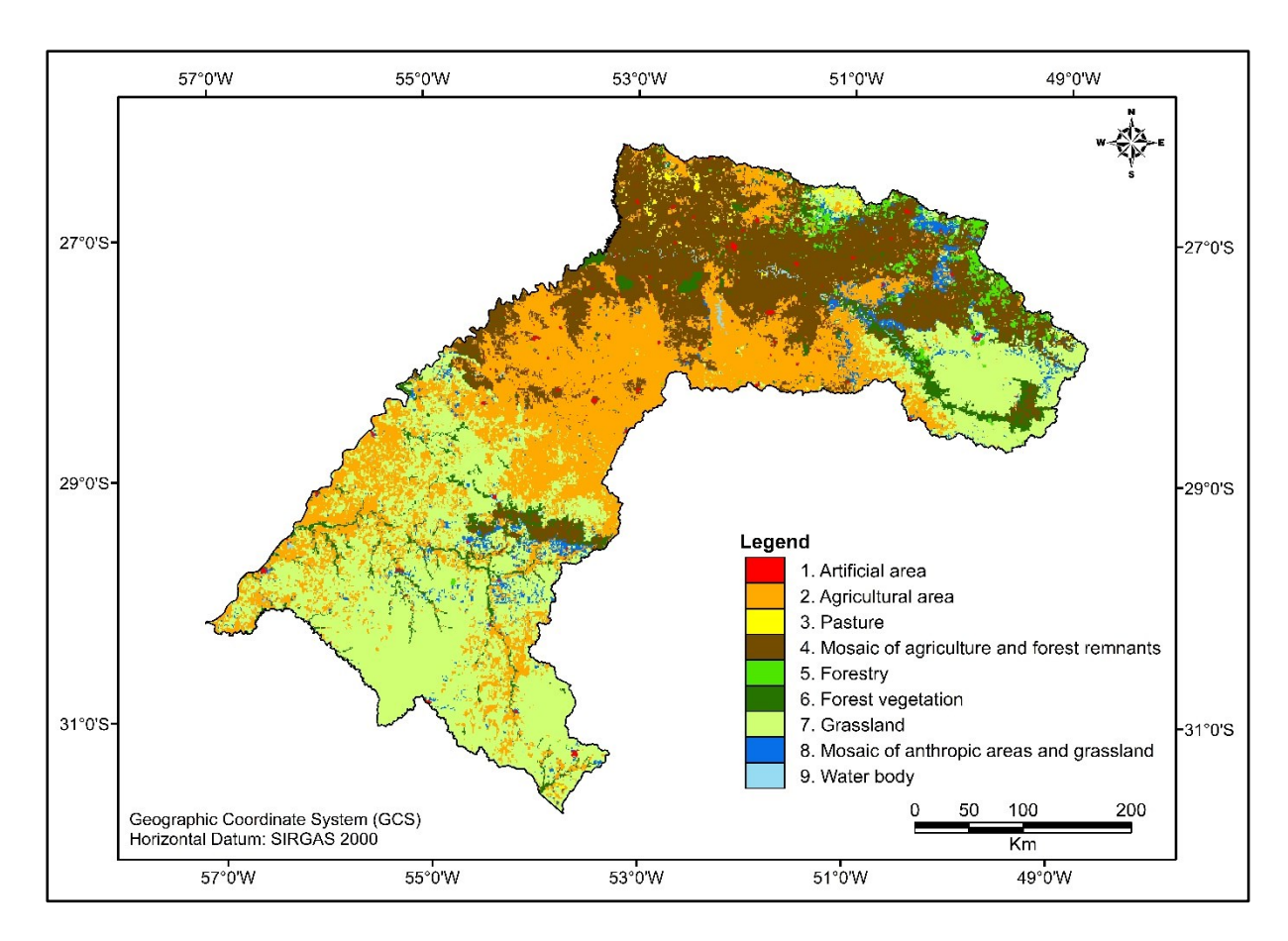


Figure 3.2 – LULC in the hydrographic region of Uruguay

Table 3.2 – Spatial distribution of LULC classes in the hydrographic region of Uruguay

LULC Classes	Area (km²)	Area (%)
Grassland	59,715.43	34.24
Agricultural area	54,391.06	31.19
Mosaic of agriculture and forest remnants	42,126.07	24.15
Forest vegetation	7,922.46	4.54
Mosaic of anthropic areas and grassland	5,081.91	2.91
Forestry	2,751.47	1.58
Pasture	928.31	0.53
Artificial area	783.03	0.45
Water body	712.26	0.41
Total	174,412.00	100.00

To include the LULC classes in the regression modelling, it was necessary to consider an area around each reference point from the BGN. For this purpose, we considered the average distance parameter obtained through the "Calculate Distance Band from Neighbour Count" tool (ArcGIS Desktop software - version 10.8.2) which returns the average distance to the N nearest neighbour (Esri, 2022). Since this result was 5,438 meters, we defined the buffer radius value as 5,500 meters in this analysis. Then, the independent variables of the regression models were computed as the area of each LULC class inside the buffer at each location. This approach guaranteed that the scale of analysis used to compute the independent variables derived from the LULC classes was the same, regardless of the spatial distribution of the BGN points which are not regularly distributed.

#### 3.2.3 Methods

SRTM and Topodata DEM are referenced to the EGM-96 geoid. So, we had to compute the geoidal undulation through the "Geoid Height Calculator" (UNAVCO, 2022) to transform their original geoidal into ellipsoidal altitudes (WGS 84) (Elkhrachy, 2018; Orlando, 2019). Then, it was necessary to convert these ellipsoidal altitudes into physical altitudes compatible with the Brazilian vertical datum (Imbituba) (Bettiol et al., 2021; Rodrigues et al., 2011) by using the hgeoHNOR2020 model (IBGE, 2019). We also had to convert the SRTM and Topodata

horizontal data from WGS 84 into the Brazilian official horizontal datum (SIRGAS2000) through ArcGIS Desktop software – version 10.8.2.

To derive the altimetric errors, we followed the methodology applied by Satge et al. (2016) and Shean et al. (2016). Negative altimetric errors mean that the DEM analysed overestimates the elevation and positive errors underestimate the elevation at each verified point (Brasington et al., 2003; Holmes et al., 2000).

Terrain analysis was carried out by generating maps of the following input candidate explanatory variables: aspect, curvature, distance to rivers, drainage density, roughness, relative relief, slope, TPI, TRI and VRM. Then, statistical analysis was made through the accuracy indicators calculation (Moura et al., 2014; Satge et al., 2016; Shean et al., 2016), namely the altimetric error ( $A_E$ ) (1), mean error (ME) (2), mean absolute error (MAE) (3), and root mean square error (RMSE) (4).

$$A_{E} = A_{REF} - A_{DEM} \tag{1}$$

$$ME = \frac{1}{n} \sum_{i=1}^{n} (A_{REF} - A_{DEM})$$
 (2)

MAE = 
$$\frac{1}{n} \sum_{i=1}^{n} |A_{REF} - A_{DEM}|$$
 (3)

$$RMSE = \sqrt{\frac{1}{n} \sum_{i=1}^{n} (A_E - ME)^2}$$
 (4)

where  $A_{REF}$  is the altitude of the reference point from the BGN,  $A_{DEM}$  is the altitude extracted from Topodata DEM, and n is the number of reference points.

The MAE is a statistical measure that computes the average absolute difference between the value considered the true (BGN) and the value extracted from the Topodata DEM. The RMSE measures the uncertainty in the computed values, defining the degree of correspondence between the reference values and those extracted from the DEM. Thus, lower MAE and RMSE values indicate better results (Rawat et al., 2019).

We performed the Exploratory Spatial Data Analysis (ESDA) through Voronoi tessellation, Hot Spot Analysis (Getis & Ord, 1992), and Local and Global Moran's I statistics (Anselin, 1995; Moran, 1950). Finally, the altimetric error modelling was performed using OLS, GWR (Brunsdon et al., 1996; Fotheringham et al., 2002) and MGWR (Fotheringham et al., 2017) on the 1,068 reference points from the BGN (Figure 3.1). A 5% significance level was considered in all statistical tests, otherwise stated.

Voronoi tessellation is a concept proposed by Georgy Voronoi in 1907 based on a computational geometry data structure that has been applied in many scientific areas (Kastrisios & Tsoulos, 2018). Voronoi maps or Voronoi diagrams are built from polygons generated around a sample point. Each Voronoi polygon is obtained by intersecting perpendicular bisectors of adjacent points, where the nearest neighbour of any point inside the polygon is the sample point (i.e., the generator of the polygon) (Nene & Nayar, 1997; Safar, 2005).

Hot spot analysis is a spatial analysis technique used to identify statistically significant clusters of high (hot spots) or low values (cold spots) within a dataset using the Getis-Ord Gi\* statistic (Getis & Ord, 1992).

The Global Moran's I is an inferential statistic used to measure the spatial autocorrelation in a dataset and to test whether the observed spatial pattern in the dataset is randomly distributed (null hypothesis) or spatially autocorrelated (alternative hypothesis). A significant positive index reveals evidence of spatial clustering of similar values, and a negative one provides evidence of a dispersion pattern of dissimilar values (Moran, 1950; Prasannakumar et al., 2011). The Local Moran's I examines the significance of local spatial autocorrelation by calculating the Moran's I statistic for each location using neighbouring values to identify local clusters or spatial outliers (Anselin, 1995). Clusters with high or low values are defined as high-high (HH) or low-low (LL), respectively, and correspond to statistically significant positive spatial autocorrelation. A high-low (HL) outlier corresponds to a high value correlated with surrounding low values, and a low value correlated with surrounding high values is defined as a low-high (LH) outlier. Spatial outliers correspond to statistically significant negative spatial autocorrelation (Anselin et al., 2007).

OLS, GWR and MGWR are linear regression models, but each one operates at different spatial scales and makes different assumptions regarding the spatial heterogeneity of the data set. OLS is a global model assuming a single coefficient to explain the relationship between each explanatory and the altimetric error in the whole study area, whereas GWR and MGWR are local regression models that allow the coefficients to vary in space. Moreover, MGWR also allows each independent variable to adopt a different spatial scale of analysis.

ArcGIS Desktop software (version 10.8.2) was used to run the ESDA and OLS analysis. We investigated all possible combinations of the 22 independent variables in 539,909 exploratory OLS models considering their statistical significance, the variance inflation factors (VIF), and the models' Adjusted R<sup>2</sup>. The OLS model which has presented the highest Adjusted R<sup>2</sup>, without multicollinearity issues, included four significant variables: aspect  $(X_1)$ , curvature  $(X_2)$ , elevation  $(X_3)$  and LULC\_1 (artificial area)  $(X_4)$ . These variables were then included in the GWR and MGWR models that were estimated using the MGWR 2.2 software (Oshan et al., 2019).

All variables in the MGWR model were standardized to increase the interpretability of the bandwidths of the spatial kernel. An adaptive bisquare kernel was applied in both GWR and MGWR models as the distance-weighting function to control the optimal number of nearest neighbours to be included in the local model fitting (5) (Fotheringham et al., 2017):

$$w_{ij} = \left[1 - (d_{ij}/b_i)^2\right]^2 \text{ if } d_{ij} < b_i; \ w_{ij} = 0 \text{ otherwise}$$
 (5)

where  $w_{ij}$  is the weight between points i and j,  $d_{ij}$  is the Euclidean distance between points i and j, and the bandwidth  $b_i$  is the distance from focal point i to its  $M^{th}$  nearest neighbor. The optimal number of neighbours (M) is determined by the lowest corrected Akaike's Information Criterion (AICc) that is obtained from multiple comparisons. The MGWR model is formulated in Equation 6.

$$Y_{i} = \beta_{bw0}(u_{i}, v_{i}) + \beta_{bw1}(u_{i}, v_{i})X_{i1} + \beta_{bw2}(u_{i}, v_{i})X_{i2} + \beta_{bw3}(u_{i}, v_{i})X_{i3} + \beta_{bw4}(u_{i}, v_{i})X_{i4} + \varepsilon_{i}$$
(6)

where bwk denotes the specific optimal bandwidth used in the calibration of the intercept and  $k^{th}$  conditional relationship (k=1,...,4), and ( $u_i,v_i$ ) are location coordinates for each focal point i (i=1,...,1068). Model diagnostics and inference-related diagnostics are computed for local parameter estimates (Fotheringham et al., 2019; Yu et al., 2020).

In the GWR model, the notation bwk was removed because the optimal bandwidth used is the same for the intercept and all k conditional relationships. That notation was also removed from the OLS model, as well as the  $(u_i, v_i)$  location coordinates because the OLS (global) model is specified using a single regression equation: the  $\beta_k$  parameters (k=0,1,...,4) are the same for all locations and they are estimated using the whole data set. For further details see Fotheringham et al. (2002).

#### 3.3 RESULTS

#### 3.3.1 Statistical analysis

The altimetric errors of the Topodata DEM range from –36.68 to 39.23 meters, and 75% of them are smaller than 1.22 meters (Table 3.3). There is very a strong correlation between the elevations extracted from SRTM and Topodata DEM when they are compared with the reference points from the BGN as the coefficient of determination (R2) of a simple linear regression is higher than 0.99 in both cases (Appendix A1/A2).

Table 3.3 – Statistical accuracy indicators of the Topodata DEM

Indicators	A <sub>E</sub> min	A <sub>E</sub> max	ME	MAE	RMSE	ER*	Q1**	Q2***	Q3****
(m)	-36.68	39.23	-0.73	4.26	6.46	75.91	-3.73	-1.48	1.22

<sup>\*</sup>Error range; \*\* 1st quartile; \*\*\* 2<sup>nd</sup> quartile (median); \*\*\*\* 3rd quartile.

The histogram indicates that the altimetric errors are negatively biased (overestimated) which is reinforced by the median value already shown in Table 3.3. Despite that, they present a distribution a little close to a normal curve (Appendix A3).

The boxplots of the elevation differences are shown in Appendix A4, where it is possible to notice that the SRTM and Topodata elevation are very similar to the BGN altitudes and that more than 50% of the altitudes are below 500 meters, an expected fact since Brazil is considered a low-lying country being 41% of its territory below 200 meters and barely 7% above 800 meters (Alvares et al., 2013). Even though it can be observed in Appendix A4 that almost 25% of the point altitudes are above 800 meters.

The altimetric errors are higher in areas with slopes above 30% (Appendix B1). Furthermore, we observe that the MAE and the RMSE increase as the slope also increases. Likewise, the altimetric errors are higher in places where the elevation is higher than 1,200 meters (Appendix B2), despite the altimetric errors being also higher in regions where elevation is between 900 and 1,200 meters when compared with places lower than 900 meters. Regarding the LULC, the classes that presented the highest altimetric errors were 'forest vegetation' and 'artificial area' (Appendix B3). The Pearson's correlation coefficient between elevation and altimetric error is approximately 0.22. The correlation matrix of all the candidate explanatory variables (Appendix C) shows that some of them are significantly correlated with each other, such as relative relief, VRM, and TPI.

# 3.3.1.1 Spatial effects in altimetric errors

The Voronoi map of the altimetric error shows that most samples (82%) present altimetric errors between –6.46 and 6.46 meters and that they are evenly distributed (Figure 3.3). There is no apparent trend of the altimetric error over the study area.

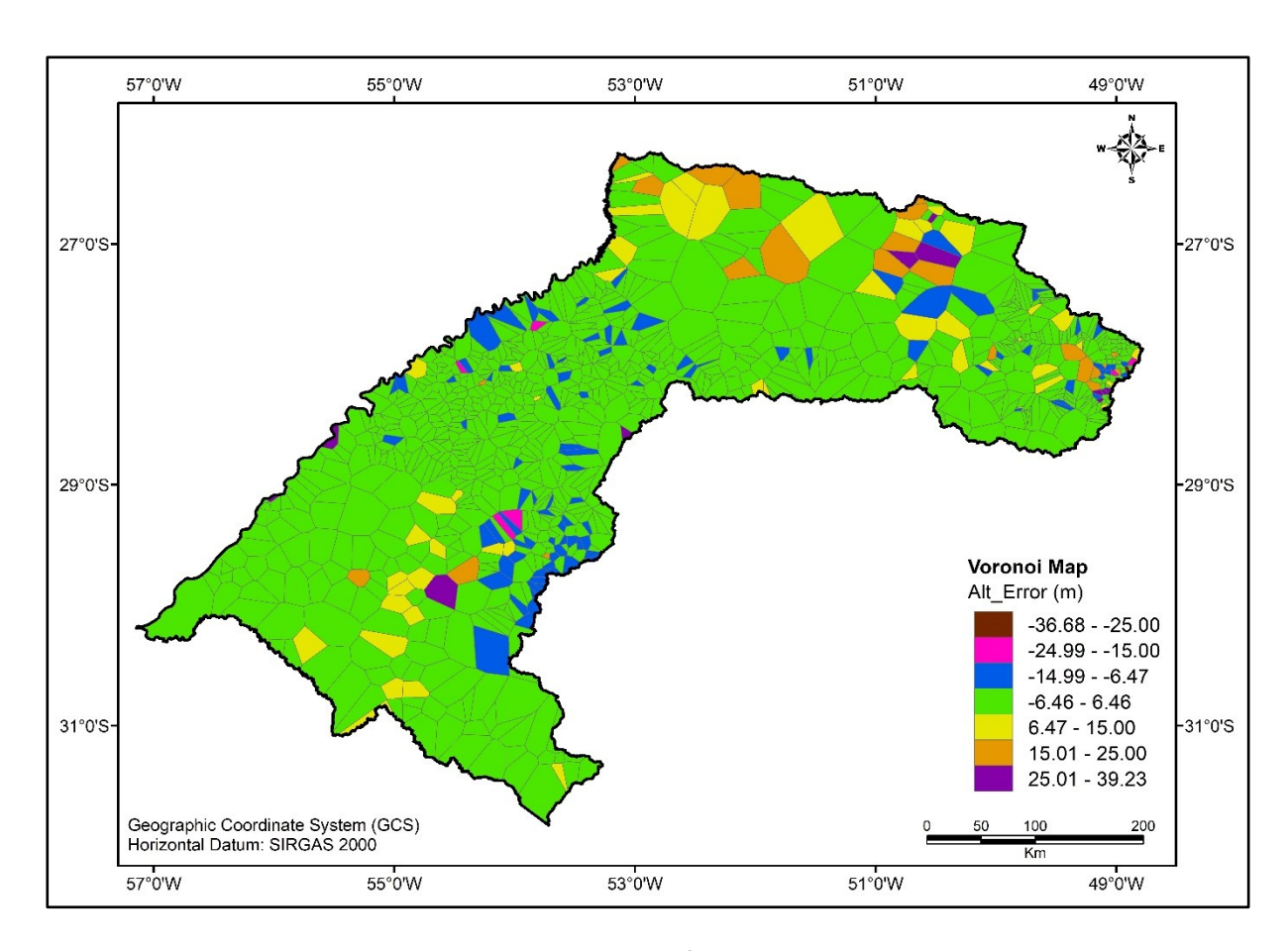


Figure 3.3 – Voronoi map of the altimetric error

The Global Moran's I statistic revealed that the altimetric error did not have a significant spatial autocorrelation (index  $\approx$  0.02; p-value = 0.98), thus the altimetric error pattern does not appear to be significantly different from random.

Anselin's Local Moran's I, represented in Figure 3.4a, shows that 23 of the 1,068 points (≈ 2%) have significant positive (15 high-high and 3 low-low clusters) and negative (3 low-high and 2 high-low outliers) spatial autocorrelation. The high-high clusters (high altimetric errors surrounded by high altimetric errors) are in the upper watershed course, and 2 of the 3 low-low clusters (low altimetric errors surrounded by low altimetric errors) are in the middle watershed course. Figure 3.4a also shows that 3 low-high outliers (low altimetric errors surrounded by high altimetric errors) are in the upper watershed course whereas there is 1 high-low outlier in the upper watershed course and 1 in the middle watershed course.

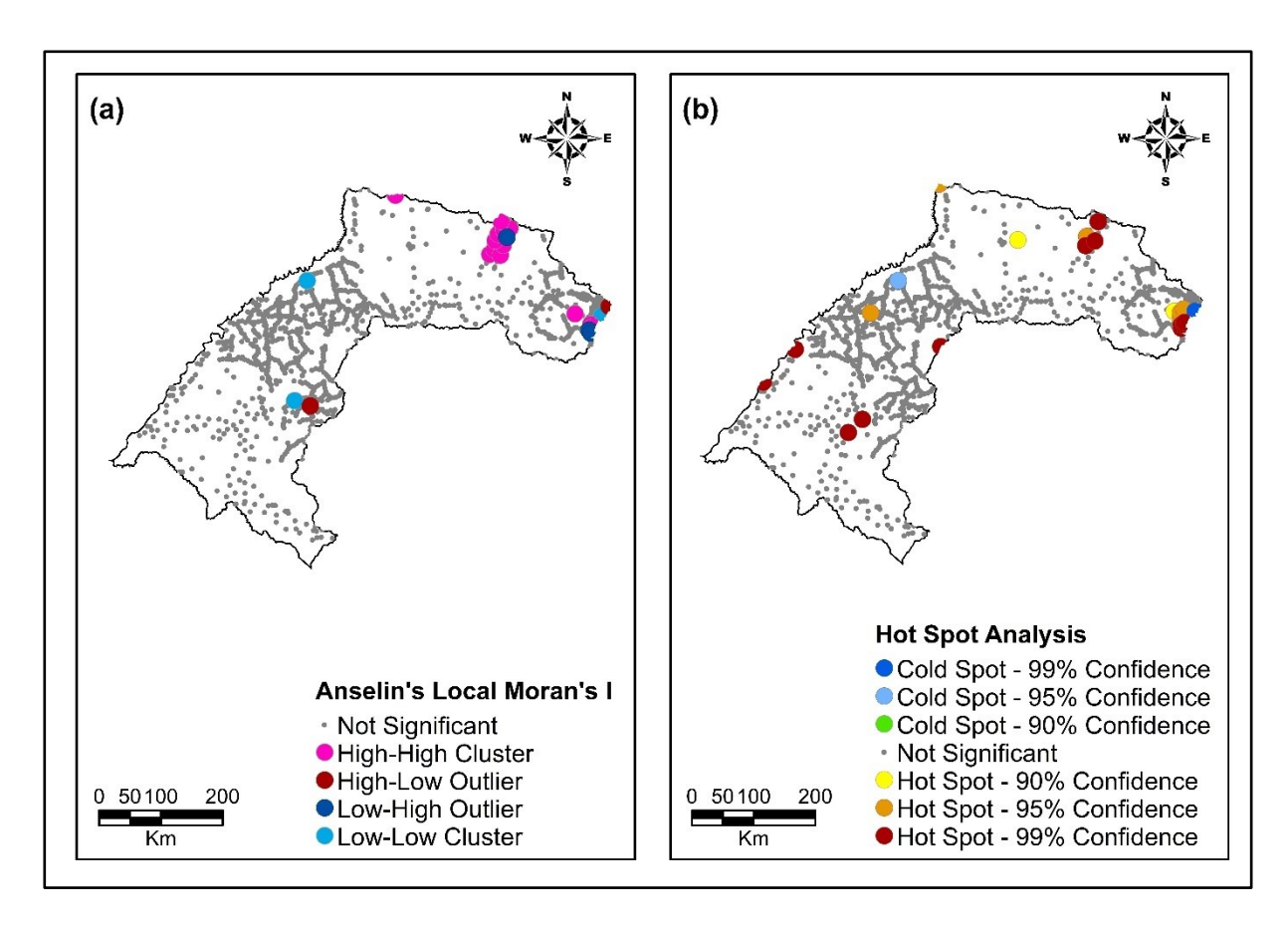


Figure 3.4 – Local Moran's I statistic (a) and Hot Spot Analysis (b) of the altimetric error

Hot Spot Analysis (Getis–Ord Gi\* statistic) reveals both high altimetric errors (hot spot) and low altimetric errors (cold spot) values clustered spatially (Figure 3.4b). In this analysis, results demonstrate the existence of 7 hot spots in the upper region, 5 in the middle and lower region of the watershed at the 1% significance level, 6 in the upper and 1 in the middle part of the watershed at the 5% significance level, and 2 in the upper region of the watershed at the 10% significance level. In addition, this analysis also shows cold spots in the upper region (3 points) and 1 in the middle region of the watershed at 1% and 5% significance levels, respectively (Figure 3.4b).

# 3.3.2 Models' performance and diagnostics

# **3.3.2.1** OLS results

The summary of OLS results in Table 3.4 shows that all variables have a statistically significant coefficient. Furthermore, the low VIF values indicate that there is no evidence of redundancy among the explanatory variables.

Table 3.4 – Parameter estimates for the OLS model

Variable	Coefficient	Robust standard error	Robust t-value	Robust p-value	VIF
Intercept	-1.042677	0.399711	-2.608579	0.009213*	
Aspect	-0.011987	0.001704	-7.034715	0.000000*	1.003166
Curvature	4.057187	0.702850	5.772483	0.000000*	1.012770
Elevation	0.003335	0.000616	5.411528	0.000000*	1.010463
LULC_1 (artificial area)	0.000000	0.000000	3.542069	0.000429*	1.001225

<sup>\*</sup>Statistically significant coefficient

#### 3.3.2.2 GWR and MGWR results

Results of the MGWR model executed with the same variables as the OLS and GWR models show an improvement of the proposed model since it had a higher Adjusted R<sup>2</sup> (0.41) and a lower AICc (2,602.14) than the OLS and GWR models (Table 3.5). It was also noticed a decrease in the residual sum of squares (RSS).

Table 3.5 – Metrics of OLS, GWR and MGWR models

	R <sup>2</sup>	Adj. R <sup>2</sup>	AIC	AICc	RSS
OLS	0.18	0.18	-	6,812.44	873.921
GWR	0.40	0.35	2,639.44	2,651.28	642.014
MGWR	0.47	0.41	2,577.98	2,602.14	571.794

Given the spatially varying nature of MGWR, the map of the Local R<sup>2</sup> (Figure 3.5a) highlights the areas where the local regressions have a better goodness-of-fit and provides insights on the locations where important variables may be missing. The Local R<sup>2</sup> ranges from 0.18 to 0.74

(Figure 3.5a). Low values of the Local R<sup>2</sup> in the flatter regions located in the middle of the study domain indicate that other factors may affect the altimetric error besides aspect and elevation, which have significant coefficients in that region (Figure 3.6a and Figure 3.6c). The Local R<sup>2</sup> was higher than 0.5 in approximately 25% of the local regressions obtained with the MGWR model (Table 3.6). These areas, where the Local R<sup>2</sup> ranges from 0.50 to 0.74, overlap with the areas where the curvature presents significant local coefficients (Figure 3.6b). Therefore, the inclusion of curvature contributed to improving the goodness-of-fit of the MGWR model in the northern and southern parts of the study domain.

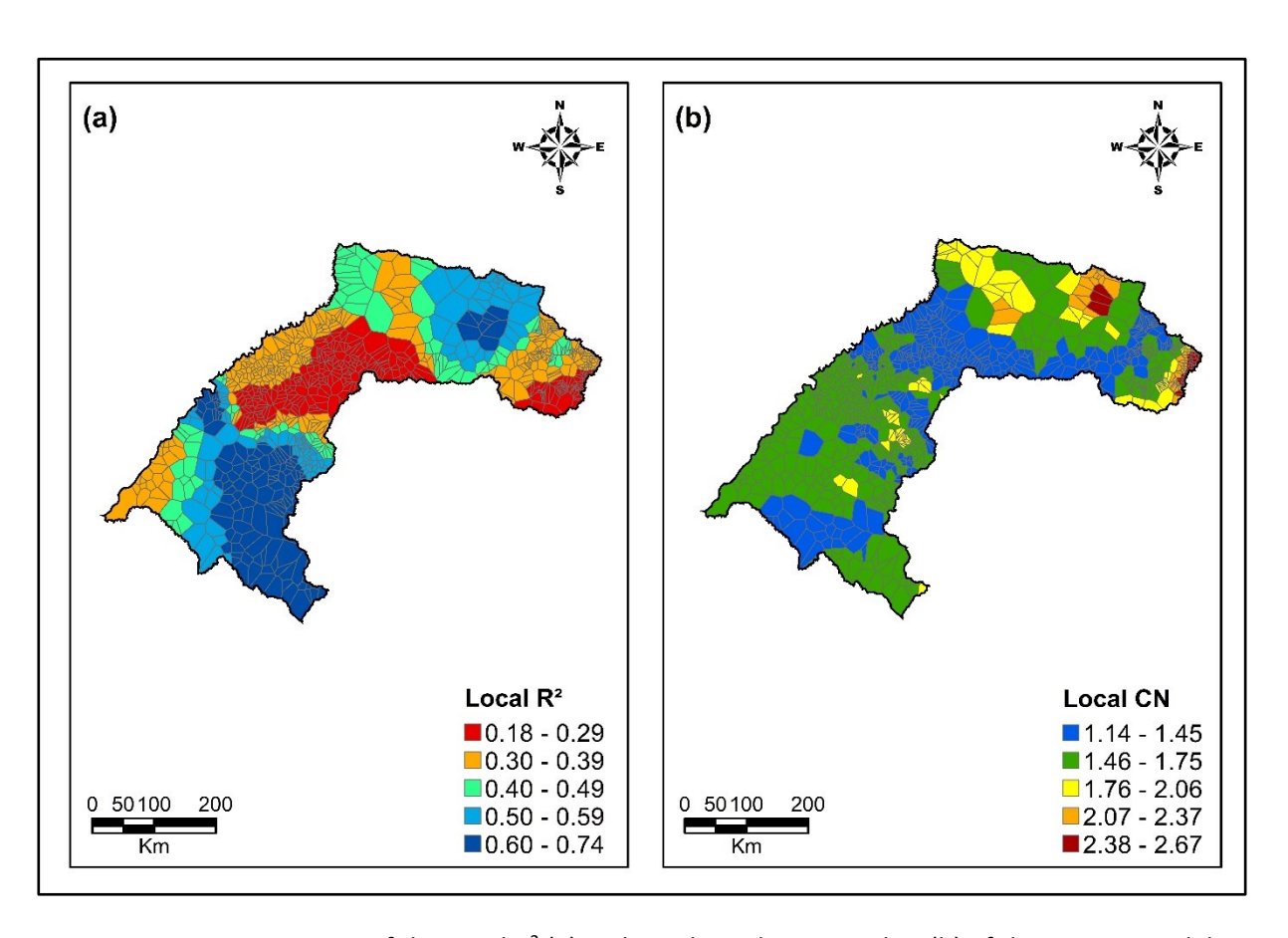


Figure 3.5 – Voronoi map of the Local R<sup>2</sup> (a) and Local Condition Number (b) of the MGWR model

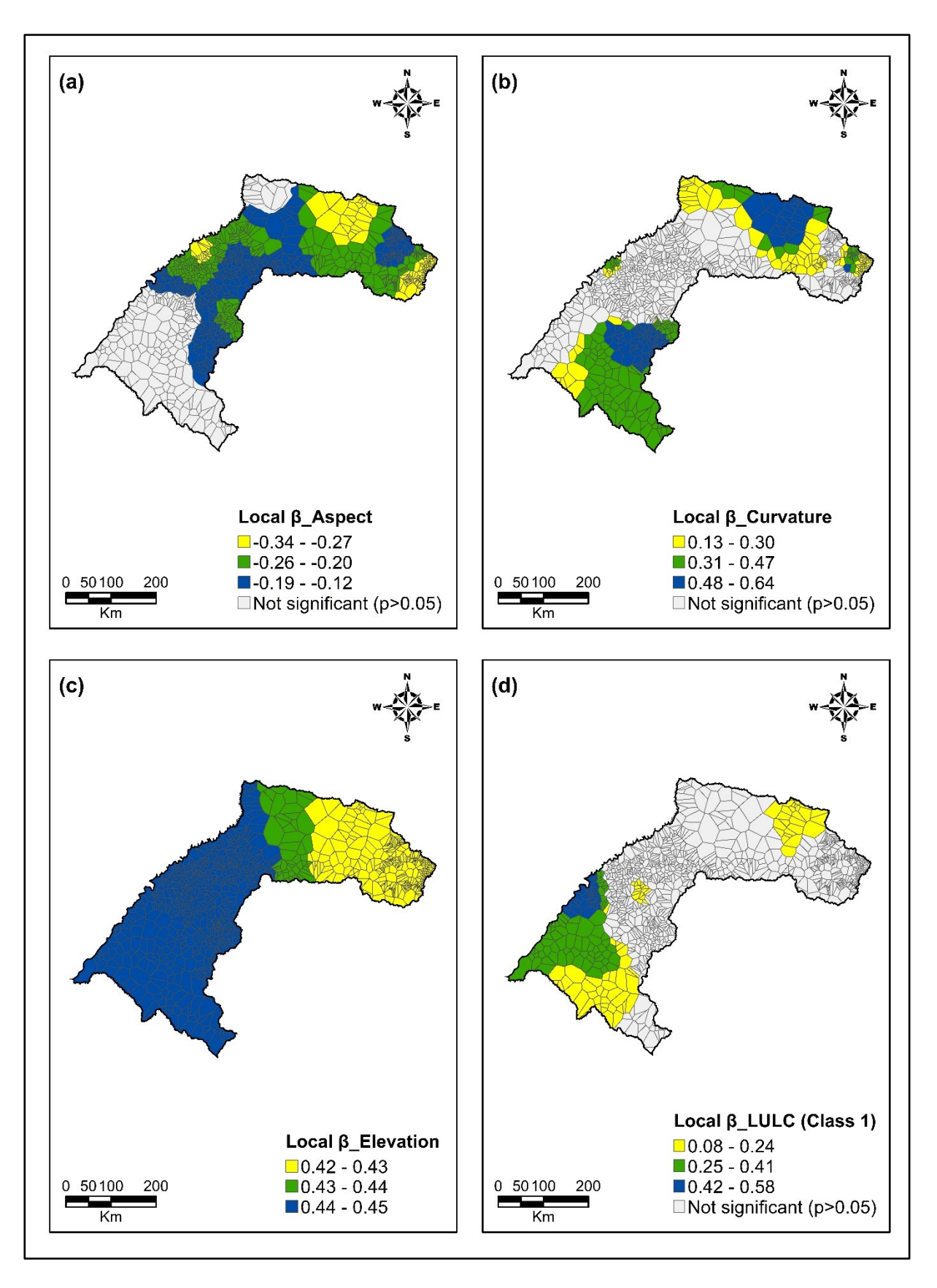


Figure 3.6 – Voronoi map of the spatial distribution of MGWR local coefficients: (a) aspect, (b) curvature, (c) elevation, (d) LULC (class 1 – Artificial area)

Table 3.6 – Frequency distribution of Local R2 values of the MGWR model

Local R <sup>2</sup>	Count	Percentage
0.18 - 0.29	324	30.34
0.30 - 0.39	375	35.11
0.40 - 0.49	105	9.83
0.50 - 0.59	118	11.05
0.60 - 0.74	146	13.67
Total	1,068	100%

There is no evidence of spatial autocorrelation in the residuals of the MGWR model over the study area because the value of the Global Moran's I statistic was equal to -0.01, and it was not statistically different from zero (z-score = -0.01; p-value = 0.99). Hence, the spatial pattern of the residuals does not appear to be significantly different from random.

A Local Condition Number (Local\_CN) greater than 30 indicates that there might be a multicollinearity problem in the model (Oshan et al., 2019). In this way, there is also no evidence of multicollinearity among the independent variables because the Local\_CNs range from 1.14 to 2.67 (Figure 3.5b).

# 3.3.2.3 Spatial pattern analysis of the coefficients

The optimal bandwidths of the coefficients obtained from GWR and MGWR models are shown in Table 3.7. The GWR model presented a very restrictive bandwidth (173) compared with the bandwidth of the MGWR model since it is approximately half of the average bandwidth of the MGWR model (337). Furthermore, GWR assumes that the aspect, curvature, elevation and LULC\_1 (artificial area) influence the altimetric error on the same scale, which is refuted by MGWR model results. The MGWR bandwidth of the curvature variable with 102 nearest neighbours indicates that this variable operates on a local scale. The MGWR bandwidths of the LULC\_1 (artificial area) and aspect variables show that these variables operate on a regional scale. The MGWR bandwidth of the elevation variable reveals that this variable influences the altimetric error on a global scale because its bandwidth is exactly the possible maximum number of neighbours (1,067).

Table 3.7 – Summary of local regression results

	Optimal	Bandwidths	Statistics for MGWR parameter estimates				
Variable	GWR	MGWR	Mean	STD*	Min	Median	Max
Intercept	173	52	-0.019	0.426	-1.415	-0.101	1.246
Curvature	173	102	0.170	0.184	-0.197	0.126	0.640
LULC_1	173	222	0.107	0.118	-0.131	0.080	0.577
Aspect	173	242	-0.187	0.077	-0.345	-0.191	0.043
Elevation	173	1067	0.433	0.008	0.420	0.438	0.441

<sup>\*</sup> Standard deviation

The MGWR bandwidth and the standard deviation parameter estimates of the variables are inversely related because a large bandwidth of a variable influences the dependent variable on a large scale which means small heterogeneity and, consequently, a small standard deviation of parameter estimates (Fotheringham et al., 2019). Likewise, a short bandwidth influences the dependent variable on a local scale where the standard deviation of the local parameter is large (Table 3.7).

MGWR local coefficients of each explanatory variable are shown in Figure 3.6, where blank areas indicate that the coefficients are not significantly different from zero. Hence, the explanatory variable does not significantly affect the altimetric error in those locations. The significant coefficients of the aspect variable are all negative and appear in the upper and middle course of the hydrographic region of Uruguay (Figure 3.6a). On the other hand, the non-significant coefficients of this variable are mostly in the lower part of the study area. Therefore, the explanatory variable does not significantly correlate with the altimetric error in those locations. Figure 3.6b shows the variation of the curvature local parameters where the coefficients are all positive in parts of the upper and lower course of the watershed, considering only regions with significant values. Figure 3.6c reveals that the elevation variable significantly influences the altimetric error at a global scale and its coefficients are very similar across the whole study area, as they range from 0.42 to 0.45. All significant coefficients of the LULC\_1 (artificial area) variable also presented positive values, and they are mainly in the lower course of the watershed (Figure 3.6d).

The percentage of locations with significant coefficients (p≤0.05 of t-test) of aspect, curvature, elevation, and LULC\_1 were 82%, 36%, 100%, and 18%, respectively (Appendix D).

#### 3.4 DISCUSSION

Despite covering 2% of Brazil's territory, the area of the Brazilian part of the Uruguay River watershed is approximately equal to double the area of some countries such as Azerbaijan (86,600 km2), Hungary (93,030 km2) or Portugal (92,212 km2). Other regions of the Brazilian territory were discarded, and that area was chosen because of the reasonable coverage of points from the BGN, where we could identify 1,068 reference points satisfactorily distributed over the study domain. Being the Topodata model exclusively developed for the Brazilian territory, it is expected that the altimetric range of the study area (32 to 1822 meters above sea level) may adequately represent the average of the national territory elevation.

The statistical analysis results demonstrated that the elevation and slope variables affect the accuracy of the Topodata DEM because higher places and steeper areas presented higher altimetric errors. In fact, the highest altimetric error residuals are related to the highest slope classes, and this result was also observed in similar studies (Gdulová et al., 2020; González-Moradas & Viveen, 2020; Gorokhovich & Voustianiouk, 2006; Sandip Mukherjee et al., 2013; Varga & Bašić, 2015). Additionally, altimetric errors are higher on higher-elevation surfaces, which was also found by Mukherjee et al. (2013) and Pandey et al. (2017). Nevertheless, some authors did not find a significant relationship between altimetric error and elevation (González-Moradas & Viveen, 2020; Varga & Bašić, 2015).

There is evidence of the influence of LULC on altimetric errors of the Topodata DEM since the artificial areas and forest vegetation presented higher altimetric errors when compared with the other classes as shown in the statistical analysis. Previous studies have already verified the LULC effect on altimetric error (Satgé et al., 2015; Yap et al., 2019), especially in vegetated areas (Dong & Shortridge, 2019; Gdulová et al., 2020; Leon et al., 2014) but such effect was also found in artificial areas (Dong & Shortridge, 2019; González-Moradas & Viveen, 2020), although smaller altimetric errors have been observed in built and homogeneous environments such as houses, roads and bare land (Leon et al., 2014). Despite the statistical analysis having shown some influence of the forest vegetation class on the altimetric error, this variable was not included in the local regression models because it was only significant in 0.02% of all the exploratory OLS investigated models. The best OLS regression model identified in this analysis included aspect, curvature, elevation and LULC\_1 (artificial area) as explanatory variables of the altimetric error in the Topodata DEM. Nonetheless, Random Forest Regression

(Breiman, 2001) could be considered in future studies for the selection of a reduced number of factors from a large set of potential explanatory variables.

The analysis of spatial effects in altimetric errors highlighted the pattern of spatial heterogeneity of the altimetric error. Generally, GWR outperforms global regression models because of its capability to deal with spatial non-stationarity. However, GWR uses a single optimized bandwidth for all independent variables to define the local neighbourhoods, thus assuming that all relationships vary at the same spatial scale across all covariates (Fotheringham et al., 2002; Fotheringham et al., 2019). Nevertheless, we assume that they may operate at different scales. In this sense, the MGWR approach is more appropriate since it computes an optimal bandwidth for each independent variable (Fotheringham et al., 2017). In fact, MGWR outperforms GWR because it allows examining the spatial scales in different processes by enabling the optimization of covariate-specific bandwidths (Fotheringham et al., 2019; Yu et al., 2020).

GWR and MGWR models were estimated using the same covariates of the best OLS model previously identified. Regression analysis results based on the Adjusted R<sup>2</sup> and AICc values proved that the MGWR outperforms the OLS and GWR models as expected. Moreover, our findings allow us to state that GWR may not be suitable for modelling the altimetric errors of a DEM because not all the explanatory variables influence the altimetric error on the same scale. Our results confirm the hypothesis that each explanatory variable operates on a different scale as the curvature variable affects the altimetric error on a local scale, the LULC\_1 (artificial area) and aspect on a regional scale, and the elevation influences the dependent variable on a global scale.

MGWR local coefficients of different variables can be directly compared because the dependent and independent variables were standardized. MGWR coefficients analysis showed that high positive altimetric errors are mainly where the aspect and curvature variables coefficients are significant. Most of the highest positive altimetric errors (high-high clusters/hot spots) are placed in regions with the lowest coefficients of the aspect variable, which exhibits a negative relationship with the altimetric error. On the other hand, the curvature coefficients showed a positive relationship. Therefore, as the curvature values increase, so do the altimetric errors. However, it is possible to verify a (low-low) cluster of

points with negative altimetric errors overlapping regions with the highest values of the curvature coefficients. Negative altimetric errors (low-low clusters) are mostly in the middle region of the study area, where only aspect and elevation variables have significant coefficients. Furthermore, negative errors occurred almost exclusively where the LULC\_1 coefficients are not significant.

One of the limitations of this study is the use of the SRTM DEM to derive some explanatory variables as this product also has accuracy issues (Weydahl et al., 2007). Nevertheless, future work should consider the development of algorithms capable of dealing with the error arising from some of the explanatory variables addressed in this study aiming to reduce altimetric discrepancies in the DEM products.

#### 3.5 CONCLUSION

This study performed a vertical accuracy analysis of the Topodata DEM in the hydrographic region of Uruguay assuming the hypothesis that its vertical accuracy would be related to terrain characteristics. The results of the statistical analysis showed that the MAE and RMSE values are sensitive to elevation, slope and some LULC classes, namely forest vegetation and artificial area. We performed a linear regression analysis through OLS, GWR and MGWR models to identify the factors that may explain the spatial patterns in the altimetric error of the Topodata DEM. The MGWR model showed better results than OLS and GWR because it models the relationship between the altimetric error and the factors influencing DEM vertical accuracy considering the geographic scale at which individual process occurs. The aspect, curvature, and artificial areas variables operate at much smaller scales than elevation which influences the altimetric error on a global scale. This implies that elevation is more relevant throughout the whole study area, whilst the other variables are relevant in certain areas since they operate on local or regional scales.

Our findings proved that different terrain characteristics operate at different scales and their relationships with altimetric error vary in space. In this way, this research provides a better understanding of the global and local processes influencing the quality of Topodata products and highlights the importance of terrain characteristics in effective DEM product development, besides shedding light on some limitations of regression modelling applications.

# 4 FINAL CONSIDERATIONS

The primary objective of this study is to enhance the comprehension of both the global and local factors that impact the quality of DEM products. In this regard, Chapter 2 presents a comprehensive assessment of the vertical accuracy of four DEM, namely ALOS PALSAR, GMTED2010, SRTM, and Topodata, with the primary goal of classifying their accuracy according to the Brazilian cartographic standard. This chapter's outcomes establish the suitability of these DEM for mapping at scales up to 1:100,000, in compliance with the Brazilian cartographic accuracy standard.

Notably, ALOS PALSAR and SRTM emerged as the top performers in the analysis. ALOS PALSAR exhibited the lowest Mean Error (ME) and Mean Absolute Error (MAE), while SRTM showcased the lowest Root Mean Square Error (RMSE) and the smallest error range. Topodata, a refinement of the SRTM data, demonstrated slightly larger errors when compared to ALOS PALSAR and SRTM. The primary reason for the less favourable performance of the GMTED2010, despite its potential compatibility with the same scale according to the Brazilian PEC standard, was attributed to its larger pixel size of 231 meters.

Through the categorization of DEM accuracy in alignment with the Brazilian cartographic accuracy standard, this chapter emphasises the importance of adhering to quality assurance guidelines to ensure that DEM accurately represent the Earth's surface, enhancing our comprehension of their suitability for a wide range of mapping applications.

This analysis raised questions about the influence of terrain characteristics on DEM accuracy. While some prior studies have identified a strong correlation between elevation/slope and altimetric error, our results did not reveal significant correlation coefficients between these variables. These observations underscore the intricacies involved in assessing DEM accuracy and highlight that while terrain characteristics are a contributing factor, their effects can vary. The findings of this chapter not only contribute to the understanding of DEM accuracy but also shed light on the implications of terrain characteristics and the potential limitations in assessing DEM accuracy.

In Chapter 3 of this dissertation, a meticulous analysis of the vertical accuracy of the Topodata DEM was conducted in the hydrographic region of Uruguay, with a focus on terrain

characteristics and their role in influencing DEM accuracy. The findings of this chapter unveil significant insights into the intricate relationship between topographic characteristics, LULC, and DEM accuracy.

The study area, comprising the Brazilian part of the Uruguay River watershed, may constitute only 2% of Brazil's vast territory, but its geographic significance and the presence of 1,068 adequately distributed reference points from the Brazilian geodetic network provided a robust database for analysis. Given that the Topodata model was exclusively designed for the Brazilian landscape, it was anticipated that this area would offer a representative altimetric range, spanning from 32 to 1822 meters above sea level, thereby reflecting the national elevation average.

A valuable revelation of this study is the impact of elevation and slope on Topodata DEM accuracy since higher elevations and steeper terrains consistently corresponded with increased altimetric errors. This finding helps us to answer our first research question and underscores the importance of considering terrain characteristics in DEM vertical accuracy assessments. In addition, Chapter 3 also provides compelling evidence of the LULC's influence on altimetric errors in the Topodata DEM. Noticeably, areas characterized by artificial structures and forest vegetation exhibited higher altimetric errors compared to other LULC classes. This observation aligns with prior research that has highlighted the effect of LULC on DEM accuracy, especially in vegetated regions. These findings also accentuate the necessity of accounting for LULC when assessing DEM accuracy.

The research conducted in this chapter also underscores the importance of DEM error spatial variation analysis. By employing GWR and MGWR models, we discovered that not all explanatory variables exert the same influence on altimetric error. These results accentuate the significance of addressing error spatial non-stationarity in the context of DEM accuracy assessment and cover our second research question since the spatial analysis of DEM uncertainties revealed the presence of spatial heterogeneity in altimetric errors.

GWR and MGWR models were employed to account for the spatial non-stationarity of Topodata DEM error. The results underscored that terrain characteristics operate at different scales and exhibit varying relationships with altimetric error. While GWR has proven utility in

addressing spatial non-stationarity, the MGWR approach emerged as more suitable for examining the distinct spatial scales at which each explanatory variable operates.

It was further demonstrated that elevation operates on a global scale, affecting altimetric error uniformly across the study area. In contrast, the aspect, curvature, and LULC\_1 (artificial area) variables operate at different local and regional scales. These results respond to our third research question, reiterating the importance of considering the geographic scale at which each variable impacts altimetric error.

The detailed analysis of MGWR coefficients provided a nuanced understanding of how terrain characteristics influence altimetric errors at the local scale. It was observed that high altimetric errors were primarily associated with areas where aspect and curvature variables exhibited significant coefficients. In this way, this study enhances our understanding of the DEM altimetric errors, highlighting some particularities of their spatial patterns.

In summary, this chapter presents a substantial contribution to the understanding of DEM accuracy and the role of terrain characteristics in shaping it. The results not only provide insights into the spatial variations of DEM accuracy but also underscore the importance of employing appropriate geospatial techniques to address this variability. As the field of geospatial analysis continues to evolve, the findings here offer valuable guidance for researchers, practitioners, and decision-makers working with DEM, ultimately enhancing the effective use of geospatial data in diverse applications. By highlighting the significance of terrain characteristics and the challenges related to spatial heterogeneity, this research contributes valuable insights to the field of geospatial data quality assessment, ultimately enabling better-informed decisions in various applications that rely on DEM data.

#### 5 LIMITATIONS AND RECOMMENDATIONS FOR FUTURE WORKS

Recognizing that DEM accuracy assessment relies heavily on the availability of accurate data and specific standardized guidelines, the study calls attention to the critical role of DEM in enabling efficient mapping and geospatial analysis. The Chapter 2 findings, despite being quite informative, are constrained by the limited distribution of control points from the Brazilian geodetic network within the Balsas River watershed since they are primarily along highways.

To address this limitation and further advance research in this field, future studies are encouraged to delve into the accuracy of DEM in other areas considering specific applications. In addition, exploration into other factors that may influence altimetric errors, such as watershed roughness, vegetation coverage, and land use, is recommended. By refining the understanding of DEM accuracy and the impacts of terrain characteristics, researchers can better harness these essential tools for geospatial applications, supporting informed decision-making in various domains.

The limitations of Chapter 3, including the use of SRTM DEM data to derive some explanatory variables, were acknowledged, and the need for addressing such limitations was highlighted. This Chapter's outcomes point to avenues for future research, particularly in the development of algorithms capable of mitigating errors introduced by certain explanatory variables. Furthermore, it is advisable to employ algorithms that can efficiently choose a limited set of factors from a vast array of potential explanatory variables while also addressing the issue of multicollinearity among these factors.

#### **REFERENCES**

- Abdelkarim, A., Al-Alola, S. S., Alogayell, H. M., Mohamed, S. A., Alkadi, I. I., & Youssef, I. Y. (2020). Mapping of gis-flood hazard using the geomorphometric-hazard model: Case study of the al-shamal train pathway in the city of qurayyat, kingdom of saudi arabia. *Geosciences (Switzerland)*, 10(9), 1-32. <a href="https://doi.org/10.3390/geosciences10090333">https://doi.org/10.3390/geosciences10090333</a>
- Abrams, M., Crippen, R., & Fujisada, H. (2020). ASTER global digital elevation model (GDEM) and ASTER global water body dataset (ASTWBD). *Remote Sensing*, *12*(7), 1156.
- Aerts, J. C., Goodchild, M. F., & Heuvelink, G. B. (2003). Accounting for spatial uncertainty in optimization with spatial decision support systems. *Transactions in GIS*, 7(2), 211-230.
- Ahmad, I. (2018). Digital elevation model (DEM) coupled with geographic information system (GIS): an approach towards erosion modeling of Gumara watershed, Ethiopia. Environmental monitoring and assessment, 190(10), 568.
- Altunel, A. O. (2019). Evaluation of TanDEM-X 90 m digital elevation model. *International journal of remote sensing*, 40(7), 2841-2854.
- Alvares, C. A., Stape, J. L., Sentelhas, P. C., & de Moraes Gonçalves, J. L. (2013). Modeling monthly mean air temperature for Brazil. *Theoretical and applied climatology*, *113*, 407-427.
- Amatulli, G., Domisch, S., Tuanmu, M. N., Parmentier, B., Ranipeta, A., Malczyk, J., & Jetz, W. (2018). Data Descriptor: A suite of global, cross-scale topographic variables for environmental and biodiversity modeling. *Scientific Data*, 5. <a href="https://doi.org/10.1038/sdata.2018.40">https://doi.org/10.1038/sdata.2018.40</a>
- ANA. (2022). Agência Nacional de Águas e Saneamento Básico. Base Hidrográfica

  Ottocodificada da Bacia do Rio Uruguai. Retrieved 12 March 2022 from

  <a href="https://metadados.snirh.gov.br/geonetwork/srv/por/catalog.search#/metadata/3d6">https://metadados.snirh.gov.br/geonetwork/srv/por/catalog.search#/metadata/3d6</a>

  a7031-5b18-45ea-ab41-39911975e51a
- Andrades Filho, C. d. O., & Rossetti, D. d. F. (2012). Effectiveness of SRTM and ALOS-PALSAR data for identifying morphostructural lineaments in northeastern Brazil. *International Journal of Remote Sensing*, 33(4), 1058-1077. https://doi.org/https://doi.org/10.1080/01431161.2010.549852

- Anselin, L. (1995). Local indicators of spatial association—LISA. *Geographical analysis*, *27*(2), 93-115.
- Anselin, L., Sridharan, S., & Gholston, S. (2007). Using exploratory spatial data analysis to leverage social indicator databases: the discovery of interesting patterns. *Social Indicators Research*, 287-309.
- Arabameri, A., Pradhan, B., Rezaei, K., & Lee, C.-W. (2019). Assessment of landslide susceptibility using statistical-and artificial intelligence-based FR–RF integrated model and multiresolution DEMs. *Remote Sensing*, 11(9), 999. <a href="https://doi.org/https://doi.org/10.3390/rs11090999">https://doi.org/https://doi.org/10.3390/rs11090999</a>
- Arosio, R., Hobley, B., Wheeler, A. J., Sacchetti, F., Conti, L. A., Furey, T., & Lim, A. (2023). Fully convolutional neural networks applied to large-scale marine morphology mapping. *Frontiers in Marine Science*.
- Athmania, D. a. A. H. (2014). External validation of the ASTER GDEM2, GMTED2010 and CGIAR-CSI- SRTM v4.1 free access digital elevation models (DEMs) in Tunisia and Algeria.

  \*Remote Sensing, 6(5), 4600-4620. <a href="https://doi.org/10.3390/rs6054600">https://doi.org/10.3390/rs6054600</a>
- Bettiol, G. M., Ferreira, M. E., Motta, L. P., Cremon, É. H., & Sano, E. E. (2021). Conformity of the NASADEM\_HGT and ALOS AW3D30 dem with the altitude from the brazilian geodetic reference stations: A case study from Brazilian Cerrado. *Sensors*, *21*(9), 2935.
- Brasington, J., Langham, J., & Rumsby, B. (2003). Methodological sensitivity of morphometric estimates of coarse fluvial sediment transport. *Geomorphology*, *53*(3-4), 299-316.
- Decreto n° 89.817 de 20 de Junho, Presidência da República Casa Civil Subchefia para Assuntos Jurídicos (1984).
- Brazil. (2006). *Caderno da Região Hidrográfica do Uruguai*. Ministério do Meio Ambiente, Secretaria de Recursos Hídricos. Brasília: MMA, 2006.
- Brazil. (2012). Secretaria do Planejamento e da Modernização da Gestão Pública (SEPLAN).

  Superintendência de Pesquisa e Zoneamento Ecológico Econômico. Diretoria de Zoneamento Ecológico-Econômico. Palmas, Tocantins.

- Norma da Especificação Técnica para Aquisição de Dados Geoespaciais Vetoriais de Defesa da Força Terrestre, Diretoria de Serviço Geográfico (DSG) Geoportal do Exército Brasileiro 2ª Edição (2016).
- Breiman, L. (2001). Random Forests. *Machine Learning*, *45*(1), 5-32. https://doi.org/10.1023/A:1010933404324
- Brunsdon, C., Fotheringham, A. S., & Charlton, M. E. (1996). Geographically Weighted Regression: A method for exploring spatial nonstationarity. *Geographical analysis*, 28(4), 281-298.
- Bui, D. T., Tsangaratos, P., Nguyen, V. T., Liem, N. V., & Trinh, P. T. (2020). Comparing the prediction performance of a Deep Learning Neural Network model with conventional machine learning models in landslide susceptibility assessment. *Catena*, *188*. https://doi.org/10.1016/j.catena.2019.104426
- Bui, D. T., Tuan, T. A., Klempe, H., Pradhan, B., & Revhaug, I. (2016). Spatial prediction models for shallow landslide hazards: a comparative assessment of the efficacy of support vector machines, artificial neural networks, kernel logistic regression, and logistic model tree. *Landslides*, *13*(2), 361-378. https://doi.org/10.1007/s10346-015-0557-6
- Carlisle, B. H. (2005). Modelling the spatial distribution of DEM error. *Transactions in GIS*, *9*(4), 521-540. https://doi.org/10.1111/j.1467-9671.2005.00233.x
- Carrol, D., & Morse, M. (1996). A national digital elevation model for resource and environmental management. *Cartography*, *25*(2), 43-49.
- Chang, H., Ge, L., Rizos, C., & Milne, T. (2004). Validation of DEMs derived from radar interferometry, airborne laser scanning and photogrammetry by using GPS-RTK. IGARSS 2004. 2004 IEEE International Geoscience and Remote Sensing Symposium,
- Chang, K., Merghadi, A., Yunus, A. P., Pham, B. T., & Dou, J. (2019). Evaluating scale effects of topographic variables in landslide susceptibility models using GIS-based machine learning techniques. *Scientific Reports*, *9*(1), 12296. <a href="https://doi.org/10.1038/s41598-019-48773-2">https://doi.org/10.1038/s41598-019-48773-2</a>

- Chaplot, V., Darboux, F., Bourennane, H., Leguédois, S., Silvera, N., & Phachomphon, K. (2006).

  Accuracy of interpolation techniques for the derivation of digital elevation models in relation to landform types and data density. *Geomorphology*, 77(1-2), 126-141.
- Chen, C., Hu, B., & Li, Y. (2021). Easy-to-use spatial random-forest-based downscaling-calibration method for producing precipitation data with high resolution and high accuracy. *Hydrology and Earth System Sciences*, *25*(11), 5667-5682. <a href="https://doi.org/10.5194/hess-25-5667-2021">https://doi.org/10.5194/hess-25-5667-2021</a>
- Chen, C., & Yue, T. (2010). A method of DEM construction and related error analysis.

  \*\*Computers\*\* & Geosciences, 36(6), 717-725.

  https://doi.org/https://doi.org/10.1016/j.cageo.2009.12.001
- Chen, X., & Chen, W. (2021). GIS-based landslide susceptibility assessment using optimized hybrid machine learning methods. *Catena*, 196. <a href="https://doi.org/10.1016/j.catena.2020.104833">https://doi.org/10.1016/j.catena.2020.104833</a>
- Danielson, J. J., & Gesch, D. B. (2011). Global multi-resolution terrain elevation data 2010 (GMTED2010). In: US Department of the Interior, US Geological Survey.
- Darnell, A. R., Tate, N. J., & Brunsdon, C. (2008). Improving user assessment of error implications in digital elevation models. *Computers, Environment and Urban Systems*, 32(4), 268-277.
- Das, S., Patel, P. P., & Sengupta, S. (2016). Evaluation of different digital elevation models for analyzing drainage morphometric parameters in a mountainous terrain: a case study of the Supin–Upper Tons Basin, Indian Himalayas. *SpringerPlus*, 5(1), 1-38.
- Demirkesen, A. C. (2012). Multi-risk interpretation of natural hazards for settlements of the Hatay province in the east Mediterranean region, Turkey using SRTM DEM. *Environmental Earth Sciences*, *65*, 1895-1907.
- DeWitt, J., Warner, T., & Conley, J. (2015). Comparison of DEMS derived from USGS DLG, SRTM, a statewide photogrammetry program, ASTER GDEM and LiDAR: implications for change detection. *GlScience & Remote Sensing*, *52*(2), 179-197.

- Dhont, D., & Chorowicz, J. (2006). Review of the neotectonics of the Eastern Turkish–Armenian Plateau by geomorphic analysis of digital elevation model imagery. *International Journal of Earth Sciences*, *95*, 34-49.
- Dong, Y., & Shortridge, A. M. (2019). A regional ASTER GDEM error model for the Chinese Loess Plateau. *International Journal of Remote Sensing*, 40(3), 1048-1065.
- Drăguţ, L., & Eisank, C. (2011). Object representations at multiple scales from digital elevation models. *Geomorphology*, *129*(3-4), 183-189.
- Ehlschlaeger, C. R. (2002). Representing multiple spatial statistics in generalized elevation uncertainty models: moving beyond the variogram. *International Journal of Geographical Information Science*, *16*(3), 259-285.
- Elkhrachy, I. (2018). Vertical accuracy assessment for SRTM and ASTER Digital Elevation Models: A case study of Najran city, Saudi Arabia. *Ain Shams Engineering Journal*, *9*(4), 1807-1817.
- Erdoğan, S. (2010). Modelling the spatial distribution of DEM error with geographically weighted regression: An experimental study. *Computers & Geosciences*, *36*(1), 34-43. https://doi.org/10.1016/j.cageo.2009.06.005
- Esri. (2022). Geographic Information System company. Calculate Distance Band from Neighbor Count (Spatial Statistics). <a href="https://pro.arcgis.com/en/pro-app/latest/tool-reference/spatial-statistics/calculate-distance-band-from-neighbor-count.htm">https://pro.arcgis.com/en/pro-app/latest/tool-reference/spatial-statistics/calculate-distance-band-from-neighbor-count.htm</a>
- Ferreira, Z., & Cabral, P. (2021). Vertical accuracy assessment of ALOS PALSAR, GMTED2010, SRTM and Topodata Digital Elevation Models. *Proceedings of the 7th International Conference on Geographical Information Systems Theory, Applications and Management (GISTAM 2021)*, 116-124. <a href="https://doi.org/10.5220/0010404001160124">https://doi.org/10.5220/0010404001160124</a>
- Ferreira, Z., & Cabral, P. (2022). A comparative study about vertical accuracy of four freely available Digital Elevation Models: A case study in the Balsas River Watershed, Brazil.

  \*ISPRS\*\* International Journal of Geo-Information, 11(2), 106.

  https://doi.org/10.3390/ijgi11020106
- Ferreira, Z., Costa, A. C., & Cabral, P. (2023). Analysing the spatial context of the altimetric error pattern of a digital elevation model using multiscale geographically weighted

- regression. *European Journal of Remote Sensing*, 56(1), 2260092. https://doi.org/10.1080/22797254.2023.2260092
- Fisher, P. (1998). Improved modeling of elevation error with geostatistics. *GeoInformatica*, *2*, 215-233.
- Florinsky, I. V. (1998). Combined analysis of digital terrain models and remotely sensed data in landscape investigations. *Progress in physical geography*, *22*(1), 33-60.
- Fotheringham, A. S., Brunsdon, C., & Charlton, M. (2002). *Geographically Weighted Regression: The analysis of spatially varying relationships*. John Wiley & Sons.
- Fotheringham, A. S., Yang, W., & Kang, W. (2017). Multiscale Geographically Weighted Regression (MGWR). *Annals of the American Association of Geographers*, *107*(6), 1247-1265. https://doi.org/10.1080/24694452.2017.1352480
- Fotheringham, A. S., Yue, H., & Li, Z. (2019). Examining the influences of air quality in China's cities using multi-scale geographically weighted regression. *Transactions in GIS*, 23(6), 1444-1464. <a href="https://doi.org/10.1111/tgis.12580">https://doi.org/10.1111/tgis.12580</a>
- Gallay, M., Lloyd, C., & McKinley, J. (2010). Using geographically weighted regression for analysing elevation error of high-resolution DEMs. Proceedings of the Ninth International Accuracy Symposium,
- Ganie, P. A., Posti, R., Aswal, A. S., Bharti, V. S., Sehgal, V. K., Sarma, D., & Pandey, P. K. (2023).

  A comparative analysis of the vertical accuracy of multiple open-source digital elevation models for the mountainous terrain of the north-western Himalaya.

  Modeling Earth Systems and Environment, 9(2), 2723-2743.

  https://doi.org/10.1007/s40808-022-01641-x
- Garofalo, D. F. T., & Liesenberg, V. (2015). Análise comparativa da informação altimétrica presente nos modelos digitais de elevação ASTER GDEM 1 e 2, SRTM e TOPODATA.

  Anais XVII Simpósio Brasileiro de Sensoriamento Remoto-SBSR. João Pessoa-PB:[sn], 2867-2875.
- Gdulová, K., Marešová, J., & Moudrý, V. (2020). Accuracy assessment of the global TanDEM-X digital elevation model in a mountain environment. *Remote Sensing of Environment*, 241, 111724. <a href="https://doi.org/10.1016/j.rse.2020.111724">https://doi.org/10.1016/j.rse.2020.111724</a>

- Gens, R. (2015). *ASF radiometric terrain corrected products* (Algorithm Theoretical Basis Document, Issue.
- Getis, A., & Ord, J. K. (1992). The analysis of spatial association by the use of distance statistics. *Geographical Analysis*, 24(2), 189–206.
- Gonga-Saholiariliva, N., Gunnell, Y., Petit, C., & Mering, C. (2011). Techniques for quantifying the accuracy of gridded elevation models and for mapping uncertainty in digital terrain analysis. *Progress in Physical Geography*, *35*(6), 739-764.
- González-Moradas, M. d. R., & Viveen, W. (2020). Evaluation of ASTER GDEM2, SRTMv3. 0, ALOS AW3D30 and TanDEM-X DEMs for the Peruvian Andes against highly accurate GNSS ground control points and geomorphological-hydrological metrics. *Remote Sensing of Environment*, 237, 111509.
- Gorini, M. A. V., & Mota, G. L. A. (2016). Dealing with double vagueness in DEM morphometric analysis. *International Journal of Geographical Information Science*, *30*(8), 1644-1666. https://doi.org/10.1080/13658816.2016.1150484
- Gorokhovich, Y., & Voustianiouk, A. (2006). Accuracy assessment of the processed SRTM-based elevation data by CGIAR using field data from USA and Thailand and its relation to the terrain characteristics. *Remote sensing of Environment*, 104(4), 409-415. <a href="https://doi.org/https://doi.org/10.1016/j.rse.2006.05.012">https://doi.org/https://doi.org/10.1016/j.rse.2006.05.012</a>
- Griffin, J., Latief, H., Kongko, W., Harig, S., Horspool, N., Hanung, R., . . . Hossen, J. (2015). An evaluation of onshore digital elevation models for modeling tsunami inundation zones. *Frontiers in Earth Science*, *3*, 32.
- Guth, P. L. (2006). Geomorphometry from SRTM. *Photogrammetric Engineering & Remote Sensing*, 72(3), 269-277.
- Guth, P. L., Van Niekerk, A., Grohmann, C. H., Muller, J.-P., Hawker, L., Florinsky, I. V., . . . Strobl, P. (2021). Digital Elevation Models: Terminology and Definitions. *Remote Sensing*, *13*(18), 3581.
- Habib, M. (2021). Evaluation of DEM interpolation techniques for characterizing terrain roughness. *Catena*, *198*, 105072.

- Hammer, R., Young, F., Haithcoate, T., Wollenhaupt, N., & Barney, T. (1995). Slope class maps from soil survey and digital elevation models. *Soil Science Society of America Journal*, *59*(2), 509-519.
- Hancock, G., Martinez, C., Evans, K., & Moliere, D. (2006). A comparison of SRTM and high-resolution digital elevation models and their use in catchment geomorphology and hydrology: Australian examples. *Earth Surface Processes and Landforms: THe Journal of the British Geomorphological Research Group*, *31*(11), 1394-1412.
- Hawker, L., Neal, J., & Bates, P. (2019). Accuracy assessment of the TanDEM-X 90 Digital Elevation Model for selected floodplain sites. *Remote Sensing of Environment*, 232, 111319. <a href="https://doi.org/10.1016/j.rse.2019.111319">https://doi.org/10.1016/j.rse.2019.111319</a>
- Hirano, A., Welch, R., & Lang, H. (2003). Mapping from ASTER stereo image data: DEM validation and accuracy assessment. *ISPRS Journal of Photogrammetry and Remote Sensing*, *57*(5), 356-370. <a href="https://doi.org/10.1016/S0924-2716(02)00164-8">https://doi.org/10.1016/S0924-2716(02)00164-8</a>
- Hirt, C., Filmer, M. S., & Featherstone, W. E. (2010). Comparison and validation of the recent freely available ASTER-GDEM ver1, SRTM ver4.1 and GEODATA DEM-9S ver3 digital elevation models over Australia. *Australian Journal of Earth Sciences*, *57*(3), 337-347. https://doi.org/10.1080/08120091003677553
- Hladik, C., & Alber, M. (2012). Accuracy assessment and correction of a LIDAR-derived salt marsh digital elevation model. *Remote Sensing of Environment*, 121, 224-235. <a href="https://doi.org/10.1016/j.rse.2012.01.018">https://doi.org/10.1016/j.rse.2012.01.018</a>
- Hodgson, M. E., Jensen, J. R., Schmidt, L., Schill, S., & Davis, B. (2003). An evaluation of LIDAR-and IFSAR-derived digital elevation models in leaf-on conditions with USGS Level 1 and Level 2 DEMs. *Remote Sensing of Environment*, 84(2), 295-308. https://doi.org/10.1016/S0034-4257(02)00114-1
- Holmes, K., Chadwick, O., & Kyriakidis, P. C. (2000). Error in a USGS 30-meter digital elevation model and its impact on terrain modeling. *Journal of Hydrology*, *233*(1-4), 154-173.
- Horton, R. E. (1932). Drainage-basin characteristics. *Transactions, American geophysical union*, *13*(1), 350-361.

- Hu, Z., Peng, J., Hou, Y., & Shan, J. (2017). Evaluation of recently released open global digital elevation models of Hubei, China. *Remote Sensing*, *9*(3), 262. <a href="https://doi.org/https://doi.org/10.3390/rs9030262">https://doi.org/https://doi.org/10.3390/rs9030262</a>
- Hutcheson, G. D. (2011). Ordinary least-squares regression. *L. Moutinho and GD Hutcheson,*The SAGE dictionary of quantitative management research, 224-228.
- IBGE. (2007). *Instituto Brasileiro de Geografia e Estatística. Manual técnico de pedologia*. <a href="https://biblioteca.ibge.gov.br/biblioteca-catalogo.html?id=237318&view=detalhes">https://biblioteca.ibge.gov.br/biblioteca-catalogo.html?id=237318&view=detalhes</a>
- IBGE. (2009). Instituto Brasileiro de Geografia e Estatística. Coordenação de Recursos Naturais e Estudos Ambientais. Manual técnico de geomorfologia. In (pp. 182). Rio de Janeiro.
- IBGE. (2015). Instituto Brasileiro de Geografia e Estatística. Modelo de ondulação geoidal MAPGEO2015: Sobre a publicação. Diretoria de Geociências DGC. Coordenação de Geodésia CGED. Retrieved 28 November 2020 from <a href="https://www.ibge.gov.br/geociencias/modelos-digitais-de-superficie/modelos-digitais-de-superficie/10855-modelo-de-ondulacao-geoidal.html?=&t=sobre">https://www.ibge.gov.br/geociencias/modelos-digitais-de-superficie/modelos-digitais-de-superficie/10855-modelo-de-ondulacao-geoidal.html?=&t=sobre</a>
- IBGE. (2017). *Instituto Brasileiro de Geografia e Estatística. Monitoramento da cobertura e uso da terra do Brasil 2000 2010 2012 2014.* Retrieved June 17, 2023 from

  <a href="https://biblioteca.ibge.gov.br/visualizacao/livros/liv101469.pdf">https://biblioteca.ibge.gov.br/visualizacao/livros/liv101469.pdf</a>
- IBGE. (2019). Instituto Brasileiro de Geografia e Estatística. Reajustamento da Rede Altimétrica com Números Geopotenciais 2 ed. Instituto Brasileiro de Geografia e Estatística Coordenação de Geodésia. Retrieved 14 July 2020 from https://biblioteca.ibge.gov.br/visualizacao/livros/liv101666.pdf
- IBGE. (2022a). Instituto Brasileiro de Geografia e Estatística. Banco de dados geodésicos.

  Retrieved 19 March 2022 from <a href="https://www.ibge.gov.br/geociencias/informacoes-sobre-posicionamento-geodesico/rede-geodesica/16327-banco-de-dados-geodesicos.html?=&t=o-que-e">https://www.ibge.gov.br/geociencias/informacoes-sobre-posicionamento-geodesico/rede-geodesica/16327-banco-de-dados-geodesicos.html?=&t=o-que-e</a>
- IBGE. (2022b). Instituto Brasileiro de Geografia e Estatística. Monitoramento da Cobertura e

  Uso da Terra. Retrieved 26 March 2022 from

  <a href="https://www.ibge.gov.br/geociencias/informacoes-ambientais/cobertura-e-uso-da-terra/15831-cobertura-e-uso-da-terra-do-brasil.html?=&t=notas-tecnicas">https://www.ibge.gov.br/geociencias/informacoes-ambientais/cobertura-e-uso-da-terra-do-brasil.html?=&t=notas-tecnicas</a>

- INPE. (2008). Insitituto Nacional de Pesquisas Espaciais. TOPODATA Banco de Dados Geomorfométricos do Brasil. Retrieved 12 October 2022 from http://www.dsr.inpe.br/topodata/index.php
- Iorio, M. M., Lastoria, G., Mioto, C. L., Albrez, E. d. A., & Paranhos Filho, A. C. (2012). Avaliação de modelos digitais de elevação extraídos de imagem ALOS/PRISM e comparação com os modelos disponibilizados gratuitamente na web. *Geociências (São Paulo), 31*(4), 650-664.
- Jain, A. O., Thaker, T., Chaurasia, A., Patel, P., & Singh, A. K. (2018). Vertical accuracy evaluation of SRTM-GL1, GDEM-V2, AW3D30 and CartoDEM-V3. 1 of 30-m resolution with dual frequency GNSS for lower Tapi Basin India. *Geocarto International*, *33*(11), 1237-1256. <a href="https://doi.org/https://doi.org/10.1080/10106049.2017.1343392">https://doi.org/https://doi.org/10.1080/10106049.2017.1343392</a>
- Janiec, P. a. G. S. (2020). A comparison of two machine learning classification methods for remote sensing predictive modeling of the forest fire in the north-eastern Siberia.

  \*Remote Sensing\*, 12(24), 1-20. https://doi.org/10.3390/rs12244157
- JAXA. (2020a). *Japan Aerospace Exploration Agency. About ALOS: Overview and Objectives*.

  Retrieved 16 July 2020 from <a href="https://www.eorc.jaxa.jp/ALOS/en/about/about">https://www.eorc.jaxa.jp/ALOS/en/about/about</a> index.htm
- JAXA. (2020b). *Japan Aerospace Exploration Agency. Advanced Land Observing Satellite* "DAICHI" (ALOS). Retrieved 16 July 2020 from <a href="https://global.jaxa.jp/projects/sat/alos/">https://global.jaxa.jp/projects/sat/alos/</a>
- Kaliraj, S., Chandrasekar, N., & Magesh, N. (2015). Morphometric analysis of the River Thamirabarani sub-basin in Kanyakumari District, South west coast of Tamil Nadu, India, using remote sensing and GIS. *Environmental Earth Sciences*, 73, 7375-7401.
- Kastrisios, C., & Tsoulos, L. (2018). Voronoi tessellation on the ellipsoidal earth for vector data. *International Journal of Geographical Information Science*, 32(8), 1541-1557.
- Krebs, P., Stocker, M., Pezzatti, G. B., & Conedera, M. (2015). An alternative approach to transverse and profile terrain curvature. *International Journal of Geographical Information Science*, 29(4), 643-666. <a href="https://doi.org/10.1080/13658816.2014.995102">https://doi.org/10.1080/13658816.2014.995102</a>
- Laurencelle, J., Logan, T., & Gens, R. (2015). *ASF Radiometrically Terrain Corrected ALOS PALSAR Products* (Alaska Satellite Facility: Fairbanks, Alaska, Issue.

- Lee, S., & Sambath, T. (2006). Landslide susceptibility mapping in the Damrei Romel area, Cambodia using frequency ratio and logistic regression models. *Environmental Geology*, *50*, 847-855.
- Lei, X., Chen, X., Yang, Z., He, S., Zhu, L., & Liang, H. (2022). A simple and robust MPM framework for modelling granular flows over complex terrains. *Computers and Geotechnics*, *149*, 104867.
- Leon, J. X., Heuvelink, G. B., & Phinn, S. R. (2014). Incorporating DEM uncertainty in coastal inundation mapping. *PLoS one*, *9*(9), e108727. <a href="https://doi.org/10.1371/journal.pone.0108727">https://doi.org/10.1371/journal.pone.0108727</a>
- Li, J., Zhao, Y., Bates, P., Neal, J., Tooth, S., Hawker, L., & Maffei, C. (2020). Digital Elevation Models for topographic characterisation and flood flow modelling along low-gradient, terminal dryland rivers: A comparison of spaceborne datasets for the Río Colorado, Bolivia. *Journal of Hydrology*, 591, 125617. <a href="https://doi.org/https://doi.org/10.1016/j.jhydrol.2020.125617">https://doi.org/https://doi.org/10.1016/j.jhydrol.2020.125617</a>
- Li, L., Nearing, M. A., Nichols, M. H., Polyakov, V. O., Guertin, D. P., & Cavanaugh, M. L. (2020).

  The effects of DEM interpolation on quantifying soil surface roughness using terrestrial LiDAR. *Soil and Tillage Research*, *198*, 104520.
- Li, S., Xiong, L., Tang, G., & Strobl, J. (2020). Deep learning-based approach for landform classification from integrated data sources of digital elevation model and imagery. *Geomorphology*, 354, 107045. https://doi.org/10.1016/j.geomorph.2020.107045
- Lindsay, J. B. (2016). Whitebox GAT: A case study in geomorphometric analysis. *Computers and Geosciences*, 95, 75-84. <a href="https://doi.org/10.1016/j.cageo.2016.07.003">https://doi.org/10.1016/j.cageo.2016.07.003</a>
- Liu, Z., Zhu, J., Fu, H., Zhou, C., & Zuo, T. (2020). Evaluation of the Vertical Accuracy of Open Global DEMs over Steep Terrain Regions Using ICESat Data: A Case Study over Hunan Province, China. *Sensors*, *20*(17), 4865.
- Mahalingam, R., & Olsen, M. J. (2016). Evaluation of the influence of source and spatial resolution of DEMs on derivative products used in landslide mapping. *Geomatics, Natural Hazards and Risk, 7*(6), 1835-1855. <a href="https://doi.org/10.1080/19475705.2015.1115431">https://doi.org/10.1080/19475705.2015.1115431</a>

- Manfreda, S., & Samela, C. (2019). A digital elevation model based method for a rapid estimation of flood inundation depth. *Journal of Flood Risk Management*, *12*, e12541.
- Mansour, S., Al-Belushi, M., & Al-Awadhi, T. (2020). Monitoring land use and land cover changes in the mountainous cities of Oman using GIS and CA-Markov modelling techniques. *Land use policy*, *91*, 104414.
- Mantelli, L. R., Barbosa, J. M., & Bitencourt, M. D. (2011). Assessing ecological risk through automated drainage extraction and watershed delineation. *Ecological Informatics*, 6(5), 325-331. https://doi.org/https://doi.org/10.1016/j.ecoinf.2011.04.003
- Merghadi, A., Yunus, A. P., Dou, J., Whiteley, J., ThaiPham, B., Bui, D. T., . . . Abderrahmane, B. (2020). Machine learning methods for landslide susceptibility studies: A comparative overview of algorithm performance. *Earth-Science Reviews*, 207. <a href="https://doi.org/10.1016/j.earscirev.2020.103225">https://doi.org/10.1016/j.earscirev.2020.103225</a>
- Mesa-Mingorance, J. L., & Ariza-López, F. J. (2020). Accuracy Assessment of Digital Elevation Models (DEMs): A Critical Review of Practices of the Past Three Decades. *Remote Sensing*, 12(16), 2630. <a href="https://doi.org/10.3390/rs12162630">https://doi.org/10.3390/rs12162630</a>
- Miceli, B. S., Dias, F. D. M., Seabra, F. M., Santos, P., & Fernandes, M. D. C. (2011). Avaliação vertical de modelos digitais de elevação (MDEs) em diferentes configurações topográficas para médias e pequenas escalas. *Revista Brasileira de Cartografia*, *63*(1), 191-201.
- Miller, A., Sirguey, P., Morris, S., Bartelt, P., Cullen, N., Redpath, T., . . . Bühler, Y. (2022). The impact of terrain model source and resolution on snow avalanche modeling. *Nat. Hazards Earth Syst. Sci.*, 22(8), 2673-2701. <a href="https://doi.org/10.5194/nhess-22-2673-2022">https://doi.org/10.5194/nhess-22-2673-2022</a>
- Mondal, A., Khare, D., Kundu, S., Mukherjee, S., Mukhopadhyay, A., & Mondal, S. (2017).

  Uncertainty of soil erosion modelling using open source high resolution and aggregated DEMs. *Geoscience Frontiers*, 8(3), 425-436. https://doi.org/10.1016/j.gsf.2016.03.004
- Moran, P. A. (1950). Notes on continuous stochastic phenomena. *Biometrika*, 37(1/2), 17-23.

- Moura, L. Z., Bias, E. d. S., & Brites, R. (2014). Avaliação da acurácia vertical de modelos digitais de elevação (MDEs) nas bacias do Paranoá e São Bartolomeu. *Revista Brasileira de Cartografia*, 66(1), ISSN 1808-0936.
- Mouratidis, A., & Ampatzidis, D. (2019). European digital elevation model validation against extensive global navigation satellite systems data and comparison with SRTM DEM and ASTER GDEM in Central Macedonia (Greece). *ISPRS International Journal of Geo-Information*, 8(3), 108. https://doi.org/https://doi.org/10.3390/ijgi8030108
- Mukherjee, I., & Singh, U. K. (2020). Delineation of groundwater potential zones in a droughtprone semi-arid region of east India using GIS and analytical hierarchical process techniques. *Catena*, 194, 104681.
- Mukherjee, S., Joshi, P. K., Mukherjee, S., Ghosh, A., Garg, R. D., & Mukhopadhyay, A. (2013). Evaluation of vertical accuracy of open source Digital Elevation Model (DEM). International Journal of Applied Earth Observation and Geoinformation, 21, 205-217. https://doi.org/10.1016/j.jag.2012.09.004
- Mukherjee, S., Mukherjee, S., Garg, R. D., Bhardwaj, A., & Raju, P. (2013). Evaluation of topographic index in relation to terrain roughness and DEM grid spacing. *Journal of Earth System Science*, 122, 869-886.
- Munoth, P., & Goyal, R. (2020). Impacts of land use land cover change on runoff and sediment yield of Upper Tapi River Sub-Basin, India. *International Journal of River Basin Management*, 18(2), 177-189.
- Mustak, S., Bhagmar, N., & Ratre, C. (2012). Measurement of Dissection India of Pairi River Basin Using Remote Sensing and GIS. *National Geographical Journal of India*, *58*(2), 97-106.
- Naderpour, M., Rizeei, H. M., Khakzad, N., & Pradhan, B. (2019). Forest fire induced Natech risk assessment: A survey of geospatial technologies. *Reliability Engineering & System Safety*, *191*, 106558.
- Nadi, S., Shojaei, D., & Ghiasi, Y. (2020). Accuracy assessment of DEMs in different topographic complexity based on an optimum number of GCP formulation and error propagation analysis. *Journal of Surveying Engineering*, *146*(1), 04019019.

- NASA. (2013). National Aeronautics and Space Administration. Shuttle Radar Topography Mission Global 1 arc second. Version 3. NASA EOSDIS Land Processes DAAC. USGS Earth Resources Observation and Science (EROS) Center: Sioux Falls, SD, USA. https://doi.org/10.5067/MEaSUREs/SRTM/SRTMGL1.003
- NASA. (2020). *National Aeronautics and Space Administration. Shuttle Radar Topography Mission*. Shuttle Radar Topography Mission. Retrieved 16 July 2020 from <a href="https://www2.jpl.nasa.gov/srtm/index.html">https://www2.jpl.nasa.gov/srtm/index.html</a>
- NASA. (2022). *National Aeronautics and Space Administration. Shuttle Radar Topography Mission*. Shuttle Radar Topography Mission. Retrieved 15 July 2022 from <a href="https://www2.jpl.nasa.gov/srtm/index.html">https://www2.jpl.nasa.gov/srtm/index.html</a>
- Nene, S. A., & Nayar, S. K. (1997). A simple algorithm for nearest neighbor search in high dimensions. *IEEE Transactions on pattern analysis and machine intelligence*, *19*(9), 989-1003.
- Ohlmacher, G. C. (2007). Plan curvature and landslide probability in regions dominated by earth flows and earth slides. *Engineering Geology*, *91*(2), 117-134. https://doi.org/https://doi.org/10.1016/j.enggeo.2007.01.005
- Oksanen, J. (2006). Digital elevation model error in terrain analysis. Finnish Geodetic Institute.
- Oksanen, J., & Sarjakoski, T. (2006). Uncovering the statistical and spatial characteristics of fine toposcale DEM error. *International Journal of Geographical Information Science*, 20(4), 345-369.
- Orlando, F. C. (2019). Análise da potencialidade do uso de MDE global em trabalho de grande escala ao longo de todo o território brasileiro.
- Oshan, T. M., Li, Z., Kang, W., Wolf, L. J., & Fotheringham, A. S. (2019). MGWR: A Python Implementation of Multiscale Geographically Weighted Regression for Investigating Process Spatial Heterogeneity and Scale. *ISPRS International Journal of Geo-Information*, 8(6), 269.
- Pakoksung, K. a. T. M. (2021). Effect of DEM sources on distributed hydrological model to results of runoff and inundation area. *Modeling Earth Systems and Environment*, 7(3), 1891-1905. <a href="https://doi.org/10.1007/s40808-020-00914-7">https://doi.org/10.1007/s40808-020-00914-7</a>

- Pandey, P., Manickam, S., Bhattacharya, A., Ramanathan, A., Singh, G., & Venkataraman, G. (2017). Qualitative and quantitative assessment of TanDEM-X DEM over western Himalayan glaciated terrain. *Geocarto International*, *32*(4), 442-454.
- Peterson, E. E., Theobald, D. M., & Ver Hoef, J. M. (2007). Geostatistical modelling on stream networks: developing valid covariance matrices based on hydrologic distance and stream flow. *Freshwater biology*, *52*(2), 267-279.
- Pipaud, I., Loibl, D., & Lehmkuhl, F. (2015). Evaluation of TanDEM-X elevation data for geomorphological mapping and interpretation in high mountain environments A case study from SE Tibet, China. *Geomorphology*, 246, 232-254. https://doi.org/https://doi.org/10.1016/j.geomorph.2015.06.025
- Polidori, L., & El Hage, M. (2020). Digital Elevation Model Quality Assessment Methods: A Critical Review. *Remote Sensing*, *12*(21), 3522.
- Polidori, L., El Hage, M., & Valeriano, M. D. M. (2014). Digital elevation model validation with no ground control: application to the topodata DEM in Brazil. *Boletim de Ciências Geodésicas*, 20(2), 467-479. <a href="https://doi.org/https://doi.org/10.1590/S1982-21702014000200027">https://doi.org/https://doi.org/10.1590/S1982-21702014000200027</a>
- Prasannakumar, V., Vijith, H., Charutha, R., & Geetha, N. (2011). Spatio-temporal clustering of road accidents: GIS based analysis and assessment. *Procedia-social and behavioral sciences*, *21*, 317-325.
- Rabby, Y. W., Ishtiaque, A., & Rahman, M. (2020). Evaluating the Effects of Digital Elevation Models in Landslide Susceptibility Mapping in Rangamati District, Bangladesh. *Remote Sensing*, 12(17), 2718. <a href="https://doi.org/https://doi.org/10.3390/rs12172718">https://doi.org/https://doi.org/10.3390/rs12172718</a>
- Rawat, K. S., Singh, S. K., Singh, M. I., & Garg, B. (2019). Comparative evaluation of vertical accuracy of elevated points with ground control points from ASTERDEM and SRTMDEM with respect to CARTOSAT-1DEM. *Remote Sensing Applications: Society and Environment*, 13, 289-297.
- Reuter, H. I., Hengl, T., Gessler, P., & Soille, P. (2009). Preparation of DEMs for geomorphometric analysis. *Developments in Soil Science*, *33*, 87-120.

- Riley, S. J., DeGloria, S. D., & Elliot, R. (1999). Index that quantifies topographic heterogeneity. intermountain Journal of sciences, 5(1-4), 23-27.
- Rizzoli, P., Martone, M., Gonzalez, C., Wecklich, C., Borla Tridon, D., Bräutigam, B., . . . Moreira, A. (2017). Generation and performance assessment of the global TanDEM-X digital elevation model. *ISPRS Journal of Photogrammetry and Remote Sensing*, *132*, 119-139. <a href="https://doi.org/https://doi.org/10.1016/j.isprsjprs.2017.08.008">https://doi.org/https://doi.org/10.1016/j.isprsjprs.2017.08.008</a>
- Rodrigues, T. G., Paradella, W. R., & Oliveira, C. G. (2011). Evaluation of the altimetry from SRTM-3 and planimetry from high-resolution PALSAR FBD data for semi-detailed topographic mapping in the Amazon Region. *Anais da Academia Brasileira de Ciências*, 83, 953-966.
- Roostaee, M., & Deng, Z. (2020). Effects of digital elevation model resolution on watershed-based hydrologic simulation. *Water Resources Management*, *34*, 2433-2447.
- Safar, M. (2005). K nearest neighbor search in navigation systems. *Mobile Information Systems*, 1(3), 207-224.
- Saleem, N., Huq, M. E., Twumasi, N. Y. D., Javed, A., & Sajjad, A. (2019). Parameters derived from and/or used with digital elevation models (DEMs) for landslide susceptibility mapping and landslide risk assessment: a review. *ISPRS International Journal of Geo-Information*, 8(12), 545.
- Sappington, J. M., Longshore, K. M., & Thompson, D. B. (2007). Quantifying landscape ruggedness for animal habitat analysis: a case study using bighorn sheep in the Mojave Desert. *The Journal of wildlife management*, *71*(5), 1419-1426.
- Sarma, C. P., Dey, A., & Krishna, A. M. (2020). Influence of digital elevation models on the simulation of rainfall-induced landslides in the hillslopes of Guwahati, India. *Engineering Geology*, 268. <a href="https://doi.org/10.1016/j.enggeo.2020.105523">https://doi.org/10.1016/j.enggeo.2020.105523</a>
- Satge, F., Denezine, M., Pillco, R., Timouk, F., Pinel, S., Molina, J., . . . Bonnet, M.-P. (2016).

  Absolute and relative height-pixel accuracy of SRTM-GL1 over the South American Andean Plateau. *ISPRS Journal of Photogrammetry and Remote Sensing*, 121, 157-166.
- Satgé, F., Bonnet, M.-P., Timouk, F., Calmant, S., Pillco, R., Molina, J., . . . Garnier, J. (2015).

  Accuracy assessment of SRTM v4 and ASTER GDEM v2 over the Altiplano watershed

- using ICESat/GLAS data. *International Journal of Remote Sensing*, *36*(2), 465-488. https://doi.org/10.1080/01431161.2014.999166
- Schwendel, A. C., & Milan, D. J. (2020). Terrestrial structure-from-motion: Spatial error analysis of roughness and morphology. *Geomorphology*, *350*, 106883.
- Shaikh, M., Yadav, S., & Manekar, V. (2021). Accuracy Assessment of Different Open-Source Digital Elevation Model Through Morphometric Analysis for a Semi-arid River Basin in the Western Part of India. *Journal of Geovisualization and Spatial Analysis*, *5*(2), 23. https://doi.org/10.1007/s41651-021-00089-4
- Sharma, M., Garg, R. D., Badenko, V., Fedotov, A., Min, L., & Yao, A. (2021). Potential of airborne LiDAR data for terrain parameters extraction. *Quaternary International*, *575*, 317-327.
- Shean, D. E., Alexandrov, O., Moratto, Z. M., Smith, B. E., Joughin, I. R., Porter, C., & Morin, P. (2016). An automated, open-source pipeline for mass production of digital elevation models (DEMs) from very-high-resolution commercial stereo satellite imagery. *ISPRS Journal of Photogrammetry and Remote Sensing*, 116, 101-117.
- Silva, J. F. d., Queiroga Miranda, R. d., & Candeias, A. L. B. (2022). Análise dos Modelos Digitais de Elevação (PE3D, SRTM-30, SRTM-90, ASTER GDEM, TOPODATA, TANDEM-X, ALOS PALSAR e ALOS AW3D30) e a necessidade da produção de dados altimétricos em excelência no Brasil. *Revista Brasileira de Geografia Física*, *15*(03), 1543-1555.
- Smith, A. G. G., Fox, M., Schwanghart, W., & Carter, A. (2022). Comparing methods for calculating channel steepness index. *Earth-Science Reviews*, *227*, 103970. <a href="https://doi.org/10.1016/j.earscirev.2022.103970">https://doi.org/10.1016/j.earscirev.2022.103970</a>
- Smith, G.-H. (1935). The Relative Relief of Ohio. *Geographical Review*, 25(2), 272-284. https://doi.org/10.2307/209602
- Soliman, A., & Han, L. (2019). Effects of vertical accuracy of digital elevation model (DEM) data on automatic lineaments extraction from shaded DEM. *Advances in Space Research*, 64(3), 603-622. <a href="https://doi.org/10.1016/j.asr.2019.05.009">https://doi.org/10.1016/j.asr.2019.05.009</a>
- Suliman, A. H. A., Gumindoga, W., Awchi, T. A., & Katimon, A. (2021). DEM resolution influences on peak flow prediction: a comparison of two different based DEMs through

- various rescaling techniques. *Geocarto International*, *36*(7), 803-819. https://doi.org/10.1080/10106049.2019.1622599
- Szypuła, B. (2019). Quality assessment of DEM derived from topographic maps for geomorphometric purposes. *Open Geosciences*, *11*(1), 843-865.
- Sánchez-Guillamón, O., Fernández-Salas, L. M., Vázquez, J. T., Palomino, D., Medialdea, T., López-González, N., . . . León, R. (2018). Shape and size complexity of deep seafloor mounds on the canary basin (West to Canary islands, Eastern Atlantic): A DEM-based geomorphometric analysis of domes and volcanoes. *Geosciences (Switzerland)*, 8(2). https://doi.org/10.3390/geosciences8020037
- Taheri, M., Dolatabadi, N., Nasseri, M., Zahraie, B., Amini, Y., & Schoups, G. (2020). Localized linear regression methods for estimating monthly precipitation grids using elevation, rain gauge, and TRMM data. *Theoretical and Applied Climatology*, *142*(1-2), 623-641. <a href="https://doi.org/10.1007/s00704-020-03320-2">https://doi.org/10.1007/s00704-020-03320-2</a>
- Tan, M., L., F. D., Dixon, B., L., I. A., Z., Y., & V., C. (2015). Impacts of DEM resolution, source, and resampling technique on SWAT-simulated streamflow. *Applied Geography*, *63*, 357-368. https://doi.org/10.1016/j.apgeog.2015.07.014
- Tan, Z., Guan, Q., Lin, J., Yang, L., Luo, H., Ma, Y., . . . Wang, N. (2020). The response and simulation of ecosystem services value to land use/land cover in an oasis, Northwest China. *Ecological Indicators*, *118*, 106711.
- Tang, F., Fu, M., Wang, L., & Zhang, P. (2020). Land-use change in Changli County, China: Predicting its spatio-temporal evolution in habitat quality. *Ecological Indicators*, *117*, 106719.
- Temme, A., Heuvelink, G., Schoorl, J., & Claessens, L. (2009). Geostatistical simulation and error propagation in geomorphometry. *Developments in soil science*, *33*, 121-140. https://doi.org/10.1016/S0166-2481(08)00005-6
- Thomas, J., Joseph, S., Thrivikramji, K., & Arunkumar, K. (2014). Sensitivity of digital elevation models: The scenario from two tropical mountain river basins of the Western Ghats, India. *Geoscience Frontiers*, 5(6), 893-909. <a href="https://doi.org/https://doi.org/10.1016/j.gsf.2013.12.008">https://doi.org/https://doi.org/10.1016/j.gsf.2013.12.008</a>

- Thomas, J., Prasannakumar, V., & Vineetha, P. (2015). Suitability of spaceborne digital elevation models of different scales in topographic analysis: an example from Kerala, India. *Environmental Earth Sciences*, 73(3), 1245-1263. <a href="https://doi.org/https://doi.org/10.1007/s12665-014-3478-0">https://doi.org/https://doi.org/10.1007/s12665-014-3478-0</a>
- Tran, T.-N.-D., Nguyen, B. Q., Vo, N. D., Le, M.-H., Nguyen, Q.-D., Lakshmi, V., & Bolten, J. D. (2023). Quantification of global Digital Elevation Model (DEM) A case study of the newly released NASADEM for a river basin in Central Vietnam. *Journal of Hydrology:* Regional Studies, 45, 101282. <a href="https://doi.org/10.1016/j.ejrh.2022.101282">https://doi.org/10.1016/j.ejrh.2022.101282</a>
- Tucker, G. E., Catani, F., Rinaldo, A., & Bras, R. L. (2001). Statistical analysis of drainage density from digital terrain data. *Geomorphology*, *36*(3), 187-202. https://doi.org/https://doi.org/10.1016/S0169-555X(00)00056-8
- UNAVCO. (2022). EarthScope Consortium. Geoid Height Calculator. Retrieved 28 March 2022

  from <a href="https://www.unavco.org/software/geodetic-utilities/geoid-height-calculator.html">https://www.unavco.org/software/geodetic-utilities/geoid-height-calculator.html</a>
- Uysal, M., Toprak, A. S., & Polat, N. (2015). DEM generation with UAV Photogrammetry and accuracy analysis in Sahitler hill. *Measurement*, 73, 539-543. https://doi.org/10.1016/j.measurement.2015.06.010
- Valeriano, M. d. M. (2008). *Topodata: Guia para utilização de dados geomorfológicos locais*. São José dos Campos: Instituto Nacional de Pesquisas Espaciais (INPE), 72.
- Valeriano, M. d. M., & Rossetti, D. d. F. (2008). *Topodata: Seleção de coeficientes* geoestatísticos para o refinamento unificado de dados SRTM. São José dos Campos: INPE.
- Valeriano, M. d. M., & Rossetti, D. d. F. (2012). Topodata: Brazilian full coverage refinement of SRTM data. *Applied Geography*, *32*(2), 300-309. <a href="https://doi.org/https://doi.org/10.1016/j.apgeog.2011.05.004">https://doi.org/https://doi.org/10.1016/j.apgeog.2011.05.004</a>
- Varga, M., & Bašić, T. (2015). Accuracy validation and comparison of global digital elevation models over Croatia. *International journal of remote sensing*, *36*(1), 170-189. https://doi.org/10.1080/01431161.2014.994720

- Vignesh, K. S., Anandakumar, I., Ranjan, R., & Borah, D. (2021). Flood vulnerability assessment using an integrated approach of multi-criteria decision-making model and geospatial techniques. *Modeling Earth Systems and Environment*, 7(2), 767-781. https://doi.org/10.1007/s40808-020-00997-2
- Walker, J. P., & Willgoose, G. R. (1999). On the effect of digital elevation model accuracy on hydrology and geomorphology. *Water Resources Research*, *35*(7), 2259-2268.
- Wechsler, S. P. (2003). Perceptions of digital elevation model uncertainty by DEM users. *Urisa Journal*, *15*(2), 57-64.
- Wechsler, S. P. (2007). Uncertainties associated with digital elevation models for hydrologic applications: a review. *Hydrology and Earth System Sciences*, *11*(4), 1481-1500.
- Weiss, A. (2001). Topographic position and landforms analysis. Poster presentation, ESRI user conference, San Diego, CA,
- Wessel, B., Huber, M., Wohlfart, C., Marschalk, U., Kosmann, D., & Roth, A. (2018). Accuracy assessment of the global TanDEM-X Digital Elevation Model with GPS data. *ISPRS Journal of Photogrammetry and Remote Sensing*, 139, 171-182. <a href="https://doi.org/https://doi.org/10.1016/j.isprsjprs.2018.02.017">https://doi.org/https://doi.org/10.1016/j.isprsjprs.2018.02.017</a>
- Weydahl, D. J., Sagstuen, J., Dick, O. B., & Ronning, H. (2007). SRTM DEM accuracy assessment over vegetated areas in Norway. *International Journal of Remote Sensing*, *28*(16), 3513-3527. https://doi.org/10.1080/01431160600993447
- Williams, R. (2012). DEMs of difference. *Geomorphological Techniques*, 2(3.2).
- Wise, S. (2000). Assessing the quality for hydrological applications of digital elevation models derived from contours. *Hydrological Processes*, 14(11-12), 1909-1929. <a href="https://doi.org/10.1002/1099-1085(20000815/30)14:11/12%3C1909::AID-HYP45%3E3.0.CO;2-6">https://doi.org/10.1002/1099-1085(20000815/30)14:11/12%3C1909::AID-HYP45%3E3.0.CO;2-6</a>
- Wise, S. (2012). Information entropy as a measure of DEM quality. *Computers & Geosciences*, 48, 102-110.
- Xiong, L., Tang, G., Yang, X., & Li, F. (2021). Geomorphology-oriented digital terrain analysis: Progress and perspectives. *Journal of Geographical Sciences*, *31*, 456-476.

- Xu, S., Wu, C., Wang, L., Gonsamo, A., Shen, Y., & Niu, Z. (2015). A new satellite-based monthly precipitation downscaling algorithm with non-stationary relationship between precipitation and land surface characteristics. *Remote sensing of environment, 162,* 119-140.
- Xu, Y., Zhu, H., Hu, C., Liu, H., & Cheng, Y. (2021). Deep learning of DEM image texture for landform classification in the Shandong area, China. *Frontiers of Earth Science*. https://doi.org/10.1007/s11707-021-0884-y
- Yap, L., Kandé, L. H., Nouayou, R., Kamguia, J., Ngouh, N. A., & Makuate, M. B. (2019). Vertical accuracy evaluation of freely available latest high-resolution (30 m) global digital elevation models over Cameroon (Central Africa) with GPS/leveling ground control points. *International Journal of Digital Earth*, 12(5), 500-524. https://doi.org/10.1080/17538947.2018.1458163
- Yu, H., Fotheringham, A. S., Li, Z., Oshan, T., Kang, W., & Wolf, L. J. (2020). Inference in Multiscale Geographically Weighted Regression. *Geographical Analysis*, *52*(1), 87-106. https://doi.org/10.1111/gean.12189
- Zhang, W., & Montgomery, D. R. (1994). Digital elevation model grid size, landscape representation, and hydrologic simulations. *Water resources research*, *30*(4), 1019-1028.
- Zhou, Q., & Liu, X. (2002). Error assessment of grid-based flow routing algorithms used in hydrological models. *International journal of geographical information science*, *16*(8), 819-842.

## **APPENDICES**

# APPENDIX A1/A2 — CORRELATION BETWEEN THE ELEVATION OF THE REFERENCE POINTS (BGN) AND THE ELEVATION

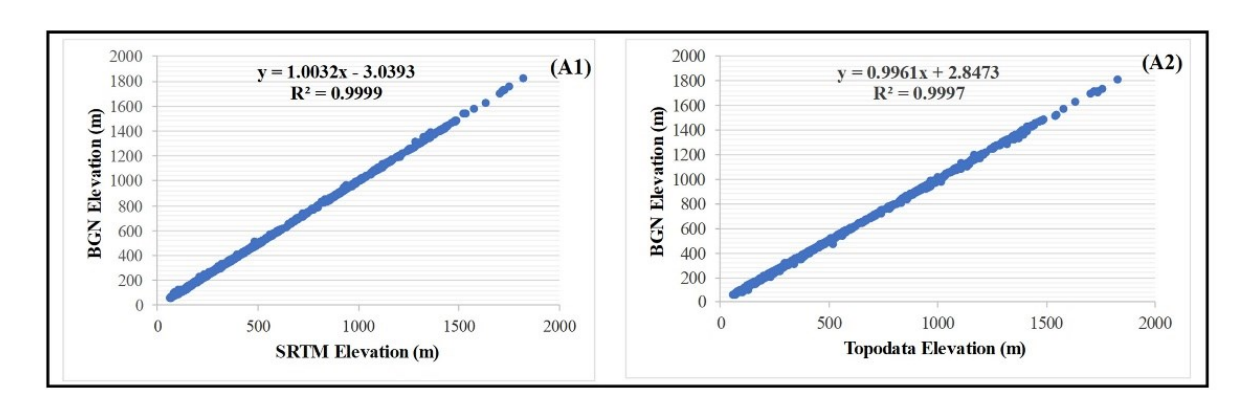


Figure A 1 / A 2 – Correlation between the elevation of the reference points (BGN) and the elevation extracted from SRTM (A1) and Topodata (A2)

## APPENDIX A3 — HISTOGRAM OF THE ALTIMETRIC ERROR

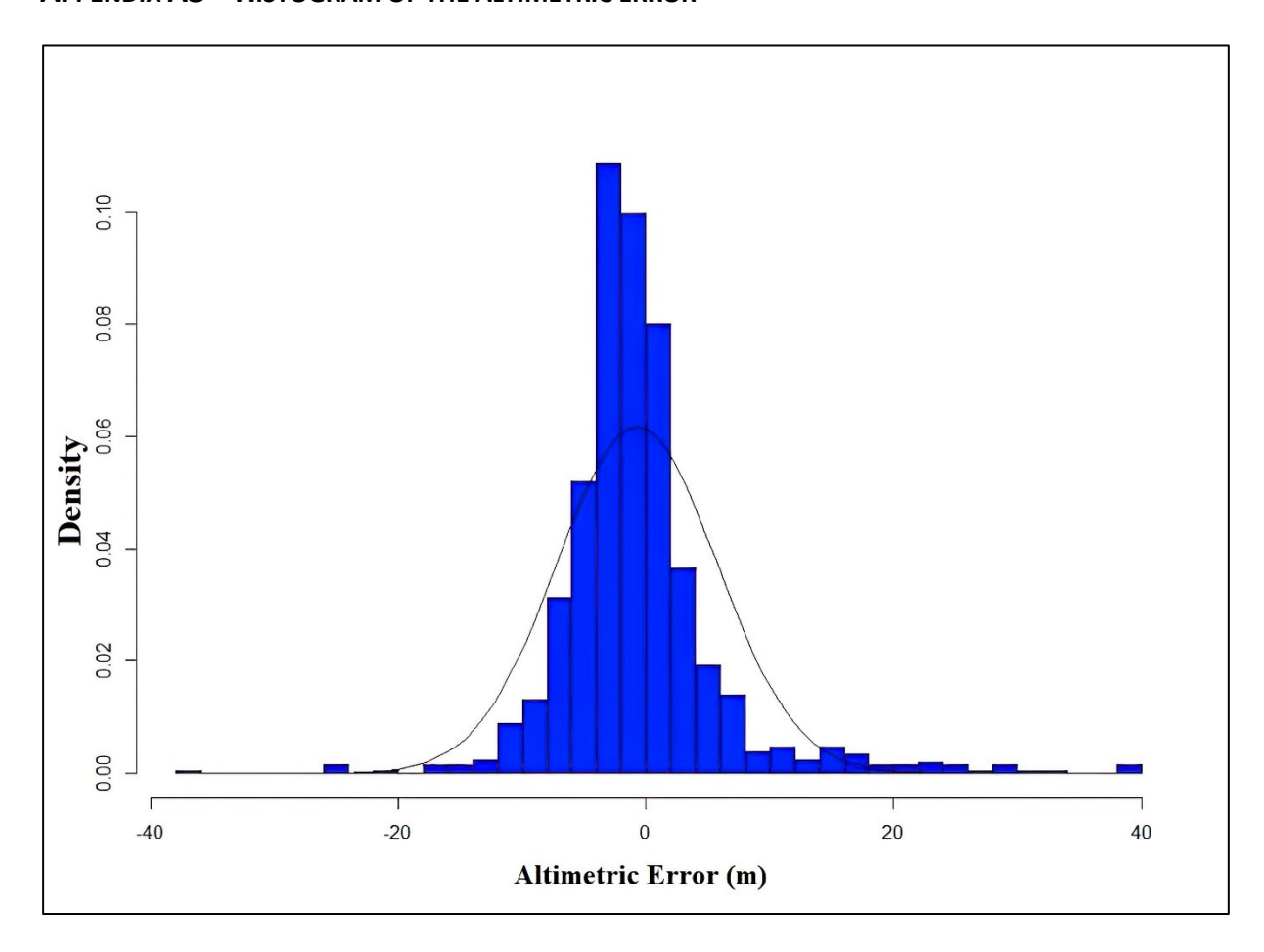


Figure A 3 – Histogram of the altimetric error

## APPENDIX A4 – BOXPLOTS OF THE ELEVATION DIFFERENCES

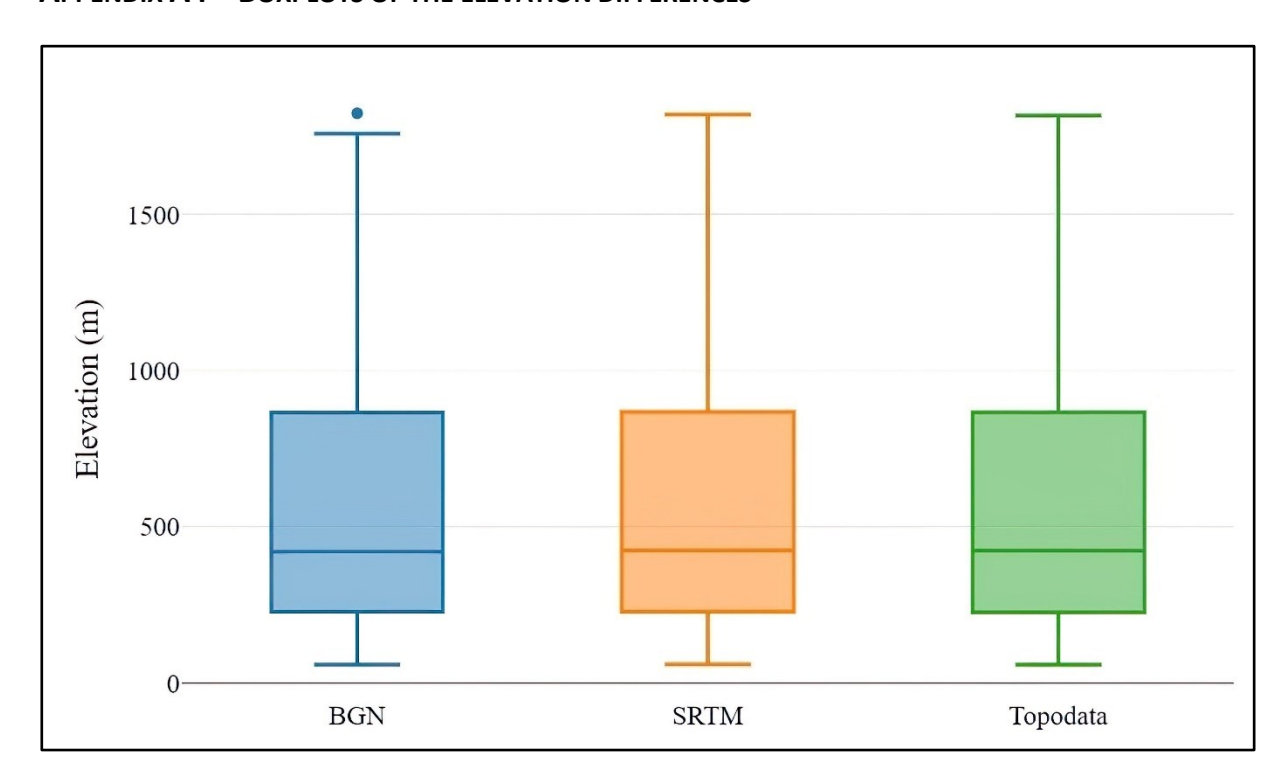


Figure A 4 – Boxplots of the elevation differences (BGN, SRTM and Topodata)

## APPENDIX B — STATISTICAL ANALYSIS OF THE ALTIMETRIC ERROR

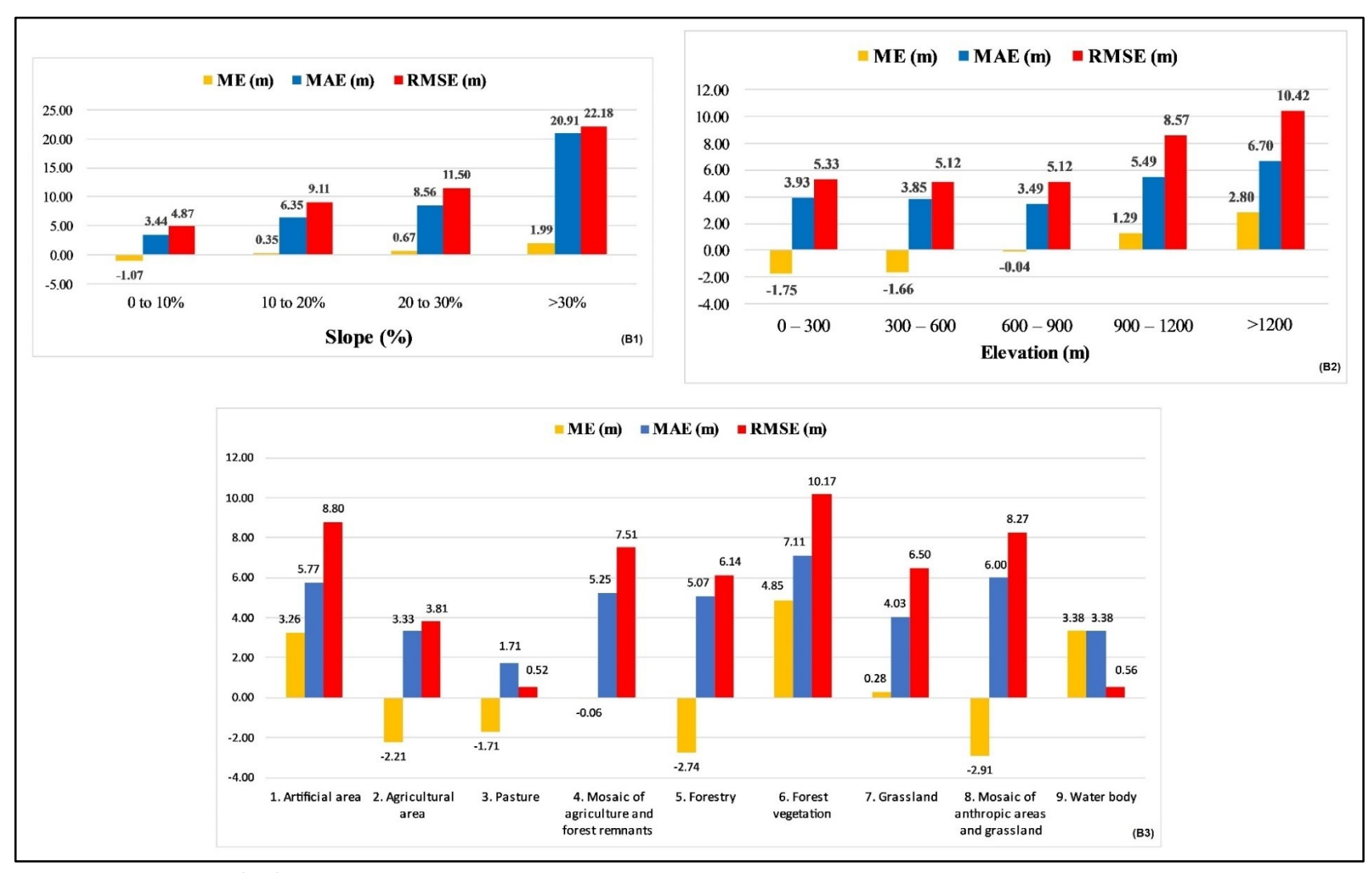


Figure B 1/B2/B3 - Statistical analysis of the altimetric error regarding slope (B1), elevation (B2) and LULC class (B3)

## APPENDIX C – CORRELATION MATRIX OF THE CANDIDATE EXPLANATORY VARIABLES

		Alt_Error	Aspect	Curv_Plan	Curv_Profi	Curvature	Dist_River	Drain_Dens	Elevation	Rel_Relief	Roughness	Slope	TRI	TPI	VRM	LULC_1	LULC_2	LULC_3	LULC_4	LULC_5	LULC_6	LULC_7	LULC_8	LULC_9
Alt_Error	Pearson's r	_																						
	p-value	_																						
Aspect	Pearson's r	-0.18 ***	-																					
	p-value	< .001	_																					
Curv_Plan	Pearson's r	0.27 ***	0.06	_																				
	p-value	< .001	0.056	-																				
Curv_Profi	Pearson's r	-0.26 ***	-0.03	-0.58 ***	_																			
	p-value	< .001	0.362	< .001	-																			
Curvature	Pearson's r	0.30 ***	0.05	0.87 ***	-0.90 ***	_																		
	p-value	< .001	0.120	< .001	< .001	-																		
Dist_River	Pearson's r	0.11 ***	-0.00	0.01	-0.07*	0.05	_																	
Drain_Dens	p-value	< .001	0.951	0.780	0.018	0.100	-																	
	Pearson's r p-value	-0.06 0.056	0.02	-0.01 0.729	0.07*	-0.05 0.112	-0.64 *** < .001	_																
Elevation																								
	Pearson's r p-value	0.22 ***	0.02	0.10 **	-0.09** 0.005	0.10 *** < .001	-0.29 *** < .001	0.44*** <.001	_															
Rel Relief		0.10 ***	0.04	0.07*	-0.02	0.05	-0.33 ***	0.56 ***	0.75***															
Rei_Reilei	Pearson's r p-value	< .001	0.237	0.020	0.518	0.112	< .001	< .001	<.001	_														
Roughness	Pearson's r	0.02	0.04	0.00	0.03	-0.01	-0.00	0.03	-0.03	0.01														
riouginicas	p-value	0.496	0.178	0.922	0.413	0.661	0.982	0.341	0.335	0.769	_													
Slope	Pearson's r	0.06	0.05	0.13 ***	-0.15***	0.16 ***	-0.17 ***	0.20 ***	0.30 ***	0.35 ***	0.01	_												
	p-value	0.066	0.127	< .001	< .001	< .001	< .001	< .001	< .001	< .001	0.681	_												
TRI	Pearson's r	-0.01	0.03	0.01	0.04	-0.02	0.01	0.02	-0.05	-0.04	0.63 ***	0.01	_											
	p-value	0.731	0.284	0.859	0.209	0.510	0.661	0.610	0.087	0.239	< .001	0.865	_											
TPI	Pearson's r	0.02	0.04	0.01	0.02	-0.01	-0.00	0.03	-0.03	0.01	1.00 ***	0.01	0.63***	_										
	p-value	0.463	0.177	0.852	0.468	0.737	0.992	0.347	0.343	0.765	< .001	0.665	< .001	_										
VRM	Pearson's r	0.01	0.04	-0.00	0.03	-0.02	0.03	0.01	-0.06*	-0.02	0.77 ***	0.01	0.82***	0.77 ***	_									
	p-value	0.802	0.160	0.967	0.286	0.509	0.362	0.710	0.048	0.428	< .001	808.0	< .001	< .001	_									
LULC_1	Pearson's r	0.13 ***	0.03	-0.01	0.02	-0.02	0.06 *	-0.05	-0.01	-0.03	-0.05	0.01	0.01	-0.05	0.01	_								
	p-value	< .001	0.388	0.748	0.420	0.530	0.037	0.110	0.703	0.317	0.098	0.852	0.735	0.098	0.678	_								
LULC_2	Pearson's r	-0.12 ***	-0.03	-0.03	0.01	-0.02	0.10 **	-0.26 ***	-0.27***	-0.40 ***	0.03	-0.16 ***	0.03	0.03	0.04	0.03	_							
	p-value	< .001	0.307	0.258	0.801	0.469	0.001	< .001	<.001	< .001	0.399	< .001	0.323	0.404	0.190	0.304	_							
LULC_3	Pearson's r	0.06	0.00	-0.02	-0.02	0.00	-0.00	0.09 **	0.11***	0.13 ***	0.01	0.02	0.01	0.01	0.01	-0.01	-0.05	_						
	p-value	0.059	0.959	0.612	0.511	0.899	0.900	0.002	< .001	< .001	0.797	0.423	0.865	0.795	0.842	0.674	0.139							
LULC_4	Pearson's r p-value	0.17 *** < .001	0.02	0.13 ***	-0.12*** <.001	0.14 *** < .001	-0.09 ** 0.004	0.10 ***	0.11***	0.24 *** < .001	0.03	0.19 *** < .001	0.02	0.03	0.03	0.16 ***	-0.17*** < .001	0.17 *** < .001	_					
IIIIC S		0.07*		0.06	-0.11***	0.09 **	-0.09 **	0.22 ***	0.21***	0.09 **		0.08**					-0.13***	0.06*	0.16 ***					
LULC_5	Pearson's r p-value	0.07	-0.00 0.905	0.065	<.001	0.003	0.003	< .001	<.001	0.09	0.01	0.006	0.01	0.01	-0.00 0.997	0.05	<.001	0.06	< .001	_				
LULC_6	Pearson's r	0.01	0.01	0.02	-0.04	0.03	0.07 *	-0.05	0.03	0.09 **	0.02	0.04	0.01	0.02	0.02	-0.02	-0.13***	0.01	0.16 ***	0.05	_			
LULC_U	p-value	0.678	0.674	0.454	0.212	0.257	0.022	0.119	0.279	0.003	0.470	0.221	0.660	0.468	0.588	0.608	< .001	0.770	< .001	0.085	_			
LULC_7	Pearson's r	0.12 ***	0.01	0.02	-0.07*	0.06	0.20 ***	-0.19 ***	-0.10***	-0.12 ***	0.00	-0.11 ***	-0.03	0.00	-0.01	-0.04	-0.22***	-0.01	-0.27 ***	-0.07 *	0.05	_		
	p-value	< .001	0.767	0.428	0.029	0.072	< .001	< .001	< .001	< .001	0.939	< .001	0.312	0.931	0.675		< .001	0.826	< .001	0.033	0.107	_		
LULC_8	Pearson's r	0.06	-0.01	0.00	-0.07*	0.04	0.06	-0.04	0.00	0.03	0.00	0.05	0.02	0.00	0.02	0.20 ***	-0.11***	0.01	-0.03	0.10 **	0.08 **	0.18 ***	_	
	p-value	0.061	0.748	0.988	0.029	0.188	0.051	0.212	0.872	0.281	0.887	0.132	0.603	0.879	0.543	< .001	< .001	0.722	0.314	0.002	0.008	< .001	_	
LULC_9	Pearson's r	0.06 *	-0.01	0.00	0.01	-0.01	0.06*	-0.05	-0.12***	-0.06 *	0.01	-0.03	0.01	0.01	0.01	0.07 *	0.04	-0.02	0.12 ***	-0.02	0.02	-0.02	-0.01	_
	p-value	0.036	0.763	0.875	0.666	0.834	0.035	0.102	< .001	0.042	0.749	0.404	0.849	0.750	0.805	0.017	0.146	0.592	< .001	0.597	0.526	0.434	0.707	_

Figure C – Correlation matrix of the candidate explanatory variables

## APPENDIX D – STATISTICS OF SIGNIFICANT COEFFICIENT ESTIMATES (MGWR)

Table D - Statistics of significant coefficient estimates (p≤0.05 of t-test) for the MGWR model of altimetric error

Variables	Minimum	Maximum	Median	Mean	<b>Standard Deviation</b>	Percentage of points
Intercept	-1.424	1.251	-0.312	0.023	0.675	35%
Aspect	-0.345	-0.123	-0.200	-0.213	0.052	82%
Curvature	0.126	0.639	0.345	0.368	0.134	36%
Elevation	0.426	0.447	0.444	0.439	0.008	100%
LULC_1	0.083	0.577	0.278	0.291	0.130	18%



NOVA Information Management School Instituto Superior de Estatística e Gestão de Informação

Universidade Nova de Lisboa